UNIVERSITY OF OKLAHOMA

GRADUATE COLLEGE

COSMOLOGY WITH A DARK REFRACTION INDEX

A DISSERTATION

SUBMITTED TO THE GRADUATE FACULTY

in partial fulfillment of the requirements for the

Degree of

DOCTOR OF PHILOSOPHY

By

BIN CHEN
Norman, Oklahoma
2009

COSMOLOGY WITH A DARK REFRACTION INDEX

A DISSERTATION APPROVED FOR THE
HOMER L. DODGE DEPARTMENT OF PHYSICS AND ASTRONOMY

BY

Ronald Kantowski, Chair

Edward Baron

David Branch

Max Forester

Chung Kao

Yun Wang

I dedicate this thesis to my father, S. Chen, and my mother, S. Cai. for their love and support.

Acknowledgements

First and foremost I would like to thank my adviser, Ronald Kantowski, it is his help all these five years that brought me from where I was to where I am now. I appreciate and enjoyed the freedom Dr. Kantowski gave me which made it possible for me to go through materials in different fields in physics, astronomy, and mathematics, which greatly extended my horizon. I learned and enjoyed from those many hours we spent together discussing physics and mathematics. I thank him for all those wise suggestions and encouragements he made whenever I was confused or frustrated.

I thank all my committee members, Edward Baron, David Branch, Max Forester, Chung Kao, and Yun Wang for their time and support. In particular, I learned all I know in the field of radiation transport and numerical analysis from Dr. Baron, I learned Supernova physics from Dr. Branch. I learned topology from Dr. Forester, and I learned cosmology from Dr. Wang. I also thank Dr. Krishnan Shankar for helpful discussion in math and for those excellent reading materials he recommended to me.

I thank the University of Oklahoma for giving me the precious chance to study in the United States.

Last but not the least, I thank my older brother Wei-Guo Chen, and my sister in

law, Xiao-Jie Huang, for taking up the responsibility of taking care of our parents during my stay abroad.

Contents

Acknowledgements iv
Abstract x

1 Introduction **1**
1.1 The Optical Metric 1
1.2 Geometrical Optics Approximation 6
1.3 Redshift and Distance Definitions 11
1.3.1 Redshift 11
1.3.2 Luminosity and Distances 12
1.4 Friedman Equation 18
1.4.1 Distance Redshift Relation in RW metric 21
1.5 Geometry of Ray Bundles and Optical Scalars 22
1.5.1 Connecting Vectors 23
1.5.2 Optical Scalars 24
1.5.3 Transport Equations 27

2 Cosmology With a Dark Refraction Index **29**
2.1 Geometrical Optics Approximation II 30
2.2 Optical Metric for Robertson-Walker Spacetimes 35
2.3 An Effective Index of Refraction Induced by the Sachs-Wolfe Effect 40
2.4 Fitting Supernova Data With A Refraction Index Model 44
2.5 Flatness of the Universe 48
2.6 Discussion 49

3 Complex Optical Metric **53**
3.1 Introduction 53
3.2 A Complex Eikonal 56
3.2.1 Plane Waves in Minkowski Spacetime 60
3.2.2 Spherical Waves in a Static Spherically Symmetric Spacetime 63
3.3 A Real Eikonal 65
3.3.1 Robertson-Walker Spacetime 67
3.4 Discussion 73

3.5 Appendix 76

4 An Optical Metric that Includes Absorption 79
4.1 Introduction 80
4.2 The "Transverse" Conformal Transformation 81
4.3 Geometrical Optics Approximation 87
4.4 A Transverse Conformal Transformation Versus Absorption 90
4.5 Absorption in Robertson-Walker Spacetimes 94
4.6 Incorporating Both Refraction and Absorption into the Optical Metric 98
4.7 The Optical Metric in FLRW Cosmology with Both Refraction and Absorption 101
4.8 An Application: FLRW Spacetime with Both Refraction and Absorption 104
4.9 Discussion 109

Conclusions 112

Bibliography 114

List of Figures

2.1 Distance modulus μ versus redshift z. Dashed curve: $\Omega_\Lambda = 0, \Omega_m = 0.3, n = 1$; Green curve: $\Omega_\Lambda = 0.7$, $\Omega_m = 0.3$, $n = 1$; Red curve: $\Omega_\Lambda = 0$, $\Omega_m = 0.04$, $n(z) = 1 + 0.1z^2 - 0.045z^3$; Blue curve: $\Omega_\Lambda = 0$, $\Omega_m = 0.3$, $n(z) = 1 + 0.15z^2 - 0.05z^3$. $\Delta\mu(z)$ are given in the inset. The difference is taken with respect to the fiducial case where $\Omega_\Lambda = 0, \Omega_m = 0.3, n = 1$. 47

2.2 $H(z)$ (upper panel) and $\dot{R}(z)/R_o$ (lower panel) curves for the two $n \neq 1$ models. Left column parameters: $\Omega_\Lambda = 0$, $\Omega_m = 0.04$, $n(z) = 1 + 0.1z^2 - 0.045z^3$; Right column parameters: $\Omega_\Lambda = 0$, $\Omega_m = 0.3$, $n(z) = 1 + 0.15z^2 - 0.05z^3$. 47

2.3 Dashed curve: $\Omega_\Lambda = 0$, $\Omega_m = 0.3$, $n(z) = 1$; Blue Curve: $\Omega_\Lambda = 0$, $\Omega_m = 0.3$, $n(z) = 1 + 4.45 \times 10^{-7} z^2 - 1.25 \times 10^{-10} z^3$; Green curve: $\Omega_\Lambda = 0.7$, $\Omega_m = 0.3$, $n = 1$. 49

3.1 Distance modulus μ versus redshift z. The two red and one solid black curves are open models, the two green curves are flat models, and the blue curve is a closed model. (looking downward at redshift $z = 1.5$) Dotted red curve: $\Omega_\Lambda = 0$, $\Omega_\mathrm{m} = 0.05$, $\alpha(z) = 6 \times 10^{-5}$ Mpc^{-1}. Short dashed red curve : $\Omega_\Lambda = 0$, $\Omega_\mathrm{m} = 0.3$, $\alpha(z) = 1.2 \times 10^{-4}$ Mpc^{-1}. Solid black curve (our best fit): $\Omega_\Lambda = 0$, $\Omega_\mathrm{m} = 0.73$, $\alpha(z) = 2.2 \times 10^{-4}$Mpc^{-1}. Solid green curve (concordance model): $\Omega_\Lambda = 0.7$, $\Omega_\mathrm{m} = 0.3$, $\alpha = 0$. Longer dashed green curve: $\Omega_\Lambda = 0$, $\Omega_\mathrm{m} = 1.0$, $\alpha(z) = 2.6 \times 10^{-4}$ Mpc^{-1}. Longest dashed blue curve: $\Omega_\mathrm{m} = 1.3$, $\alpha(z) = 3.2 \times 10^{-4}$ Mpc^{-1}. Black dashed curve: $\Omega_\Lambda = 0$, $\Omega_\mathrm{m} = 0.3$, $\alpha = 0$. Inset: $\Delta\mu$ versus z curve for each model, the fiducial model (black dashed curve): $\Omega_\Lambda = 0$, $\Omega_\mathrm{m} = 0.3$, $\alpha = 0$. . 73

3.2 α versus Ω_m. The best fitting parameters are $\Omega_\mathrm{m} = 0.73, \alpha = 2.2 \times 10^{-4}$Mpc^{-1}, with $\chi^2_\mathrm{min} = 1.04$ (per degree of freedom). The innermost contour encloses the 68.3% confident region, the next one encloses the 95.4% confidence region, and the outermost one encloses the 99.73% confidence region. 74

4.1 $\Delta\mu$ versus z. In each of the four frames the fiducial model (horizontal black dashed) is the now disfavored dark matter only model, i.e., $\Omega_\Lambda = 0, \Omega_{\rm m} = 0.3, \alpha = 0, p = 0$, and the green curve is the concordance model, $\Omega_\Lambda = 0.7, \Omega_{\rm m} = 0.3, \alpha = 0, p = 0$. Upper left panel: pure absorption models with no refraction. Dotted red curve, $\Omega_\Lambda = 0, \Omega_{\rm m} = 0.05, \alpha = 0.7 \times 10^{-4}{\rm Mpc}^{-1}, n = 1$. Short-dashed red curve, $\Omega_\Lambda = 0, \Omega_{\rm m} = 0.3, \alpha = 1.3 \times 10^{-4}{\rm Mpc}^{-1}, n = 1$. Solid black curve: $\Omega_\Lambda = 0, \Omega_{\rm m} = 0.73, \alpha = 2.2 \times 10^{-4}{\rm Mpc}^{-1}, n = 1$. Upper right panel: blue curve, $\Omega_\Lambda = 0, \Omega_{\rm m} = 1.0, \alpha = 2.5 \times 10^{-4}{\rm Mpc}^{-1}, p = 0$. Red curve, $\Omega_\Lambda = 0, \Omega_{\rm m} = 1.0, \alpha = 2.5 \times 10^{-4}{\rm Mpc}^{-1}, p = 0.024$. Bottom left panel: blue curve, $\Omega_\Lambda = 0, \Omega_{\rm m} = 1.5, \alpha = 3.3 \times 10^{-4}{\rm Mpc}^{-1}, p = 0$. Red curve, $\Omega_\Lambda = 0, \Omega_{\rm m} = 1.0, \alpha = 3.3 \times 10^{-4}{\rm Mpc}^{-1}, p = 0.042$. Bottom right panel: blue curve, $\Omega_\Lambda = 0, \Omega_{\rm m} = 2.0, \alpha = 4.1 \times 10^{-4}{\rm Mpc}^{-1}, p = 0$. Red curve, $\Omega_\Lambda = 0$, $\Omega_{\rm m} = 2.0$, $\alpha = 4.1 \times 10^{-4}{\rm Mpc}^{-1}$, $p = 0.049$. 107

4.2 Confidence contours (68.3%, 95.4%, and 99.73%) for each fixed $\Omega_{\rm m}$ model. The x coordinate is absorption coefficient α in unit of $10^{-4}{\rm Mpc}^{-1}$, and the y-axis is refraction index parameter p ($n = 1 + pz^2$). Top left panel, $\Omega_{\rm m} = 0.05$, with least chi-square (per degree of freedom) $\chi^2 = 1.09$, the best fitting parameters are $\alpha = 0.7 \times 10^{-4}{\rm Mpc}^{-1}$, $p = 0$. Top right panel, $\Omega_{\rm m} = 0.3$, least $\chi^2 = 1.05$, the best fitting parameters are $\alpha = 1.3 \times 10^{-4}{\rm Mpc}^{-1}$, $p = 0$. Middle left panel, $\Omega_{\rm m} = 0.73$, least $\chi^2 = 1.035$, the best fitting parameters are $\alpha = 2.2 \times 10^{-4}{\rm Mpc}^{-1}$, $p = 0$. Middle right panel, $\Omega_{\rm m} = 1.0$, least $\chi^2 = 1.042$, at $\alpha = 2.5 \times 10^{-4}{\rm Mpc}^{-1}$, $p = 0.024$. Bottom left, $\Omega_{\rm m} = 1.5$, least $\chi^2 = 1.05$, the best fitting parameters are $\alpha = 3.3 \times 10^{-4}{\rm Mpc}^{-1}$, $p = 0.042$. Bottom right, $\Omega_{\rm m} = 2.0$, least $\chi^2 = 1.06$, the best fitting parameters are $\alpha = 4.1 \times 10^{-4}{\rm Mpc}^{-1}$, $p = 0.049$. 108

Abstract

In this dissertation we review Gordon's optical metric theory, generalize it, and apply it to modern cosmology.

In Chapter 1, we build the notation, define important quantities (luminosity distance, angular diameter distance, etc.), derive a few key equations (reciprocity relation, transport equations of optical scalars, etc.), and develop some basic techniques which will be useful later on.

In Chapter 2 we apply Gordon's optical metric theory to Friedman-Lemaître-Robertson-Walker cosmologies. We associate a refraction index with the cosmic fluid and derive the refraction-corrected distance redshift relations. We then fit the Hubble curve of current supernova observations with a non-accelerating cosmological model. We also show that some observational effects caused by inhomogeneities, e.g., the Sachs-Wolfe effect, can be interpreted as being caused by an effective index of refraction, and hence this theory could extend to other speed of light communications such as gravitational radiation and neutrino fluxes.

In Chapter 3 we show that Gordon's optical metric on a curved spacetime can be generalized to include absorption by allowing the metric to become complex. We distinguish two different cases, i.e., strong and weak absorption, and demonstrate the use of the complex optical metric theory by giving three examples. We use one

of these examples to compute corrected distance-redshift relations for Friedman-Lemaître-Robertson-Walker models in which the cosmic fluid possesses a complex index of refraction that represents grey extinction. We then fit this corrected Hubble curve to the same supernovae data used in Chapter 2 by assuming pure absorption.

In Chapter 4 we equate the physical intensity reduction of a light wave caused by weak absorption with a geometrical reduction in intensity caused by a "transverse" conformal transformation of the spacetime metric in which the wave travels. We then modify Gordon's optical metric to include absorption via a totally different way than that of Chapter 3 in which we included absorption in Gordon's optical metric by allowing the metric to be complex. We derive the distance-redshift relation from the modified optical metric for Friedman-Lemaître-Robertson-Walker spacetimes whose cosmic fluid has associated refraction and absorption coefficients. We then fit the current supernovae data with a cosmological model containing both refraction and absorption and provide an alternate explanation (other than dark energy) of the apparent acceleration of the universe expansion.

Chapter 1

Introduction

In this introductory chapter, we build the notation, define some important quantities, prove a few key theorems, and develop some basic techniques which will be useful for discussions later on. In Sec. 1.1 we review Gordon's optical metric. In Sec. 1.2 we review the geometrical optics approximation. In Sec. 1.3 and 1.4 we define a few important astronomical quantities and prove a few key theorems. In Sec. 1.5 we discuss the optical scalars and their propagating equations in detail.

1.1 The Optical Metric

In GR type theories, a gravity field is described by a metric g_{ab} on a four dimensional manifold (we use a +2 signature here). We additionally assume the presence of an arbitrarily moving medium with normalized 4-velocity $u^a u_a = -1$ that fills spacetime. For simplicity, we also assume that the fluid's electromagnetic properties are linear, isotropic, transparent[1], and non-dispersive (frequency independent),

[1]This constraint will be dropped in Chapter 2 when we include absorption in Gordon's optical metric.

and can be summarized by two scalar functions defined on the 4-manifold, i.e., a permittivity $\epsilon(x^a)$ and a permeability $\mu(x^a)$, or equivalently by a refraction index $n \equiv \sqrt{\epsilon\mu}$. Following [30] in this section, we write the two electromagnetic bivectors as $F^{ab}(B, E)$ and $H^{ab}(H, D)$. They satisfy Maxwell's Equations[2]

$$\begin{aligned} \partial_{[a}F_{bc]} &= 0, \\ \nabla_b H^{ba} &= \frac{4\pi}{c} J^a, \end{aligned} \tag{1.1}$$

with constitutive relations

$$\begin{aligned} H^{ab}u_b &= \epsilon F^{ab}u_b, \\ F_{[ab}u_{c]} &= \mu H_{[ab}u_{c]}. \end{aligned} \tag{1.2}$$

Remark. For a familiar example, take the Minkowski spacetime with the fluid at rest, $u^a = (1, 0, 0, 0)$.

Gordon's optical metric [41] is defined as

$$\bar{g}_{ab} = g_{ab} + (1 - \frac{1}{\epsilon\mu})u_a u_b = -\frac{1}{n^2}u_a u_b + g_{\perp ab}, \tag{1.3}$$

with inverse

$$\bar{g}^{ab} = g^{ab} + (1 - \epsilon\mu)u^a u^b = -n^2 u^a u^b + g_{\perp}^{ab}, \tag{1.4}$$

where $g_{\perp ab}$ is the familiar projection tensor.

[2]Notation: square bracket $[\cdot]$ or parenthesis $(\cdot)$ symbolize respectively complete anti-symmetrization or symmetrization of the enclosed indices. A comma in front a subscript, e.g., $[\cdot]_{,\,a}$, takes partial derivative of the corresponding coordinate component. ∇ with a subscript, or a semicolon in front of a subscript, i.e., ∇_a or $[\cdot]_{;\,a}$, represents covariant differentiation.

Remark. The normalized 4-velocity with respect to the optical metric $\bar{g}_{ab}$ is

$$\bar{u}_a \equiv \frac{1}{\sqrt{\epsilon\mu}} u_a, \;\; \bar{u}^a \equiv \bar{g}^{ab}\bar{u}_b = \sqrt{\epsilon\mu}\, u^a. \tag{1.5}$$

We have almost no occasion [3] where we have to use $\bar{u}^a$ because all physical measurements such as frequency ν and energy density U of the electromagnetic wave should be measured with respect to the physical observer u^a (see Chapter 2).

To relate covariant derivatives of the two metrics and to obtain Eq. (1.14) below the relationship of the two determinants is needed[4]

$$\det \bar{g}_{ab} = \frac{1}{n^2} \det g_{ab}. \tag{1.8}$$

At this point we have one differentiable manifold with two metrics or equivalently two related spacetimes, the physical and the optical. We are primarily interested in the dynamics of a particular type of physical field (radiation) in the optical spacetime. All physical objects are described by tensor fields in physical spacetime and those of interest here have associated fields in optical spacetime. Where necessary we denote optical spacetime fields with a bar. The optical equivalent of the physical covariant Maxwell field F_{ab} is F_{ab} itself; hence the homogeneous Maxwell equations are satisfied in both spacetimes, and both share covariant 4-

[3] An exception is in Chapter 4 when we apply a transverse conformal transformation to Gordon's optical metric.

[4] **Lemma**. $\det \bar{g}_{ab} = (1/n^2) \det g_{ab}$.

Proof. Take $A^a = (1 - 1/n^2)u^a$, $B^a = u^a$. Note that $A \cdot B = -(1 - 1/n^2)$. Show first

$$\det(\delta^a{}_b + A^a B_b) = 1 + A^a B_a, \tag{1.6}$$

and then

$$\det(g_{ac}(\delta^c{}_b + A^c B_b)) = \det(g_{ab} + A_a B_b) = \det\, g_{ab} \cdot (1 + A \cdot B). \tag{1.7}$$

potentials. Using the optical metric the two constitutive equations can be written as a single equation

$$H^{ab} = \frac{1}{\mu}\bar{F}^{ab} \equiv \frac{1}{\mu}\bar{g}^{ac}\bar{g}^{bd}F_{cd}, \tag{1.9}$$

as can be seen by first expressing the contravariant Maxwell field in optical spacetime as

$$\bar{F}^{ab} = [F^{ab} - (1-\epsilon\mu)u^a F^b{}_c u^c + (1-\epsilon\mu)u^b F^a{}_c u^c], \tag{1.10}$$

and then contracting separately with u_b and $\epsilon_{abcd}u^c$. Here the metric dependent bivector $\bar{F}^{ab}$ is the metric independent 2-form F_{ab} raised using the optical metric Eq. (1.4) rather than the physical metric g_{ab}. By using the identity relating the contracted Christoffel symbols to the metric's determinant

$$\Gamma^d_{cd} = \frac{\partial_c\sqrt{-g}}{\sqrt{-g}}, \tag{1.11}$$

we find

$$\nabla_b H^{ab} = \frac{(\sqrt{-g}H^{ab})_{,\,b}}{\sqrt{-g}}. \tag{1.12}$$

Now using Eq. (1.8), Maxwell's equations (1.1) can be written using the optical metric as

$$\begin{aligned} \partial_{[a}F_{bc]} &= 0, \\ \bar{\nabla}_b\left(e^{2\phi}\,\bar{F}^{ba}\right) &= \frac{4\pi}{c}\bar{J}^a \equiv \frac{4\pi}{c}\sqrt{\epsilon\mu}\,J^a, \end{aligned} \tag{1.13}$$

where $e^{2\phi} \equiv \sqrt{\epsilon/\mu}$ and the covariant derivatives are taken using the optical metric (see [30] for details when $J^a = 0$). From now on, we work only with source-free

case, i.e., we assume the current $J^a = 0$ and correspondingly

$$\begin{aligned} \partial_{[a} F_{bc]} &= 0, \\ \bar{\nabla}_b \left(e^{2\phi}\, \bar{F}^{ba} \right) &= 0. \end{aligned} \tag{1.14}$$

The form of the inhomogeneous Maxwell equation is slightly modified and hence slightly more complicated, i.e., the $e^{2\phi}$ term is present in Eq. (1.14); however, the advantage is that there are no constitutive equations (1.2) to deal with, i.e., $\bar{F}^{ab}$ is just F_{ab} raised with the optical metric. Solutions constructed in the optical spacetime via Eq. (1.14) directly translate to solutions in physical spacetime via Eq. (1.9). Because the vacuum Maxwell equations are conformally invariant [5] any metric conformally related to Gordon's can be used to generate H^{ab}, see [30]. In the next section we show that light waves travel along null geodesics at the speed c in the optical spacetime (and hence in any conformally related spacetime), whereas

[5] **Theorem**. The vacuum Maxwell equations are conformally invariant (we will need this fact in Chapter 4). *Proof.* A conformal transformation can be written

$$\begin{aligned} \hat{g}_{ab} &= e^{2\sigma} g_{ab}, \\ \hat{g}^{ab} &= e^{-2\sigma} g^{ab}, \end{aligned} \tag{1.15}$$

where $\sigma(x^a)$ is a scalar function defined on the manifold. Define

$$\begin{aligned} \hat{F}_{ab} &= F_{ab}, \\ \hat{F}^{ab} &= e^{-4\sigma} F^{ab}. \end{aligned} \tag{1.16}$$

The homogeneous Maxwell equation immediately translates into $\hat{F}_{[ab,c]} = 0$ since it is metric independent. The inhomogeneous Maxwell equation tells us

$$\begin{aligned} \nabla_b F^{ab} &= \frac{1}{\sqrt{-g}} (\sqrt{-g} F^{ab})_{,b} = 0 \rightarrow \\ \hat{\nabla}_b \hat{F}^{ab} &= \frac{1}{\sqrt{-\hat{g}}} (\sqrt{-\hat{g}} \hat{F}^{ab})_{,b} = \frac{e^{-4\sigma}}{\sqrt{-g}} (\sqrt{-g} F^{ab})_{,b} = 0, \end{aligned} \tag{1.17}$$

where $\hat{g} \equiv \det \hat{g}_{ab} = e^{8\sigma} g$.

Corollary. The modified (source free, $J^a = 0$) Maxwell Eqs. (1.14) in Gordon's optical spacetime are conformally invariant.

the corresponding waves travel at speed c/n in physical spacetime.

1.2 Geometrical Optics Approximation

In this thesis, we will be using the Geometrical Optics (GO) approximation several times. In this section we illustrate the main procedure for the simplest case, the vacuum Maxwell equations, i.e., electromagnetic waves with no charges, no currents, and no polarizing material. There are some subtle points to make when we use the GO approximation for the modified Maxwell equations in Gordon's optical spacetime, especially for the generalized Gordon's theory including absorption and for the modified Maxwell equations caused by a transverse conformal transformation of the optical metric, etc., but the key ideas are contained in this section.

We assume that the electromagnetic wave is planar on a scale large compared with the wavelength, but small compared with the curvature radius of spacetime. We write the field tensor as

$$F_{ab} = \Re\left\{e^{iS/\lambda}\left(A_{ab} + \frac{\lambda}{i}B_{ab} + O(\lambda^2)\right)\right\}, \tag{1.18}$$

where λ is a wavelength related parameter, $S(x^a)$ is the so-called eikonal function and is real [6], and $\Re\{\cdot\}$ stands for the real part. The A_{ab} term represents the geometrical optics approximation and the B_{ab} term is its first order correction in both the physical and optical spacetimes. We define the wave vector k_a to be the gradient of the eikonal function S, i.e., $k_a = \partial_a S$.

[6] $S(x^a)$ will become complex for the strong absorption case when we include absorption into Gordon's optical metric, see Chapter 3.

Inserting Eq. (1.18) into the vacuum Maxwell equations

$$\begin{aligned} \partial_{[a}F_{bc]} &= 0, \\ \nabla_b F^{ba} &= 0, \end{aligned} \tag{1.19}$$

we obtain for oder λ^{-1}

$$\begin{aligned} A_{[ab}k_{c]} &= 0, \\ A^{ab}k_b &= 0, \end{aligned} \tag{1.20}$$

and order λ^0

$$\begin{aligned} \partial_{[a}A_{bc]} + k_{[a}B_{bc]} &= 0, \\ \nabla_b A^{ab} + B^{ab}k_b &= 0. \end{aligned} \tag{1.21}$$

Now we analyze what these equations tell us.

Contract the first of Eqs. (1.20) with k^c we find

$$k^a k_a = 0, \tag{1.22}$$

and this gives us

$$\dot{k}^a \equiv k^b \nabla_b k^a = 0, \tag{1.23}$$

by using the fact that

$$\nabla_b k_a = \nabla_a k_b. \tag{1.24}$$

Note that we can choose a vector m^a such that $k_a m^a = 1$. Contracting the first of

Eqs. (1.20) with m^c we find

$$A_{ab} = 2k_{[a}\mathcal{E}_{b]},\ \mathcal{E}_a k^a = 0, \tag{1.25}$$

where

$$\mathcal{E}_a = -A_{ab}m^b. \tag{1.26}$$

The nullity condition Eq. (1.22) for k^a and the algebraic structure of A_{ab} [Eq. (1.25)] exhaust the lowest order equations. Now plugging this form of A_{ab} into the first of Eqs. (1.21) we find

$$2A_{[ab}k_{c]} + B_{[ab}k_{c]} = 0 \rightarrow 2A_{ab} + B_{ab} = k_{[a}B_{b]}, \tag{1.27}$$

for some B_b similarly defined. Inserting Eq. (1.25) for A_{ab} and Eq. (1.27) for B_{ab} into the second of Eqs. (1.21) we obtain

$$k^b\nabla_b\mathcal{E}_a + \frac{1}{2}\mathcal{E}_a\nabla_b k^b = \frac{1}{2}k_a(B_b k^b + \nabla_b\mathcal{E}^b). \tag{1.28}$$

One fact we have not made use of is that $\mathcal{E}_a$ defined above can be subject to a gauge like transformation of the form

$$\mathcal{E}_a \rightarrow \mathcal{E}_a + fk_a \tag{1.29}$$

for an arbitrary function f. We use this fact to choose a suitable f to eliminate the right hand side of Eq. (1.28), i.e., we obtain

$$\dot{\mathcal{E}}^a + \theta\mathcal{E}^a = 0, \tag{1.30}$$

where we have defined the expansion parameter (see Sec. 1.5)

$$\theta = \frac{1}{2}\nabla_a k^a. \tag{1.31}$$

Now we split $\mathcal{E}^a$ into a real scalar amplitude $\mathcal{E}$ and a unit polarization vector e_a,

$$\mathcal{E}^a = \mathcal{E} e^a, \tag{1.32}$$

where

$$\mathcal{E} \geq 0,\ e^*_a e^a = 1,\ e_a k^a = 0 \tag{1.33}$$

($*$ is the complex conjugating operator). Now the transport equation for the amplitude $\mathcal{E}$ and the polarization vector e^a becomes

$$\begin{aligned} \dot{\mathcal{E}} + \theta\mathcal{E} &= 0, \\ \dot{e}^a &= 0. \end{aligned} \tag{1.34}$$

Note the remarkable fact that the polarization vector e^a is parallel transported along the null geodesics.

The GO approximation is just the $O(\lambda^0)$ of Eq. (1.18), i.e.,

$$F_{ab} = 2\mathcal{E} \cdot \Re\{e^{iS} k_{[a} e_{b]}\}. \tag{1.35}$$

Inserting the above expression into the energy momentum tensor

$$T^{ab} \equiv -\frac{1}{4\pi}\left[F^{ac}F_{cb} - \frac{1}{4}\delta^a_b F^{dc}F_{cd}\right], \tag{1.36}$$

we obtain

$$T^{ab} = \frac{\mathcal{E}^2}{2} k^a k^b (1 - \Re\{e^{2iS} e_a e^a\}). \tag{1.37}$$

After averaging with time, we finally obtain

$$T^{ab} = \frac{\mathcal{E}^2}{2} k^a k^b. \tag{1.38}$$

Remark (Another WKB derivation). The homogeneous Maxwell equation tells us there exists a vector potential A^a such that $F_{ab} = \partial_a A_b - \partial_b A_a$. We choose a gauge condition $\nabla_a A^a = 0$, and write $A^a = \mathcal{E}^a e^{\frac{i}{\lambda} S}$ where the exponential oscillates much faster than the amplitude E^a changes. We define $k_a = S_{,\,a}$ as before. First we find from the gauge condition that

$$\mathcal{E}^a k_a = 0, \quad \nabla_a \mathcal{E}^a = 0, \tag{1.39}$$

and then from Maxwell's equation

$$k^a k_a = 0, \quad \dot{k}^a = 0, \tag{1.40}$$

and

$$\dot{\mathcal{E}}^a + \theta \mathcal{E}^a = 0, \quad (\mathcal{E}^a)^{;b}{}_{;b} = R^a{}_b \mathcal{E}^b, \tag{1.41}$$

where $R^a{}_b$ is the Ricci tensor. For details, refer to [35].

1.3 Redshift and Distance Definitions

In this section we define a few quantities important in astrophysics and cosmology, such as redshift z, angular diameter distance d_A, and luminosity distance d_L, and we then review a classical result in this field: the reciprocity relation [38, 51, 78, 11, 63].

1.3.1 Redshift

From the results of the GO approximation, we can treat k^a as tangent to light rays. We now think about the frequency of the light ray k^a. With the appropriately chosen affine parameter ξ we can write

$$k^a = \frac{dx^a}{d\xi} = p^a, \tag{1.42}$$

where p^a is the 4-momentum of the photon. For an observer u^a, the energy of the photon is measured as $-k^a u_a$. For two different observers u_1^a and u_2^a, we have the frequency ratio

$$\frac{\nu_1}{\nu_2} = \frac{(k_a u^a)_1}{(k_a u^a)_2}. \tag{1.43}$$

Definition (Redshift). The redshift z of a source S (emitter) measured by an observer O is defined in terms of wavelengths by

$$z = \frac{\lambda_o - \lambda_e}{\lambda_e} = \frac{\Delta\lambda}{\lambda_e}, \tag{1.44}$$

therefore

$$1 + z = \frac{(k_a u^a)_e}{(k_a u^a)_o}. \tag{1.45}$$

Note that the source itself has a 4-velocity u_s^a, and it is not usually at the same spacetime point as the observer u_o^a.

Remark. An useful trick is to split the null vector k^a into its time and spatial part with respect to the observer u^a, i.e., we write

$$k^a = (-u_b k^b)(u^a + \hat{k}^a) \tag{1.46}$$

with $\hat{k}^a$ defined by

$$\hat{k}^a = \frac{g_\perp^{ab} k_b}{g_{\perp cd} k^c k^d}, \tag{1.47}$$

where $g_\perp^{ab}$ is the projection tensor as before. $\hat{k}^a$ satisfies

$$\hat{k}^a u_a = 0, \quad \hat{k}^a \hat{k}_a = 1. \tag{1.48}$$

For a small increment of affine parameter $d\xi$, the observer would see a time elapse Δt and spatial displacement $\Delta \ell$,

$$\begin{aligned} |\Delta t| &\equiv -dx^a u_a = (-k_a u^a) d\xi \\ |\Delta \ell| &\equiv dx^a \hat{k}_a = (-k_a u^a) d\xi, \end{aligned} \tag{1.49}$$

where the photon's displacement along the null geodesic is $dx^a = k^a d\xi$. This will be useful when we talk about the propagating equation of optical scalars, see Sec. 1.5.

1.3.2 Luminosity and Distances

In cosmology, *distance* is not a directly measurable quantity, it has to be defined by theory. In Euclidean geometry, solid angle in 3-space is related to distance and

area by

$$dA = r^2 d\Omega. \tag{1.50}$$

This motivates the definitions of cosmological distances. The *corrected* luminosity distance d'_L is defined by

$$d'_L = \sqrt{\frac{dA_o}{d\Omega_s}}, \tag{1.51}$$

and the angular diameter distance (sometimes called apparent size distance) is defined by

$$d_A = \sqrt{\frac{dA_s}{d\Omega_o}}. \tag{1.52}$$

Theorem. At the same spacetime point, the cross-sectional area of a ray bundle is observer independent.

Proof. Refer to Theorem 4.1 of Sachs [76]. See also discussion in Sec. 1.5.1.

Theorem. For two observers u^a, u'^a at the same point x^a measuring the solid angle subtended by a ray bundle converging at x^a, we have

$$\frac{d\Omega'}{d\Omega} = \frac{(k_a u^a)^2}{(k_a u'^a)^2}. \tag{1.53}$$

Proof. $d\Omega = \Delta A/\Delta\ell^2$. The area ΔA of the beam is the same, but $\Delta\ell \propto (k_a u^a)$.

Theorem (Reciprocity Relation). In any spacetime, the corrected luminosity distance is related to the angular diameter distance by $d'_L = (1+z)d_A$.

Remark. This important result was originally discovered by Etherington in 1933 [38], and rediscovered by Sachs in 1961 [76] and Penrose in 1966 [63] (see also [11]). Its proof is technically demanding. The key geometrical concepts in the following (outlined) proof are the Jacobi field and the Jacobi map [15]. The reciprocity relation is a differential geometrical result which does not depend on

Einstein's general relativity and therefore is more general.

Proof. Near the source event S, the light cone is a 3-dimensional hypersurface with two parameters (e.g., in the rest frame of the source, the spherical polar angles θ, ϕ). We choose an arbitrary smooth 1-parameter subfamily of light rays in this hypersurface. Write the null geodesics as $x^a = f^a(\xi, y)$ where y is the parameter labeling the ray, and ξ the affine parameter along the ray. We fix ξ by requiring that

$$u_s^a k_a = \omega_s \rightarrow \omega_s d\xi = u_a dx^a = \Delta\ell \tag{1.54}$$

for source velocity u_s^a and a fixed angular frequency ω_s. The connecting vector between two neighboring rays can be written as

$$\delta x^a = \frac{\partial f^a}{\partial y}\delta y \tag{1.55}$$

We define the so-called Jacobi field Y^a along the central ray γ of the ray bundle as

$$Y^a = \frac{\partial f^a}{\partial y}, \quad Y^a|_s = 0. \tag{1.56}$$

The standard Jacobi equation (geodesic deviation equation) [15] gives us

$$\ddot{Y}^a = R^a{}_{bcd} k^b k^c Y^d. \tag{1.57}$$

The linearity of the Jacobi equation and the initial conditions $Y^a|_s = 0$ tell us there exists a linear transformation, the so-called Jacobi map $\Lambda^{\hat{a}}{}_f$, such that

$$Y_o^{\hat{a}} = \Lambda^{\hat{a}}{}_f(o, s)\frac{\dot{Y}_s^f}{\omega_s}. \tag{1.58}$$

Note that $\Lambda^{\hat{a}}{}_{f}$ is not a tensor; the hatted indices are with respect to the observer o, and the unhatted indices are with respect to the source event s. Our choice of affine parameter ξ tells us

$$\frac{\dot{Y}^a_s \delta y}{\omega_s} = \frac{DY^a_s \delta y}{\omega_s d\xi} = \frac{\delta x^a}{\delta \ell} = \delta\theta_s \hat{n}^a_s, \tag{1.59}$$

where $\hat{n}^a_s$ is the unit vector pointing along the Jacobi field at source s, and $\delta\theta_s$ is the angular separation between the two rays connected by δx^a. Therefore

$$\delta x^{\hat{a}}_o = \Lambda^{\hat{a}}{}_{f}(o,s) n^f_s \delta\theta_s, \tag{1.60}$$

or equivalently

$$d'_L \equiv \frac{|\delta x^{\hat{a}}|_o}{\delta\theta_s} = n_{\hat{a}}(o)\Lambda^{\hat{a}}{}_{f}(o,s) n^f(s). \tag{1.61}$$

We introduce a Jacobi field Z^a starting from the observer o and evolve it backward towards the source, i.e., $Z^a|_o = 0$. Exchanging the role of source s and observer o, we similarly obtain

$$d_A \equiv \frac{|\delta x^a|_s}{\delta\theta_o} = -n_a(s)\Lambda^{a}{}_{\hat{f}}(s,o) n^{\hat{f}}(o). \tag{1.62}$$

It is easy to show that

$$(Z_a \dot{Y}^a - Y_a \dot{Z}^a) = \text{const}, \tag{1.63}$$

which tells us that

$$Z_a \dot{Y}^a|_s = -Y_a \dot{Z}^a|_o. \tag{1.64}$$

Combining this equation with Eq. (1.58) we obtain

$$g_{ac}(s)\Lambda^{c}{}_{\hat{b}}(s,o)\frac{1}{\omega_o} = -g_{\hat{b}\hat{d}}(o)\Lambda^{\hat{d}}{}_{a}(o,s)\frac{1}{\omega_s}, \tag{1.65}$$

or equivalently

$$n_c(s)\Lambda^{c}{}_{\hat{b}}(s,o)n^{\hat{b}}(o)\frac{1}{\omega_0} = -n_{\hat{d}}(o)\Lambda^{\hat{d}}{}_{a}(o,s)n^{a}(s)\frac{1}{\omega_s}. \tag{1.66}$$

Comparing this equation with Eqs. (1.61) and (1.62) we conclude that

$$d'_L = (1+z)d_A. \tag{1.67}$$

The specific luminosity L_ν of a light source S is defined as the total energy emitted in unit time and unit frequency interval. Suppose the source is radiating spherically symmetrically. The number of photons with frequency ν_s emitted in proper time interval $d\tau_s$ and solid angle element $d\Omega_s$ is

$$N_s = \frac{L_\nu}{4\pi\nu_s}d\tau_s d\Omega_s d\nu_s. \tag{1.68}$$

Suppose this beam of photons is intercepted by an observer using a detector with cross-sectional area dA_o and frequency sensitivity $d\nu_o$. The definition of specific flux F_ν then tells us that the number of photon received is

$$N_o = \frac{F_{\nu_o}}{\nu_o}d\tau_o dA_o d\nu_o. \tag{1.69}$$

Note that the frequency interval is also redshifted. Using the conservation of photon number, $N_o = N_s$, we find

$$F_\nu = \frac{L_{(1+z)\nu}}{4\pi(1+z)d_L'^2}. \tag{1.70}$$

Integrating over all frequencies we get the bolometric flux

$$F \equiv \frac{L}{4\pi d_L^2} = \frac{L}{4\pi(1+z)^2 d_L'^2}. \tag{1.71}$$

This tells us the relation between luminosity distance d_L and corrected luminosity distance d_L' is

$$d_L = (1+z)d_L'. \tag{1.72}$$

This finally gives us the more familiar reciprocity relation

Corollary. In any spacetime, the luminosity distance d_L is related to the angular diameter distance d_A by

$$d_L = (1+z)^2 d_A. \tag{1.73}$$

Remark. The validity of the classical reciprocity relation depends crucially on two facts: first, photons travel along null geodesics in curves spacetime, and secondly, the photon number is conserved. The first assumption will not be true in case where the spacetime is filled with dielectric material, and the second fails when absorption exists. We will discuss this issue in detail later on.

Definition (Magnitudes m and M). Suppose a source radiates spherically symmetrically. Making use of Eq.(1.71), the apparent magnitude m is defined as

$$m \equiv -2.5 \log_{10} \frac{F}{F_{\odot\, 10\,\mathrm{pc}}} + 4.74, \tag{1.74}$$

and the absolute magnitude M is defined as

$$M \equiv -2.5 \log_{10} \frac{L}{L_{\odot}} + 4.74, \tag{1.75}$$

where $F_{\odot}$ and $L_{\odot}$ are respectively the bolometric flux of the sun at 10 pc, and the bolometric luminosity of the sun. The distance modulus μ is defined as

$$\mu = m - M = 5 \log_{10} \frac{d_L}{1\mathrm{Mpc}} + 25. \tag{1.76}$$

1.4 Friedman Equation

The familiar Robertson-Walker (RW) metric can be written

$$ds^2 = -c^2 dt^2 + R^2(t) \left[\frac{dr^2}{1 - kr^2} + r^2 (d\theta^2 + \sin^2 \theta d\phi^2) \right], \tag{1.77}$$

where $k = 1, 0, -1$ for a closed, flat or open universe, respectively. The non-vanishing components of the Ricci tensor of the RW metric Eq. (1.77) is easily found to be

$$\begin{aligned} R_{00} &= -3\frac{\ddot{R}}{R}, \\ R_{11} &= 2k + 2\dot{R}^2 + R\ddot{R}, \end{aligned}$$

$$R_{22} = r^2(2k + 2\dot{R}^2 + R\ddot{R}),$$
$$R_{33} = r^2 \sin^2\theta(2k + 2\dot{R}^2 + R\ddot{R}). \tag{1.78}$$

Inserting the above into the Einstein's equation, we obtain

$$3\frac{\ddot{R}}{R} = -4\pi G(\rho + 3p),$$
$$\frac{\ddot{R}}{R} + 2\frac{\dot{R}^2}{R^2} + 2\frac{k}{R^2} = 4\pi G(\rho - p). \tag{1.79}$$

Canceling the $\ddot{R}/R$ term immediately gives us the Friedman equation

$$\dot{R}^2 + k = \frac{8\pi G}{3}\rho R^2. \tag{1.80}$$

When we integrate the Friedman equation, it is very convenient to cast the equation into one where all quantities are dimensionless [42]. A dimensionless scale factor and time coordinate can be defined by

$$a = \frac{R(t)}{R(t_0)} = \frac{1}{1+z}, \tag{1.81}$$

and

$$\tau = H_0 t, \tag{1.82}$$

where H_0 is the current Hubble constant. We define the critical density $\rho_{\rm cr}$ as

$$\rho_{\rm cr}(t) = \frac{3H^2(t)}{8\pi G}. \tag{1.83}$$

Now the dimensionless density parameter of dust, radiation and vacuum are defined

as

$$\Omega_m = \frac{\rho_m}{\rho_{\rm cr}},\ \Omega_r = \frac{\rho_r}{\rho_{\rm cr}},\ \ \Omega_\Lambda = \frac{\rho_\Lambda}{\rho_{\rm cr}} \tag{1.84}$$

with the total density parameter $\Omega = \Omega_r + \Omega_m + \Omega_\Lambda$. The Friedman equation can be written

$$\Omega(t) - 1 = \frac{c^2 k}{(HR)^2}. \tag{1.85}$$

The rescaled Friedman equation is now

$$\frac{1}{2}\dot{a}^2 + U_{\rm eff}(a) = \frac{1}{2}\Omega_k, \tag{1.86}$$

where the effective potential $U_{\rm eff}$ is defined by

$$U_{\rm eff} = -\frac{1}{2}(\Omega_\Lambda a^2 + \frac{\Omega_m}{a} + \frac{\Omega_r}{a^2}), \tag{1.87}$$

and the curvature density parameter is defined by

$$\Omega_k = -\frac{c^2 k}{H_0^2 R^2(t)} = 1 - \Omega, \tag{1.88}$$

The Hubble parameter $H(z)$ can be immediately found to be

$$H(z) = H_0\sqrt{\Omega_\Lambda + \Omega_k(1+z)^2 + \Omega_m(1+z)^3 + \Omega_r(1+z)^4}, \tag{1.89}$$

and the expansion parameter is

$$\frac{da}{dt} = H_0 a = H_0\sqrt{\frac{\Omega_\Lambda}{(1+z)^2} + \Omega_k + \Omega_m(1+z) + \Omega_r(1+z)^2}. \tag{1.90}$$

Another useful parameter, i.e., the deceleration parameter q_0 is defined as

$$q = -\frac{\ddot{R}R}{\dot{R}^2} = -\frac{\ddot{R}}{R}\frac{1}{H^2} = \Omega_r - \Omega_\Lambda + \frac{1}{2}\Omega_m, \tag{1.91}$$

where we have made use of Eq. (1.79). A Friedman-Lemaître-Robertson-Walker (FLRW) universe is determined by four cosmological parameters $\Omega_m, \Omega_r, \Omega_\Lambda$, and H_0. The density parameters fix the dimensionless Friedman equation, and the Hubble constant fixes the overall scale.

1.4.1 Distance Redshift Relation in RW metric

From Eq. (1.77) we obtain the angular diameter distance d_A of a source at the origin as measured by an observer at co-moving radial coordinate r to be

$$d_A = R(t_e)r, \tag{1.92}$$

and the corrected luminosity distance to be

$$d'_L = R(t_o)r, \tag{1.93}$$

where t_e and t_o correspond to the emission and observation time. The luminosity distance-redshift relation in FLRW universe is then

$$\begin{aligned} d_L(z) &= (1+z)^2 d_A(z) \\ &= (1+z)^2 R(t_e) r \\ &= (1+z)\frac{c}{H_0}\frac{1}{\sqrt{|\Omega_k|}}\text{sinn}\sqrt{|\Omega_k|}\int_0^z \frac{dz'}{h(z')}, \end{aligned} \tag{1.94}$$

where we have defined sinn$[r]$,

$$\text{sinn}[r] \equiv \begin{cases} \sin[r] & \text{k=+1} \\ r & \text{k=0} \\ \sinh[r] & \text{k=-1,} \end{cases} \tag{1.95}$$

the dimensionless Hubble parameter $h(z)$,

$$h(z) = \sqrt{\Omega_\Lambda + \Omega_k(1+z)^2 + \Omega_m(1+z)^3 + \Omega_r(1+z)^4}, \tag{1.96}$$

and where in the last step we have made use of the Friedman equation.

1.5 Geometry of Ray Bundles and Optical Scalars

In this last section of the first chapter we go a little bit deeper into the details than is actually needed for the later part of this thesis[7]. We talk about the geometry of ray bundles, introduce the concept of optical scalars, and derive a few classical equations in this field. The derivation of this section follows closely that of [80] and of [35]. Other important references include Kristian & Sachs [51], Penrose [63], Sachs [76], and Raychadhuri [66, 67].

[7] This review section reminds me of those hard times I sweated blood getting started on general relativity.

1.5.1 Connecting Vectors

We now study rays associated with an eikonal function $S(x^a)$. A bundle of light rays can be parametrized by an affine parameter ξ and 3 other parameters y^i as

$$x^a = f^a(\xi, y^i) \tag{1.97}$$

(in this section indices i and j run through 1, 2 and 3). This parametrization is not unique, i.e., , we can change parametrization by

$$\begin{aligned} y^i &= g^i(\tilde{y}^j), \\ \xi &= \tilde{\xi} + h(\tilde{y}^j), \end{aligned} \tag{1.98}$$

and correspondingly

$$x^a = \tilde{f}^a(\tilde{\xi}, \tilde{y}^j) = f^a(\tilde{\xi} + h(\tilde{y}^j), g^i(\tilde{y}^j)). \tag{1.99}$$

Suppose the central ray of the bundle is labeled by y^i, and a neighboring ray is labeled by $y^i + \delta y^i$. The connecting vector between the two rays (same ξ value) is

$$\delta x^a = \frac{\partial f^a}{\partial y^i} \delta y^i. \tag{1.100}$$

Reparametrization as above gives us

$$\begin{aligned} \delta \tilde{x}^a &= \frac{\partial \tilde{f}^a}{\partial \tilde{y}^i} \delta \tilde{y}^i \\ &= \frac{\partial f^a}{\partial y^i} \delta y^i + k^a \delta h \\ &= \delta x^a + k^a \delta h, \end{aligned} \tag{1.101}$$

where $k_a = \partial_a S$ is the wave vector. We know that two rays connected by δx^a have the same phase iff $k^a \delta x_a = 0$. This property is parametrization independent since $\delta \tilde{x}^a k_a = \delta x^a k_a$ by Eq. (1.101). Suppose an observer with four-velocity u^a sees the light ray at a spacetime point P. A parametrization can be chosen such that all vectors δx^a connecting γ to its neighbors satisfy $\delta x^a u_a = 0$, i.e., they connect events simultaneous with respect to observer u^a. The intersection of the hypersurface of constant $S(x^a)$ with the 3-D space as seen by u^a at P, i.e., the wave surface seen by u^a at that instant, is orthogonal to the ray direction k^a. It consists of photons arriving at observer u^a at P simultaneously. The important point is that this **simultaneity** is true for any observer at P. This observer independence makes it possible to define a **beam** as a collection of such photons. Furthermore, for two rays γ_1, γ_2 (on the same hypersurface of constant S) neighboring to γ, we have

$$g_{ab} \delta \tilde{x}_1^a \delta \tilde{x}_2^b = g_{ab} \delta x_1^a \delta x_2^b. \tag{1.102}$$

This means that the size and shape of the cross-section of an infinitesimal beam at the event P is observer independent. Note that these two invariant properties all come from the key fact that k^a is a null vector, i.e., $k^a k_a = 0$.

1.5.2 Optical Scalars

We find from Eq. (1.100) that

$$\frac{\partial \delta x^a}{\partial \xi} = k^a_{\ ,b} \delta x^b. \tag{1.103}$$

This gives us the transport equation of the connecting vector

$$\dot{\delta x}^a = \frac{D\delta x^a}{d\xi} = k^a{}_{;b}\delta x^b. \tag{1.104}$$

Now we choose parallel transported observers u^a along γ (without any loss of generality because of the observer independence established in the previous section). We next choose a pair of unit vector $e^a_{(A)}$ (A runs through 1 and 2) orthogonal to each other as well to u^a and k^a. We define

$$\varepsilon^a = e^a_{(1)} + ie^a_{(2)}. \tag{1.105}$$

We also parallel transport $e^a_{(A)}$ along γ. We furthermore fix the affine parameter ξ by requiring that

$$k_a u^a = -1 \tag{1.106}$$

everywhere on γ. The complex vector ε^a satisfies algebraic relations

$$u_a\varepsilon^a = k_a\varepsilon^a = \varepsilon_a\varepsilon^a = 0,\ \varepsilon^*_a\varepsilon^a = 2. \tag{1.107}$$

We define the projection tensor P_{ab}, which projects vectors into the 2-D space orthogonal to k^a and u^a, i.e., $\mathrm{span}\{e^a_{(1)}, e^a_{(2)}\}$, as

$$P_{ab} = g_{ab} - k_a k_b + k_a u_b + u_a k_b, \tag{1.108}$$

and is equivalent to

$$P_{ab} = \frac{1}{2}(\varepsilon_a\varepsilon^*_b + \varepsilon^*_a\varepsilon_b). \tag{1.109}$$

We now find

$$\begin{aligned} k_{a;\,b} &= k_{c;\,d}\delta^c_{\ a}\delta^d_{\ b} \\ &= k_{c;\,d}P^c_{\ a}P^d_{\ b} + P_{(a}k_{b)} \\ &= \frac{1}{2}\Re\{\varepsilon_a\varepsilon_b k_{c;\,d}\varepsilon^{*c}\varepsilon^{*d} + \varepsilon_{(a}\varepsilon^*_{b)}k_{c;\,d}\varepsilon^{*c}\varepsilon^d\} + P_{(a}k_{b)} \\ &= \sigma_{ab} + \theta P_{ab} + P_{(a}k_{b)}, \end{aligned} \tag{1.110}$$

where

$$\begin{aligned} P_a &\equiv -2P^c_{\ a}k_{c;\,d}u^d - k_a(u^c k_{c;\,d}u^d), \\ \theta &\equiv \frac{1}{2}k^a_{\ ;\,a}, \\ \sigma &\equiv \frac{1}{2}k_{a;\,b}\varepsilon^{*a}\varepsilon^{*b}, \\ \sigma_{ab} &\equiv \Re(\sigma\varepsilon_a\varepsilon_b). \end{aligned} \tag{1.111}$$

The vector P^a satisfies $P_a k^a = 0$ but is of no interest to us; θ, σ are the well known optical scalars and σ_{ab} is the shear tensor. It can be easily checked that σ_{ab} satisfies

$$\begin{aligned} \sigma^a_{\ a} &= 0, \\ \frac{1}{2}\sigma_{ab}\sigma^{ab} = |\sigma|^2 &= \frac{1}{2}k_{a;\,b}k^{a;\,b} - \frac{1}{4}(k^a_{\ ;\,a})^2. \end{aligned} \tag{1.112}$$

Writing $\delta x^a = \ell\,\hat{n}^a$ with $\hat{n}^a\hat{n}_a = 1$, we find from Eq. (1.104) and Eq. (1.110) that

$$\frac{\dot{\ell}}{\ell} = \theta + \sigma_{ab}\hat{n}^a\hat{n}^b. \tag{1.113}$$

Since the 2-dimensional shear tensor is symmetric and trace free, it has two orthogonal eigen-directions and two eigenvalues $\pm|\sigma|$. Therefore we get the two extreme

rates of stretching

$$\max \frac{\dot{\ell}}{\ell} = \theta + |\sigma|, \ \min \frac{\dot{\ell}}{\ell} = \theta - |\sigma|, \tag{1.114}$$

and the rate of area distortion

$$\frac{\dot{A}}{A} = 2\theta = k^{a}_{\ ;\, a}. \tag{1.115}$$

1.5.3 Transport Equations

We obtain transport equations of optical scalars via the Ricci identity

$$k_{b;\, cd} - k_{b;\, dc} = R_{abcd} k^{a}. \tag{1.116}$$

First, by covariantly differentiating

$$\theta = \frac{1}{2} k^{a}_{\ ;\, a}, \tag{1.117}$$

we obtain

$$\dot{\theta} = -\frac{1}{2} k^{a}_{\ ;\, b} k^{b}_{\ ;\, a} - \frac{1}{2} R_{ab} k^{a} k^{b}. \tag{1.118}$$

With the help of Eq. (1.112) we obtain the transport equation for the expansion scalar θ,

$$\dot{\theta} + \theta^2 + |\sigma|^2 = -\frac{1}{2} R_{ab} k^{a} k^{b}. \tag{1.119}$$

Second, by covariantly differentiating

$$\sigma = \frac{1}{2} k_{a;\, b} \varepsilon^{*a} \varepsilon^{*b}, \tag{1.120}$$

and making use of Ricci identity, we obtain the transport equation of σ

$$\begin{aligned}\dot{\sigma} + 2\theta\sigma &= -\frac{1}{2}R_{abcd}\varepsilon^{*a}\varepsilon^{*c}k^b k^d \\ &= -\frac{1}{2}C_{abcd}\varepsilon^{*a}\varepsilon^{*c}k^b k^d, \end{aligned} \tag{1.121}$$

where C_{abcd} is the Weyl tensor ($R_{abcd} = C_{abcd} + g_{a[c}R_{d]b} - g_{b[c}R_{d]a} - \frac{1}{3}Rg_{a[c}g_{d]b}$). The focusing equation is obtained by rewriting Eq. (1.119) with the help of Eq. (1.115) as

$$\ddot{\sqrt{A}} = -(|\sigma|^2 + \frac{1}{2}R_{ab}k^a k^b)\sqrt{A}. \tag{1.122}$$

Remark. For perfect fluid with non-negative pressure, $T_{ab} = (\rho + p/c^2)u^a u^b - pg^{ab}$, the Ricci term above is

$$\frac{1}{2}R_{ab}k^a k^b = \frac{4\pi G}{c^4}(\rho + p)(u^a k_a)^2 > 0. \tag{1.123}$$

Therefore, Eq. (1.122) implies $\ddot{\sqrt{A}} \leq 0$. Choosing a ray bundle that converges at the observer O, we have $\dot{\sqrt{A}}|_o = \sqrt{\delta\Omega_o}$ (with the appropriately chosen affine parameter ξ). At earlier times, we have $A(\xi) \leq \xi^2\delta\Omega_o$. Thus if shear is introduced into the ray bundle or if matter exists along the beam, the angular diameter distance of the source from the observer is smaller than what would have been if the ray bundles traveled through an empty, shear-free cone. This is the so-called focusing theorem [76, 80].

Chapter 2

Cosmology With a Dark Refraction Index

In this chapter [16] we apply Gordon's optical metric theory to the Friedman-Lemaître-Robertson-Walker cosmologies by associating a refraction index with the cosmic fluid. In Sec. 2.1 we make the geometrical optics approximation of the modified Maxwell's theory in Gordon's optical spacetime. In Sec. 2.2 we discuss the optical metric for the Robertson-Walker metric and derive the refraction-corrected distance-redshift relation. In Sec. 2.3 we discuss the equivalence of the inhomogeneity of the density distribution, e.g., the Sachs-Wolfe effect, with an effective refraction index. We then fit the current supernovae data with our new distance-redshift relation.

2.1 Geometrical Optics Approximation II

Recall that Gordon's optical metric is defined as

$$\bar{g}_{ab} = g_{ab} + (1 - \frac{1}{n^2})u_a u_b, \tag{2.1}$$

with inverse

$$\bar{g}^{ab} = g^{ab} + (1 - n^2)u^a u^b, \tag{2.2}$$

and the modified Maxwell's equations in Gordon's optical spacetime are

$$\begin{aligned} \partial_{[a} F_{bc]} &= 0, \\ \bar{\nabla}_b \left(e^{2\phi}\, \bar{F}^{ba} \right) &= 0, \end{aligned} \tag{2.3}$$

with

$$H^{ab} = \frac{1}{\mu} \bar{F}^{ab}. \tag{2.4}$$

In this section we follow [76] and [31] but use vectors rather than spinors to derive the transport equations for the amplitude and polarization of a geometrical optics wave. As before we write the covariant (and metric independent) field tensor as

$$F_{ab} = \Re \left\{ e^{iS/\lambda\!\!\!^{-}_0} \left(A_{ab} + \frac{\lambda\!\!\!^{-}_0}{i} B_{ab} + O(\lambda\!\!\!^{-2}_0) \right) \right\}. \tag{2.5}$$

Inserting Eq. (2.5) into the modified Maxwell Eqs. (2.3) we obtain to order $\lambda\!\!\!^{-1}_0$

$$\begin{aligned} A_{[ab} k_{c]} &= 0, \\ \bar{A}^{ab} k_b &= 0, \end{aligned} \tag{2.6}$$

and to order $(\lambda\!\!\!^{-}_0)^0$

$$\begin{aligned} \partial_{[a}A_{bc]} + k_{[a}B_{bc]} &= 0, \\ \bar{\nabla}_b\bar{A}^{ab} + \bar{B}^{ab}k_b + 2\bar{A}^{ab}\phi_{,b} &= 0. \end{aligned} \tag{2.7}$$

Remark. Eqs. (2.6) and (2.7) should be compared with Eqs. (1.20) and (1.21) of Chapter 1. The reason for the difference is two fold: First, we are now using optical metric instead of the physical metric. All barred contravariant quantities throughout are obtained by raising indices with the optical metric, e.g., $\bar{A}^{ab} = \bar{g}^{ac}\bar{g}^{bd}A_{cd}$; unbarred are obtained by raising with the physical metric g^{ab}. Second, we now work with the **modified** Maxwell equations.

Equations (2.6) tell us that $\bar{k}^a \equiv \bar{g}^{ab}k_b$ is tangent to null geodesics of the optical metric

$$\begin{aligned} \bar{k}^c k_c &= 0, \\ \bar{k}^b\bar{\nabla}_b\bar{k}^a &= 0, \end{aligned} \tag{2.8}$$

and that A_{ab} is of the form:

$$A_{ab} = -2k_{[a}\mathcal{E}_{b]}, \tag{2.9}$$

where $\mathcal{E}_a$ is spacelike and constrained by $\mathcal{E}_a\bar{k}^a = 0$ but has the remaining freedom of definition $\mathcal{E}_a \to \mathcal{E}_a + f(x)k_a$. It is $\bar{\mathcal{E}}^a$ that determines the amplitude and polarization of the GO wave seen by an observer and it is Eqs. (2.8) that establishes the speed of propagation as c.

Equation (2.7) tells us that

$$B_{ab} = 2(\mathcal{E}_{[a,b]} - k_{[a}\mathcal{D}_{b]}), \tag{2.10}$$

with a remaining freedom $\mathcal{D}_a \to \mathcal{D}_a + g(x)k_a$ and gives as the propagation equation for $\bar{\mathcal{E}}^a$

$$\dot{\bar{\mathcal{E}}}^a + \bar{\mathcal{E}}^a\theta + \bar{\mathcal{E}}^a\dot{\phi} = \frac{\bar{k}^a}{2}(\bar{\nabla}_b\bar{\mathcal{E}}^b + k_b\bar{\mathcal{D}}^b + 2\phi_{,b}\bar{\mathcal{E}}^b). \tag{2.11}$$

The affine parameter derivative symbolized by ' ˙ ' is the invariant derivative $\bar{k}^b\bar{\nabla}_b$ along the null geodesics generated by the vector field $\bar{k}^a$. If we now split $\bar{\mathcal{E}}^a$ into a scalar amplitude and a unit polarization vector, i.e.,

$$\bar{\mathcal{E}}^a = \mathcal{E}\bar{e}^a,\ \mathcal{E} \geq 0,\ \bar{e}^a\bar{e}^*_a = 1, \tag{2.12}$$

where $*$ means complex conjugate, the transport equation for the amplitude $\mathcal{E}$ becomes [this should be compared with Eq. (1.30)]

$$\dot{\mathcal{E}} + \mathcal{E}\theta + \mathcal{E}\dot{\phi} = 0, \tag{2.13}$$

where θ is the expansion rate of the null rays defined by the vector field $\bar{k}^a$. It is defined by the divergence of $\bar{k}^a$

$$\theta \equiv \frac{1}{2}\bar{\nabla}_a\bar{k}^a = \frac{\dot{\sqrt{A}}}{\sqrt{A}}, \tag{2.14}$$

and is related to the fractional rate of change of the observer independent area A of a small beam of neighboring rays (see [76] and discussions in Sec. 1.5.2). Given

A, we are able to integrate Eq. (2.13)

$$\mathcal{E}\left(\frac{\epsilon}{\mu}\right)^{1/4}\sqrt{A} = \mathcal{E}_e\left(\frac{\epsilon_e}{\mu_e}\right)^{1/4}\sqrt{A_e}\ , \tag{2.15}$$

where the subscript e means evaluate at (or close to) the emitter.

For the calculation at hand we need the amplitude $\mathcal{E}$ only, however, if we were interested in the wave's polarization a suitable choice for $f(x)$ makes the right hand side of Eq. (2.11) vanish and also makes $\dot{\bar{e}}^a = 0$, i.e., a particular choice for a polarization vector can be made that is parallel transported along the null geodesics of the GO wave.

The GO approximation is just the $(\lambda\!\!\!^{-}_0)^0$ order term in Eq. (2.5), i.e.,

$$\bar{F}^{ab} = -2\mathcal{E}\,\Re\{e^{iS/\lambda\!\!\!^{-}_0}\bar{k}^{[a}\bar{e}^{b]}\}. \tag{2.16}$$

The frequency and wavelength seen by observers co-moving with the fluid can be computed using the fact that the phase of the wave changes by 2π when the observer ages by one period of the wave τ, or respectively steps a spatial distance of one wavelength λ in the direction of the wave, $\hat{k}^a$,

$$\begin{aligned} 2\pi &= -(c\tau\, u^a)\partial_a\left(\frac{S}{\lambda\!\!\!^{-}_0}\right) = -\frac{c\tau}{\lambda\!\!\!^{-}_0}(u^a k_a), \\ 2\pi &= (\lambda\,\hat{k}^a)\partial_a\left(\frac{S}{\lambda\!\!\!^{-}_0}\right) = -\frac{\lambda}{\lambda\!\!\!^{-}_0}n\,(u^a k_a), \end{aligned} \tag{2.17}$$

where

$$\begin{aligned} \bar{k}^a &= (-\bar{u}_b\bar{k}^b)(\bar{u}^a + \hat{k}^a) \\ &= (-nu_b k^b)(nu^a + \hat{k}^a), \end{aligned} \tag{2.18}$$

and $\hat{k}^a$ is a unit vector in both the physical and the optical metric since $u_a\hat{k}^a = 0$. The natural choice of the constant parameter $\lambda\!\!\!^{-}_0$ is the rationalized wavelength $(\lambda_0/2\pi)$ at the observer. This requires the eikonal satisfy $n_0(k_a u^a)_0 = -1$.

The energy and momentum of this wave as seen by a co-moving observer in physical spacetime ($u^a g_{ab} u^b = -1$) is contained in the Poynting 4-vector

$$\begin{aligned}\mathcal{S}^a &= -c\,T^a_{\ b}u^b \\ &= \frac{c}{4\pi}\left[H^{ac}F_{cb} - \frac{1}{4}\delta^a_b H^{dc}F_{cd}\right]u^b,\end{aligned} \tag{2.19}$$

where all quantities in Eq. (2.19) are evaluated in the physical spacetime. When evaluated using Eqs. (2.4) and (2.16)

$$\begin{aligned}\mathcal{S}^a &= \frac{c}{4\pi\mu}\left[\bar{F}^{ac}F_{cb} - \frac{1}{4}\delta^a_b \bar{F}^{dc}F_{cd}\right]u^b \\ &= -\frac{c}{8\pi\mu}\mathcal{E}^2\bar{k}^a(k_b u^b).\end{aligned} \tag{2.20}$$

In the last equality the oscillations have been averaged over. The energy density and 3-D Poynting vector seen by observer u^a are respectively

$$\begin{aligned}U &= -\frac{1}{c}\mathcal{S}^a u_a = \frac{1}{8\pi\mu}\mathcal{E}^2(\bar{k}^a u_a)(k_b u^b) = \frac{n^2}{8\pi\mu}\mathcal{E}^2(k_a u^a)^2, \\ \mathcal{S}^a_\perp &= \mathcal{S}^a - c\,U u^a = -\frac{c}{8\pi\mu}\mathcal{E}^2(k_b u^b)\left[k^a + (k_c u^c)u^a\right],\end{aligned} \tag{2.21}$$

with magnitude

$$\mathcal{S}_\perp \equiv \sqrt{S^a_\perp \mathcal{S}_{\perp a}} = \frac{cn}{8\pi\mu}\mathcal{E}^2(k_a u^a)^2 = \mathcal{S}_{\perp e}\frac{A_e}{A}\frac{\tau_e^2}{\tau^2}. \tag{2.22}$$

In the last equality we have eliminated the amplitude $\mathcal{E}$ using Eq. (2.15) and con-

tinue using a subscript e to represent quantities evaluated near the emitter. Equation (2.22) simply says that the energy flux varies inversely with the beam's area and inversely with the square of the period, even in the presence of an index of refraction. We will use this expression in the next section to compute the luminosity distance-redshift relation for FLRW cosmologies that are filled with a transparent optical material.

2.2 Optical Metric for Robertson-Walker Spacetimes

As before RW metric is written

$$ds^2 = -c^2\,dt^2 + R^2(t)\left\{\frac{dr^2}{1-kr^2} + r^2(d\theta^2 + \sin^2\theta\,d\phi^2)\right\}, \tag{2.23}$$

where $k = 1, 0, -1$ for a closed, flat or open universe, respectively. The cosmic fluid associated with the RW metric is at rest in the co-moving spatial coordinates (r, θ, ϕ) and hence has a 4-velocity $u^a = \delta^a_t/c$. We assume that the cosmic fluid has associated with it a homogeneous and isotropic refraction index which depends only on the cosmological time t, i.e., $\sqrt{\epsilon\mu} = n(t)$. From Eq. (2.1) only the $\bar{g}_{tt}$ component of the optical metric is seen to differ from the physical metric, i.e.,

$$\bar{g}_{tt} = -\frac{c^2}{n^2(t)}\,. \tag{2.24}$$

The radial null geodesics of the optical metric are found by fixing (θ, ϕ) and integrating

$$d\bar{s}^2 = -\frac{c^2}{n^2(t)}dt^2 + R^2(t)\frac{dr^2}{1-kr^2} = 0. \tag{2.25}$$

Two such geodesics traveling between the origin and a fixed co-moving point r satisfy

$$\int_{t_e}^{t_o} \frac{c\,dt}{n(t)R(t)} = \int_{t_e+\Delta t_e}^{t_o+\Delta t_o} \frac{c\,dt}{n(t)R(t)} = \int_0^r \frac{dr}{\sqrt{1-kr^2}} = \text{sinn}^{-1}[r], \tag{2.26}$$

where sinn$[r]$ was defined in Eq. (1.95). In the above equation, (t_e, t_o) and $(t_e + \Delta t_e, t_o + \Delta t_o)$ represent the emitting and receiving times of the two respective null signals. We see from Eq. (2.26) that the differences in emission and observation times are related by

$$\frac{\Delta t_o}{n(t_o)R(t_o)} = \frac{\Delta t_e}{n(t_e)R(t_e)}, \tag{2.27}$$

and hence the redshift z_n is given by

$$1 + z_n = \frac{\Delta t_o}{\Delta t_e} = \frac{n(t_o)R(t_o)}{n(t_e)R(t_e)} = \frac{n(t_o)}{n(t_e)}(1+z). \tag{2.28}$$

We have used z_n as a measure of the observed frequency change but have also kept the usual z which measures the wavelength change. The tangent to the radial null geodesic ($\bar{k}^a k_a = 0$) can be found directly from Eq. (2.25) by a variation

$$\begin{aligned} \bar{k}^a &= \alpha\left(\frac{n}{c\,R}, \frac{\sqrt{1-kr^2}}{R^2}, 0, 0\right) \\ &= R_0\left(\frac{n}{c\,R}, \frac{\sqrt{1-kr^2}}{R^2}, 0, 0\right), \end{aligned} \tag{2.29}$$

with covariant components

$$k_a = R_0 \left(-\frac{c}{nR}, \frac{1}{\sqrt{1-kr^2}}, 0, 0 \right), \tag{2.30}$$

where α is an arbitrary constant equivalent to the freedom of choosing an affine parameter along a null geodesics, and we fix it to be R_0 (the current radius of the universe) from now on. In the physical metric the light ray has a timelike tangent vector, i.e.,

$$\bar{k}^a g_{ab} \bar{k}^b = n^2(1-n^2)(u_a k^a)^2 = \frac{R_0^2}{R^2}(1-n^2) < 0. \tag{2.31}$$

The eikonal S of the GO approximation Eq. (2.16) can easily be found for this covariant vector field k_a assuming the spherical wave originates from an emitter located at $r = 0$

$$S(t,r) = R_0 \left(-\int_{t_e}^{t} \frac{c\,dt'}{n(t')R(t')} + \text{sinn}^{-1}[r] \right). \tag{2.32}$$

To relate the constant $\lambda\!\!\!^{-}_0$ of Eq. (2.16) to co-moving wavelength, we use Eqs. (2.17) and (2.30)

$$2\pi = -\frac{c\tau}{\lambda\!\!\!^{-}_0}(u^a k_a) = \frac{c\tau(t) R_0}{\lambda\!\!\!^{-}_0 n(t) R(t)} = \frac{\lambda}{\lambda\!\!\!^{-}_0}\frac{R_0}{R(t)}. \tag{2.33}$$

The last equality establishes $\lambda\!\!\!^{-}_0 = \lambda(t_0)/2\pi$ and confirms our interpretation of the conventional $(1+z) = R_0/R_e$ as the wavelength redshift, see Eq. (2.17).

We are interested in computing the apparent-size and luminosity distances for RW models with an index of refraction $n(t)$ and must be careful in doing so. The optical metric gives the correct wave trajectories, but because it does not measure distances or times correctly, densities and rates will be incorrect. Because angles, areas, and redshifts are easier to calculate than energy fluxes we

start with the apparent size distance-redshift $d_A(z_n)$. We will then compute the luminosity distance $d_L(z_n)$ by using the 3-D Poynting vector of Eq. (2.21). We use the optical metric in the form given in Eq. (2.24) with Eq. (2.23) because the coordinates (t, r, θ, ϕ) have direct physical interpretations in the RW metric itself. For an example, in the local rest frame of the source (observer), the proper time interval is Δt_e (respectively Δt_o) instead of $\Delta t_e/n(t_e)$ (respectively $\Delta t_o/n(t_o)$), and hence the observed shift in periods, $\Delta t_o/\Delta t_e$, is correctly given by Eq. (2.28). From Eq. (2.23) the apparent size distance (also called the angular size distance) of a source at coordinates (t_e, r) is just

$$d_A = r\, R(t_e), \tag{2.34}$$

as seen by an observer at $(0, t_o)$ where the three coordinates (r, t_e, t_o) are constrained by Eq. (2.26). To give $d_A(z_n)$ we must use Eqs. (2.26) and (2.28) to eliminate (r, t_e) in terms of (z_n, t_o). We start by using Eq. (2.28) to change variables in the remaining integral of Eq. (2.26) from t to z_n. The following steps are familiar except for the presence of the index of refraction $n(x)$ and the two redshift variables (z_n, z). Friedman Equation is used to change from t to R and then to $(1 + z) = R_o/R$.

$$\begin{aligned} \mathrm{sinn}^{-1}(r) &= \int_{t_e}^{t_o} \frac{cdt}{n(t)R(t)} = \int_{R_e}^{R_0} \frac{cdR}{n(R)R\,(dR/dt)} \\ &= \frac{c}{R_0 H_0} \int_0^{z(z_n)} \frac{dz}{n(z)h(z)}\,, \end{aligned} \tag{2.35}$$

where $h(z)$ is the dimensionless Hubble parameter. The wavelength redshift $z(z_n)$ as a function of the frequency redshift z_n is found by eliminating t_e in Eq. (2.28).

From Eq. (2.34) we conclude that the apparent size distance-redshift relation for a FLRW cosmology with an index of refraction is

$$d_A(z_n) = \frac{1}{(1+z(z_n))}\frac{c}{H_0}\frac{1}{\sqrt{|\Omega_k|}}\text{sinn}\left[\sqrt{|\Omega_k|}\int_0^{z(z_n)}\frac{dz}{n(z)h(z)}\right]. \tag{2.36}$$

To derive the luminosity-redshift relation $d_L(z_n)$ knowing $d_A(z_n)$ one ordinarily uses Etherington's (see [38] and Sec. 1.3) result

$$d_L(z) = (1+z)^2 d_A(z). \tag{2.37}$$

If this result were correct with an index of refraction present, one would need to know which redshift to use, frequency z_n or wavelength z. To know what to choose we evaluate the magnitude of the Poynting vector Eq. (2.22) and arrive at the correct replacement for Eq. (2.37). To find the needed area A we evaluate the expansion θ of Eq. (2.14) using Eqs. (2.29), (2.23), (2.24), and (1.8). We find a simple result

$$\theta = \frac{(\dot{rR})}{(rR)}, \tag{2.38}$$

and hence the beam area $A \propto rR$ from which we have the needed Poynting vector magnitude, Eq. (2.22),

$$\mathcal{S}_\perp = \mathcal{S}_{\perp e}\frac{4\pi(rR)_e^2}{4\pi(rR)^2}\frac{\tau_e^2}{\tau^2} = \frac{L_e}{4\pi(rR)^2(1+z_n)^2} = \frac{L_e}{4\pi d_L^2}. \tag{2.39}$$

The latter identity defines the luminosity distance d_L in terms of the total power radiated at the emitter L_e and the flux received, i.e., the Poynting vector at the

observer,

$$\begin{aligned} d_L &= rR(1+z_n) \\ &= rR_e(1+z)(1+z_n) \\ &= (1+z_n)\frac{c}{H_0}\frac{1}{\sqrt{|\Omega_k|}}\text{sinn}\left[\sqrt{|\Omega_k|}\int_0^{z(z_n)}\frac{dz}{n(z)h(z)}\right], \end{aligned} \tag{2.40}$$

which agrees with the Etherington result Eq. (2.37) only if we use one frequency redshift factor $(1+z_n)$ from Eq. (2.28) and one wavelength redshift $(1+z)$. Equation (2.39) also confirms a conserved photon number interpretation of the radiation even in the presence of a time dependent index of refraction (which has the potential of taking energy out of the radiation field). It is equivalent to having a fixed number of photons emitted in a time Δt_e each having energy $h\nu_e$ and all being collected over an area $4\pi(rR)^2$ in a time Δt_o but with redshifted energy $h\nu_o$.

2.3 An Effective Index of Refraction Induced by the Sachs-Wolfe Effect

Up to now, we have been considering a refractive index modeled after the one generated by induced electromagnetic polarizations in inter and intra galactic media, dark or otherwise. Lensing has long been interpreted as a gravitationally induced refraction effect, and here we suggest that to 1^{st} order, inhomogeneities in the flat FLRW models are equivalent to effective indices of refraction.

Sachs & Wolfe [77] were two of the first to consider the effect of perturbations of the homogeneous and isotropic models on optical observations. In that classic paper, the authors used perturbations in the flat, i.e., $k = 0$, FLRW spacetime

to study the angular fluctuations in the Cosmic Microwave Background (CMB). They used a conformally flat version of the metric

$$ds^2 = R^2(\eta)\,[\eta_{ab} + h_{ab}]\,dx^a dx^b \tag{2.41}$$

with dimensionless coordinates and worked in a co-moving gauge to derive the equations governing the evolution of the metric perturbation h_{ab} and perturbations of the energy-momentum tensor δT_{ab}. Here the conformal time coordinate of the flat Minkowski metric $\eta_{ab} = \mathrm{diag}\,[-1, 1, 1, 1]$ is $x^0 = \eta$ and for the pressureless case is familiarly related to the co-moving FLRW time coordinate t by $\eta = (3\,tH_0/2)^{1/3}$. The three Euclidean spatial coordinates are labeled by letters of the Greek alphabet. They then considered the deviations of null geodesics from the unperturbed case and derived the now famous temperature fluctuations in the microwave background caused by h_{ab}, see Eq. (42) of Ref. [77]. Among the scalar, vector, and tensor perturbation modes in dust ($p = \delta p = 0$, see Eq. (22) of Ref. [77]), the scalar density perturbations, i.e., the relatively decreasing $A(x^\gamma)$ mode and relatively increasing $B(x^\gamma)$ mode (responsible for the famous Sachs-Wolfe effect) give

$$h_{\alpha\beta} = -\frac{1}{\eta^3}A_{,\alpha\beta} + \delta_{\alpha\beta}B + \frac{\eta^2}{10}B_{,\alpha\beta}\,, \tag{2.42}$$

and $h_{0a} = 0$. The arbitrarily specified form of the scalar modes are related to the density perturbation $\delta\rho$ through Poisson's equation

$$\delta\rho = \frac{H_0^2}{32\pi G}\nabla^2\left(\frac{6A}{\eta^9} - \frac{3B}{5\eta^4}\right), \tag{2.43}$$

(See Eq. (22) of Ref. [76]).

Remark. The time component of the perturbation h_{00} vanishes because of a co-moving gauge choice ($u^a \propto \delta^a_0$) and $h_{0\alpha}$ is only present for the rotational perturbations.

To connect this perturbed metric to Gordon's optical metric, we attempt a coordinate transformation ($x^a \to x'^a$, and $g_{ab} \to g'_{ab}$) as following

$$\begin{aligned} \eta &= \eta' - D(x'^b), \\ x^\alpha &= x'^\alpha - C^\alpha(x'^b), \end{aligned} \tag{2.44}$$

where $D(x'^a)$ and $C^\alpha(x'^a)$ are functions to be determined. First, from $g'_{0\alpha} = 0$ we found

$$\frac{\partial D}{\partial x'^\alpha} = \frac{\partial C^\alpha}{\partial \eta'}, \text{ for } \alpha = 1, 2, 3. \tag{2.45}$$

Second, from

$$\begin{aligned} g'_{\alpha\beta} &= R^2(\eta)[\delta_{\alpha\beta} + h_{\alpha\beta} + \frac{\partial C^\alpha}{\partial x'^\beta} + \frac{\partial C^\beta}{\partial x'^\alpha}] \\ &= R^2(\eta)[(1+B)\delta_{\alpha\beta} - \frac{A_{,\alpha\beta}}{\eta^3} + \frac{\eta^2}{10}B_{,\alpha\beta} - C^\alpha{}_{,\beta} - C^\beta{}_{,\alpha}] \\ &= R^2(\eta)(1+B)\delta_{\alpha\beta}, \end{aligned} \tag{2.46}$$

we obtain

$$\begin{aligned} C^\alpha &= -\frac{1}{2}\frac{A_{,\alpha}}{\eta'^3} + \frac{1}{20}\eta'^2 B_{,\alpha}, \\ D &= \frac{3}{2}\frac{A}{\eta'^4} + \frac{1}{10}\eta' B. \end{aligned} \tag{2.47}$$

Since for the flat dust only case, $R(\eta) = \frac{2}{H_0}\eta^2$ (H_0 is the Hubble parameter right

now, see[77]) we found

$$R(\eta) = R(\eta')\left(1 - \frac{D}{\eta'}\right)^2 = R(\eta')\left(1 - \frac{3}{2}\frac{A}{\eta'^5} - \frac{1}{10}B\right)^2. \quad (2.48)$$

Now we have

$$g'_{00} = -R^2(\eta)\left(1 - 2\frac{\partial D}{\partial \eta'}\right) = -R^2(\eta)(1 + \frac{12}{\eta'^5}A - \frac{1}{5}B), \quad (2.49)$$

$$g'_{\alpha\beta} = R^2(\eta)(1 + B)\delta_{\alpha\beta}, \quad (2.50)$$

and the new perturbed metric after the coordinate transformation

$$x^\alpha = x'^\alpha + \frac{1}{2\eta'^3}A_{,\alpha}(x') - \frac{\eta'^2}{20}B_{,\alpha}(x'),$$
$$\eta = \eta'\left(1 - \frac{3}{2\eta'^5}A(x') - \frac{1}{10}B(x')\right), \quad (2.51)$$

to be (up to 1^{st} order)

$$ds^2 = R^2(\eta')\left(1 - \frac{3}{\eta'^5}A(x') + \frac{3}{10}B(x')\right)^2 \times \left\{-\frac{d\eta'^2}{\left(1 - \frac{6}{\eta'^5}A(x') + \frac{3}{5}B(x')\right)^2} + dr'^2 + r'^2(d\theta^2 + \sin^2\theta d\phi^2)\right\}. \quad (2.52)$$

This simply says that the Sachs-Wolfe metric is a conformally transformed Gordon metric corresponding to a k=0, FLRW metric with a spacetime index of refraction $n = 1 - 6A(x')/\eta'^5 + 3B(x')/5$. Since conformal transformations don't alter light

cones (see [30]) we have arrived at the connection of null geodesics of Sachs-Wolfe's density perturbations with the light curves of an unperturbed FLRW spacetime possessing an index of refraction. In contrast to the homogeneous optical fluid discussed in Section 2.2, the co-moving frame of the index of refraction in Eq. (2.52) is not the same as the co-moving frame of the matter density in Eq. (2.41). However, they are related by the coordinate change of Eq. (2.51).

We have our doubts about extending the index of refraction comparison beyond linear perturbations, and make no claims as to that possibility. Such an extension would be quite interesting because old work [47, 48] on non-linear observational effects in Swiss Cheese cosmologies are again in the literature [57, 58, 60, 13] also hoping to find sources of apparent acceleration other than a cosmological constant. Work on interpreting effects of local density perturbations on the Hubble curve are numerous [24, 79, 21, 4, 5, 90, 22, 73, 50], the results of which can be compared to the above in the 1^{st} order regime.

2.4 Fitting Supernova Data With A Refraction Index Model

In this section we use the index of refraction model of Section 2.2 to fit the current supernova data [6, 28, 71, 72, 91]. We use the 178 supernova from the gold sample [1] with redshifts greater than $cz = 7000\,\mathrm{km/s}$ to avoid the so-called Hubble bubble [24, 96] , see Fig. 2.1. The Hubble constant we use is $H_0 = 65$ km/s/Mpc and since we are concerned with the matter dominated era, we exclude radiation ($\Omega_r = 0$). We compare the distance modulus versus redshift, $\mu(z)$, of the concordance model,

[1] http://braeburn.pha.jhu.edu/∼ariess/R06/.

$\Omega_\Lambda = 0.7$, $\Omega_m = 0.3$, $n = 1$ with two $n(z) > 1$ models. The first is a baryonic matter only model ($\Omega_m = 0.04$) and no cosmological constant ($\Omega_\Lambda = 0$) with $n(z) = 1 + 0.1z^2 - 0.045z^3$. The second model includes a dark matter contribution, $\Omega_m = 0.3$, no cosmological constant, and $n(z) = 1 + 0.15z^2 - 0.05z^3$. Also included is a now disfavored dark matter only model, $\Omega_\Lambda = 0$, $\Omega_m = 0.3$, $n = 1$. In the inset of Fig. 2.1, we use this case to compare with the two $n \neq 1$ models and with the concordance model. The critical redshift region is between $0.2 < z < 1.2$, where most of the supernova data is concentrated. Both $n \neq 1$ models fit the data much better in this region than models with the same Ω parameters but with no refraction. The two refraction indices are plotted in the insets of Fig. 2.2. It can be easily seen that the effects of a suitable index of refraction $n(z)$ can simulate the accelerating effects of a cosmological constant.

The Supernova data is currently considered the best evidence for the existence of dark energy because of the observed acceleration in the expansion of the universe (see Fig. 7 of Ref. [72]). For the homogeneous FLRW models, the acceleration is directly related to density and pressure by

$$\frac{\ddot{R}}{R} = -\frac{4\pi G}{3}(\rho + 3\frac{p}{c^2}). \tag{2.53}$$

A true observed acceleration, i.e., $\ddot{R} > 0$, requires $p < -\rho c^2/3$, and hence implies an unusual equation of state such as vacuum energy ($p = -\rho c^2$). What we show here is that an overlooked index of refraction can cause a misinterpretation of the Hubble curve, suggesting an acceleration. In Fig. 2.2 we plot $H(z)$ and $\dot{R}(z)/R_o = H(z)/(1+z)$ for the two $n \neq 1$ models. They can be compared with similar plots in Ref. [72]. The data points are plotted using flux averaging [92, 93] and uncorrelated

redshift binning [94] algorithms. To apply these techniques to non-flat cases, we define

$$g(z_n) \equiv \int_0^{z(z_n)} \frac{dz}{n(z)h(z)} = \frac{1}{\sqrt{|\Omega_k|}} \text{sinn}^{-1}\left[\frac{\sqrt{|\Omega_k|}}{1+z_n}\frac{H_0}{c}10^{\frac{\mu}{5}-5}\right], \tag{2.54}$$

where μ is the distance modulus defined as before and where we have made use of Eq. (2.40). We furthermore defined

$$x_i = \frac{g(z_n^{i+1}) - g(z_n^i)}{z^{i+1}(z_n^{i+1}) - z^i(z_n^i)}, \tag{2.55}$$

which when averaged inside each bin gives us an estimate of the inverse of the product of $n(z)$ with $h(z) \equiv H(z)/H_0$ (compare with Eq. (5) of Ref. [94]). The presence of an index of refraction produces a degeneracy in determining the value of $H(z)$ and hence in $\ddot{R}(t)$. A suitably decreasing $n(t)$ and a non-accelerating $R(t)$ will mimic an accelerating universe.

We can see that our index of refraction models fit the data well. However, we need to remind the reader that the binned data plotted on the $H(z)$ and $\dot{R}(z)/R_0$ curves are model dependent. The binning process as designed in Ref. [94] requires use of $d_L(x_n)$, i.e., $g(z_n)$ in Eq. (2.54). Rather than using this technique to argue for an observed accelerating $H(z)$, we argue for an observed $n(z)$ with a non-accelerating $H(z)$. The point we make is that we can fit the $\mu(z)$ data with no Λ, and are able to get rid of the acceleration.

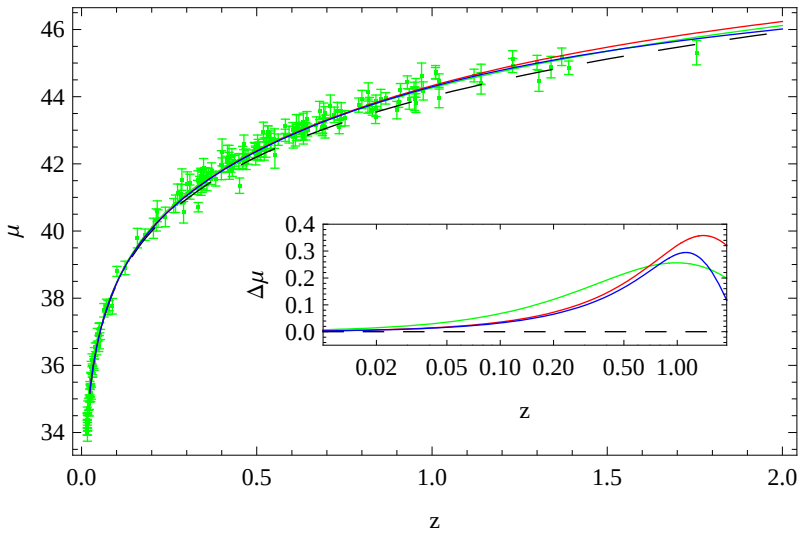

Figure 2.1: Distance modulus μ versus redshift z. Dashed curve: $\Omega_\Lambda = 0, \Omega_m = 0.3, n = 1$; Green curve: $\Omega_\Lambda = 0.7,\ \Omega_m = 0.3,\ n = 1$; Red curve: $\Omega_\Lambda = 0,\ \Omega_m = 0.04,\ n(z) = 1+0.1z^2-0.045z^3$; Blue curve: $\Omega_\Lambda = 0, \Omega_m = 0.3, n(z) = 1+0.15z^2-0.05z^3$. $\Delta\mu(z)$ are given in the inset. The difference is taken with respect to the fiducial case where $\Omega_\Lambda = 0, \Omega_m = 0.3, n = 1$.

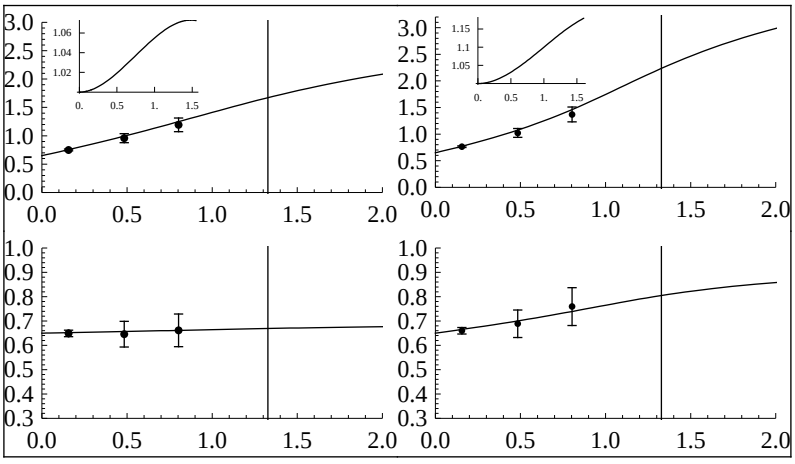

Figure 2.2: $H(z)$ (upper panel) and $\dot{R}(z)/R_o$ (lower panel) curves for the two $n \neq 1$ models. Left column parameters: $\Omega_\Lambda = 0,\ \Omega_m = 0.04,\ n(z) = 1 + 0.1z^2 - 0.045z^3$; Right column parameters: $\Omega_\Lambda = 0,\ \Omega_m = 0.3,\ n(z) = 1 + 0.15z^2 - 0.05z^3$.

2.5 Flatness of the Universe

The conclusion drawn from the latest Wilkinson Microwave Anisotropy Probe (WMAP) data, when combined with the SNe Ia Hubble curve, that vacuum energy exists, depends crucially on many unconfirmed theoretical assumptions including the adiabatic power law assumption for the initial perturbation spectrum [84, 85]. Such observations have motivated efforts to find ways to produce a perceived acceleration other than by a real Λ [4, 5, 21, 22, 24, 50, 79, 73, 90]. This section is another such effort.

The angular position of the first acoustic peak is commonly believed to be the strongest piece of evidence for the flatness of the universe. The characteristic wavelengths of the acoustic oscillations at the last scattering surface depend very weakly on Λ, but their observed angular size as seen by us now depends significantly on a combination of Ω_m and Ω_Λ, see Eq. (2.36). Assuming our Universe is of the FLRW type with no refraction index, a first acoustic peak at $\sim 0.8^o$ is almost fit by a flat universe.[2] With a suitable index of refraction and no cosmological constant we can produce an angular diameter distance comparable to the angular diameter distance of a flat cosmology at any given redshift, independent of the Hubble parameter H_0. In Fig. 2.3 we have used a $\Omega_\Lambda = 0$, $\Omega_m = 0.3$ model with an index of refraction $n(z)$ shown in the inset. We chose this $n(z)$ because it produces similar distances over the large redshift range $z > 1000$. To conclude

[2]Within the context of a power law ΛCDM model ($w = 1$), WMAP data alone does not rule out non-flat models. With a prior on the Hubble constant, $H_0 > 40\,\mathrm{kms}^{-1}\mathrm{Mpc}^{-1}$, or combined with other astronomical observations, such as SDSS LRG sample, HST constraint on the Hubble constant, or SNe data, WMAP data strongly favors a nearly flat universe with nonzero vacuum energy, see Table 12, Fig. 20, and Fig. 21 of [85]. For a more general model of dark energy, e.g., one with a time evolving equation of state parameter $w \neq 1$ instead of a cosmological constant Λ, significant spatial curvature is still allowed even under the above prior on the Hubble constant, see e.g. [44, 45].

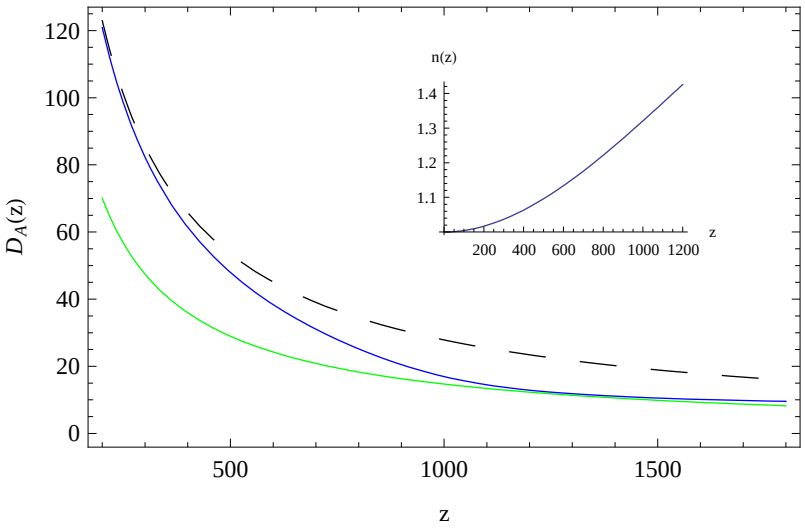

Figure 2.3: Dashed curve: $\Omega_\Lambda = 0, \Omega_m = 0.3, n(z) = 1$; Blue Curve: $\Omega_\Lambda = 0, \Omega_m = 0.3, n(z) = 1+4.45\times10^{-7}z^2-1.25\times10^{-10}z^3$; Green curve: $\Omega_\Lambda = 0.7, \Omega_m = 0.3, n = 1$.

that WMAP implies flatness requires the acceptance of the accuracy of theoretical assumptions beyond the initial perturbation spectrum; e.g., even the accuracy of the optics of homogeneous FLRW models is now being questioned as was pointed out in Section 2.3.

2.6 Discussion

In this chapter we applied Gordon's theory to the homogeneous, $\Lambda = 0$, FLRW models, derived the **Refraction**-corrected distance-redshift relation, and then estimated the refraction index needed to fit current SNe Ia and WMAP data. We found that an $n(z) \approx 1.07$ at redshift $z = 1.5$ in a baryon only model, or an $n(z) \approx 1.15$ at $z = 1.5$ in a dark matter model, could easily fit the supernova data (see Fig. 2.1, and Fig. 2.2), and that an $n(z)$ as big as 1.3 at the last scattering surface in a dark matter model would give the same angular diameter distance

$d_A(z)$ as the concordance model (see Fig. 2.3).

The question is, where could such an index of refraction come from? If it had its origin in atomic dipole moments or charges in plasmas the densities would have to be much larger than they actually are. A critical mass density now is about $8 \times 10^{-30}\,\mathrm{g \cdot cm^{-3}}$, which translates to $1 \times 10^{-20}\,\mathrm{g \cdot cm^{-3}}$ at $z = 1100$. The density of air on the earth is about $1.2 \times 10^{-3}\,\mathrm{g \cdot cm^{-3}}$, some 10^{17} times denser than the universe at recombination and yet its index of refraction is only $n = 1.0003$. We conclude that there is little hope for a baryon-lepton origin for n. A long shot would be a colorless index of refraction for the mysterious dark matter (see e.g. [39]).

Severe limits have already been estimated on direct interactions of the dark matter particles with photons caused by fractional charge [87, 27] ($q/e < 10^{-5} - 10^{-7}$ depending on the particle's mass) and by electric/magnetic dipole moments [83] (dipole moment $< 3 \times 10^{-16} e\,\mathrm{cm}$). General limits on photon interaction rates have even been estimated by requiring the associated collisional damping scale be small enough to allow structures larger than 100 kpc to form [14]. [39] recently proposed the idea of probing dark matter by investigating the frequency dependence of its refraction index. Proposing an n of unknown source is perhaps outlandish, but not much more than proposing a non-intuitive repulsive cosmological constant Λ to produce acceleration. Even though the latter has become fashionable, we wish to add a dark index of refraction theory to the community to think about.

In this chapter we developed the general framework needed for using Gordon's optical metric in cosmological observations, but have applied it only to an index of refraction model which is homogeneous and isotropic. If the dark matter and it's assumed index of refraction were truly homogeneous we could have addi-

tionally proposed a redshift dependence for $n(z)$ modeled after a dilute dielectric gas or plasma. However, such a model would still contain unknowns equivalent to ionization densities and/or molecular polarizabilities. Instead we chose a phenomenological expression in the form of a cubic containing two parameters which we adjusted (i.e., $n(z) = 1 + p * z^2 + q * z^3$). Such a simple starting point is prudent because we know the real universe is filled with low density voids, and high density condensations, as well as associated velocity perturbations all of which would modify the refraction index $n(x^a)$. If an index of refraction model such as the one proposed here has merit, future efforts can look into how such perturbations, including local variations in the magnetic field of the intergalactic medium, might impact distance-redshift. However, the optical metric theory Eq. (2.1) is still the applicable theory. We talked about the effective refraction index induced by Sachs-Wolfe effect, but have not gone very far. One reason is that the original formalism in [77] works only for flat models, whereas the more interesting case is one where the universe is open, i.e., $\Omega_m < 1, \Omega_\Lambda = 0$. Further exploration of the equivalence of the optical effects of gravitational inhomogeneities (beyond the linear perturbation results of Sachs-Wolfe in Section 2.3) and our index of refraction proposal is desirable. Complete equivalence would be quite interesting and useful in light of the current interest in Swiss Cheese optics [13, 47, 48, 57, 58, 60]. Modifications in distance-redshift caused by random spacetime perturbations could then be interpreted as being caused by an effective index of refraction. The idea of an optical metric can also be applied to other massless particles which follow null geodesics in vacuum. If the presence of material causes interference of the propagating waves of the particles, an effective refraction index should exist. For an example, gravitons and some neutrinos are massless and local inhomogeneities, such as the Sachs-Wolfe

perturbations discussed in Section 2.3, would alter propagation of their waves [97].

The idea of solving cosmological problems via a changing light speed model is not new, see [3, 7, 8]. Ellis [36] has recently pointed out consistency constraints required of such theories. Our proposal is fundamentally different from those cited above in that it is based on a classical electrodynamics analogy (the cosmological fluid simply has an unexpected refraction index which reduces the propagation speed of electromagnetic waves). Because we are not proposing a change in the vacuum light speed c or the limiting causal speed, the proposal is not subject to Ellis's criticism.

Finally we note that since an accelerating universe is consistent with other observations, such as Baryon Acoustic Peaks detected in galaxy surveys [34, 88, 89] and the interesting $H(z)$ relation obtained from ages of passively evolving galaxies in [82], additional comparisons with refraction models are in order.

In the next chapter, we will generalize Gordon's optical metric to include absorption by allowing the metric to become complex. We then derive the **Absorption & Refraction**-corrected distance-redshift relation in FLRW cosmology, and fit the same set of supernova data with our new distance-redshift relation.

Chapter 3

Complex Optical Metric

In this chapter [17] we show that Gordon's optical metric on a curved spacetime can be generalized to include absorption by allowing the metric to become complex. We demonstrate its use in the realm of geometrical optics by giving three simple examples. We use one of these examples to compute corrected distance-redshift relations for Friedman-Lemaître-Robertson-Walker models in which the cosmic fluid has an associated complex index of refraction that represents grey extinction. We then fit this corrected Hubble curve to the same set of type Ia supernovae data as used in Chapter 2.

3.1 Introduction

We assume that at some given frequency range the fluid's electromagnetic properties are linear and isotropic relative to the fluids unit 4-velocity $u_a u^a = -1$, and can be summarized by a **complex** permittivity $\epsilon(x^a)$ and a **complex** permeability $\mu(x^a)$ defined on the four dimensional spacetime manifold. Following [53] we write

a complex refraction index $N(x^a)$ as

$$N = \sqrt{\epsilon\mu} \equiv n + i\kappa, \tag{3.1}$$

where n and κ are respectively the real and imaginary parts. The real electric field/magnetic induction bivector $F_{ab}(E, B) = \Re\{F_{ab}^{\lambda\!\!\!^{-}_0}\}$ that represents a traveling monochromatic wave has a geometrical optics expansion of the form

$$F_{ab}^{\lambda\!\!\!^{-}_0} = e^{iS/\lambda\!\!\!^{-}_0} \left(A_{ab} + \frac{\lambda\!\!\!^{-}_0}{i} B_{ab} + O(\lambda\!\!\!^{-}_0{}^2) \right), \tag{3.2}$$

and satisfies the homogeneous Maxwell equation

$$\partial_{[a} F_{bc]}^{\lambda\!\!\!^{-}_0} = 0, \tag{3.3}$$

in both the physical and optical spacetimes. We designate the constant expansion parameter of geometrical optics by $\lambda\!\!\!^{-}_0$ because we use its value to fix the wave's wavelength. It's positioning as a superscript or subscript is for convenience only. The real part of $S(x^a)$ is the usual eikonal function which determines the surfaces of constant phase for the wave. The A_{ab} term represents the usual amplitude of the geometrical optics approximation and the B_{ab} term is its first order correction. The constitutive relations for the contravariant components of the real displacement/magnetic field bivector in physical spacetime $H^{ab}(D, H) = \Re\{H_{\lambda\!\!\!^{-}_0}^{ab}\}$ are given by

$$H_{\lambda\!\!\!^{-}_0}^{ab} = \frac{1}{\mu} \bar{F}_{\lambda\!\!\!^{-}_0}^{ab}, \tag{3.4}$$

where the optical metric $\bar{g}_{ab}$ of [41] (which now becomes complex) has been used to raise the covariant indices of $F^{\lambda_0}_{ab}$ to produce $\bar{F}^{ab}_{\lambda_0}$. The complex optical metric is related to the real physical metric $g_{ab} = -u_a u_b + g_{\perp\, ab}$ by

$$\bar{g}_{ab} \equiv (1 - \frac{1}{\epsilon\mu})u_a u_b + g_{ab} = -\frac{1}{N^2}u_a u_b + g_{\perp\, ab}, \tag{3.5}$$

with inverse

$$\bar{g}^{ab} = (1 - \epsilon\mu)u^a u^b + g^{ab} = -N^2 u^a u^b + g^{ab}_{\perp}. \tag{3.6}$$

The familiar source-free inhomogeneous Maxwell Equations in physical spacetime remain

$$\nabla_b H^{ba}_{\lambda_0} = 0. \tag{3.7}$$

The more familiar form of the constitutive relations

$$\begin{aligned} H^{ab}_{\lambda_0} u_b &= \epsilon F^{ab}_{\lambda_0} u_b, \\ F^{\lambda_0}_{[ab} u_{c]} &= \mu H^{\lambda_0}_{[ab} u_{c]}, \end{aligned} \tag{3.8}$$

have been replaced in Eq. (3.4) by an equivalent single equation using Gordon's metric. Just as with a real optical metric (see [30, 31, 41, 16, 17]), the source-free inhomogeneous Maxwell equation (3.7) can be rewritten as

$$\bar{\nabla}_b \left(\sqrt{\epsilon/\mu}\ \bar{F}^{ba}_{\lambda_0} \right) = 0. \tag{3.9}$$

The covariant derivative in Eq. (3.9) is with respect to the complex optical metric, and except for the reciprocal of the impedance, $Z^{-1} = \sqrt{\epsilon/\mu}$, would be the same as Maxwell's vacuum inhomogeneous equations in the optical spacetime but with-

out polarizable materials, i.e., the components of $\bar{F}^{ba}_{\lambda_0}$ were obtained in Eq. (3.4) by simply raising indices on $F^{\lambda_0}_{ab}$ using the optical metric. Because ϵ and μ are ordinarily wavelength dependent, the values of N and Z at a spacetime point depend on the particular geometrical optics wave being considered.

To proceed further with the geometrical optics approximation we must make assumptions about the size of the imaginary part, κ, of the index of refraction in Eq. (3.1) at the frequency of interest. We will consider two types: for the first type the imaginary part κ is not small compared to the real part n (at the wavelengths of interest) and for the second type it is, i.e., $\kappa << n$. The first type includes the absorption of low frequency waves in a conductor as well as the absorption of microwaves by water. The second includes a case of interest to us, the extinction of light waves traveling in a dilute gas. In the first case the eikonal S in Eq. (3.2) has an imaginary part which is not negligible compared to the real part (see Sec. 3.2) and in the second type, S can be taken as real (see Sec. 3.3). In Sec. 3.2 we include two complex eikonal examples and in Sec. 3.3 we give one real example which we then use to evaluate distance-redshift in standard cosmologies when absorption is present. Because much of the algebra of the second type is included in the first we start with a complex S.

3.2 A Complex Eikonal

In this section we develop the geometrical optics approximation for waves traveling in a medium where absorption on the scale of a wavelength cannot be neglected. Such significant absorption requires the use of a complex eikonal. By inserting

Eq. (3.2) into Maxwell's Eqs. (3.3) and (3.9) we find that A_{ab} is of the form

$$A_{ab} = -2k_{[a}\mathcal{E}_{b]}, \tag{3.10}$$

where $k_a \equiv \partial_a S$ is a complex null vector of the optical metric ($\bar{k}^a k_a = 0$) satisfying a complex geodesic like equation $\dot{\bar{k}}^a = 0$ in the optical spacetime. In general, the invariant derivative '$\cdot$' is defined by

$$\dot{} \equiv \bar{k}^b \bar{\nabla}_b, \tag{3.11}$$

and rather than being a directional derivative as it is when the metric is real, it becomes a complex partial differential operator.

Because we are interested in "homogeneous" waves, i.e., those for which the surfaces of constant phase and constant amplitude coincide [53], we require that the spatial part of $\bar{k}^a$, i.e., the part of $\bar{k}^a$ which is orthogonal to u^a, be proportional to a **real** unit spacelike vector $\hat{k}^a$, $\hat{k}^a \hat{k}_a = 1$. This direction defines the propagation direction for the wave as seen by the optical fluid. As a consequence we can write

$$\begin{aligned} \bar{k}^a &= -(S_{,b}u^b)N(Nu^a + \hat{k}^a), \\ k_a &= -(S_{,b}u^b)(u_a + N\hat{k}_a). \end{aligned} \tag{3.12}$$

The local period T and decay time T_d of the wave are related to changes in the real and imaginary parts of the eikonal as seen by an observer moving with the fluid, i.e., by

$$-(S_{,b}u^b) = \lambda\!\!\!^{-}_0 \left(\frac{2\pi}{cT} - i\frac{2}{cT_d} \right), \tag{3.13}$$

which are in turn related to the local wavelength λ and absorption coefficient α through the complex index of refraction N by

$$\frac{2\pi}{\lambda} + i\frac{\alpha}{2} = N\left(\frac{2\pi}{cT} - i\frac{2}{cT_d}\right), \tag{3.14}$$

since

$$S_{,b}\hat{k}^b = \lambda\!\!\!^{-}_0\left(\frac{2\pi}{\lambda} + i\frac{\alpha}{2}\right). \tag{3.15}$$

Maxwell's equations further restrict the electric field amplitude $\mathcal{E}_a$ in Eq. (3.10) by $\mathcal{E}_a\bar{k}^a = 0$ but leave the remaining freedom of definition $\mathcal{E}_a \to \mathcal{E}_a + f(x)k_a$ (here $f(x)$ is an arbitrary complex function). The first order (polarization dependent) correction to geometrical optics is given by

$$B_{ab} = 2(\mathcal{E}_{[a,b]} - k_{[a}\mathcal{D}_{b]}), \tag{3.16}$$

with a remaining freedom $\mathcal{D}_a \to \mathcal{D}_a + g(x)k_a$. Furthermore the propagation equation for the electric field amplitude $\bar{\mathcal{E}}^a$ is

$$\dot{\bar{\mathcal{E}}}^a + \bar{\mathcal{E}}^a\theta + \bar{\mathcal{E}}^a\dot{\phi} = \frac{\bar{k}^a}{2}(\bar{\nabla}_b\bar{\mathcal{E}}^b + k_b\bar{\mathcal{D}}^b + 2\phi_{,b}\bar{\mathcal{E}}^b), \tag{3.17}$$

where 2ϕ is the natural logarithm of the reciprocal of the impedance, i.e., $2\phi = \log\sqrt{\epsilon/\mu}$, and 2θ is the divergence of $\bar{k}^a$. It is a generalization of the expansion rate of the "null rays" defined by the complex vector field $\bar{k}^a$, i.e.,

$$\theta \equiv \frac{1}{2}\bar{\nabla}_a\bar{k}^a = \frac{\dot{\sqrt{A}}}{\sqrt{A}}, \tag{3.18}$$

and for a real metric is conventionally interpreted [76] as the fractional rate of

change of the observer independent cross-sectional area A of a small beam of neighboring rays (see Sec. 1.5). In what follows we choose a gauge where $\mathcal{E}_a u^a = 0$ which makes $\mathcal{E}_a$ spacelike and transverse to the wave's propagation direction, i.e., $\mathcal{E}_a \hat{k}^a = 0$. By contracting Eq. (3.17) with $\mathcal{E}_a$ we arrive at the propagation equation for the amplitude of plane polarized waves

$$(\mathcal{E}_a \dot{\overline{\mathcal{E}}}^a) + 2(\mathcal{E}_a \overline{\mathcal{E}}^a)(\theta + \dot{\phi}) = 0, \tag{3.19}$$

which can be simplified to read

$$\left[(\mathcal{E}_a \overline{\mathcal{E}}^a)\dot{A}\sqrt{\epsilon/\mu}\right] = 0. \tag{3.20}$$

The time averaged 4-flux seen by an observer moving with the optical fluid is in general

$$S^a \equiv \frac{c}{8\pi}\Re\left\{H^{*ac}F_{cb} - \frac{1}{4}\delta^a_b H^{*dc}F_{cd}\right\}u^b,. \tag{3.21}$$

When $\bar{F}^{ab}$ in Eq. (3.4) is restricted to the lowest order geometrical optics approximation, Eq. (3.2), and is homogeneous, i.e., satisfies Eq.(3.12), we have

$$S^a = \frac{c}{8\pi}e^{-2S_I/\lambda_0}(\mathcal{E}_a\bar{\mathcal{E}}^{*a})|S_{,b}u^b|^2\Re\left\{\sqrt{\epsilon/\mu}\right\}\left[\Re\{N\}\,u^a + \hat{k}^a\right], \tag{3.22}$$

where S_I is the imaginary part of the eikonal S, and $\Re\{N\} = n$ is the usual index of refraction, see Eq. (3.1). The coefficient of the fluid velocity u^a in S^a is the time average of the energy density ($\times c$) and the coefficient of $\hat{k}^a$ is the time average of the magnitude of the Poynting vector, both measured by observers moving with the

optical fluid. Equation (3.22) shows that energy in the single frequency geometrical optics wave is transferred in the $\hat{k}^a$ direction with a speed of c/n by this wave. In the next two subsections we give two concrete examples where S is complex.

3.2.1 Plane Waves in Minkowski Spacetime

To make contact with familiar examples in classical electrodynamics, we start with a plane wave propagating in an optical fluid which is at rest in flat spacetime. We assume ϵ and μ have only a z-dependence, and study waves propagating along the z direction, starting at $z = -\infty$. To suppress reflections and to make the geometrical optics approximation valid, we assume that ϵ and μ vary slowly over a wavelength λ, i.e., $\epsilon_{,z}\lambda \ll 1$, $\mu_{,z}\lambda \ll 1$. The physical metric is flat Minkowskian, the fluid's 4-velocity is $u^a = \delta^a_0$, and the optical metric, Eq. (3.5), is

$$\bar{ds}^2 = -\frac{(cdt)^2}{N(z)^2} + dx^2 + dy^2 + dz^2. \tag{3.23}$$

From Eq. (3.12) we find the complex wave vector

$$\begin{aligned} \bar{k}^a &= N(N, 0, 0, 1), \\ k_a &= (-1, 0, 0, N), \end{aligned} \tag{3.24}$$

with the complex eikonal

$$S \equiv S_R + iS_I = \left[-ct + \int_{-\infty}^{z} n(z')dz'\right] + i\left[\int_{-\infty}^{z} \kappa(z')dz'\right]. \tag{3.25}$$

Equations (3.13) and (3.14) reduce to

$$1 = \lambda\!\!\!^{-}_0 \left(\frac{2\pi}{cT}\right),$$
$$\frac{2\pi}{\lambda} + i\frac{\alpha}{2} = N\left(\frac{2\pi}{cT}\right), \tag{3.26}$$

which give the wave a constant frequency $\nu \equiv 1/T = c/(2\pi\lambda\!\!\!^{-}_0)$, but a z dependent wavelength $\lambda = 2\pi\lambda\!\!\!^{-}_0/n(z)$ and a z dependent absorption coefficient $\alpha = 2\kappa(z)/\lambda\!\!\!^{-}_0$. For this wave we have chosen the scale of S so that the geometrical optics expansion parameter $\lambda\!\!\!^{-}_0$ is the wave's rationalized wavelength in the absence of refractive material. This wave corresponds to a constant and uniform source (at $z = -\infty$) which resulted in $T_d = \infty$ in Eqs. (3.13) and (3.14).

The expansion defined in Eq. (3.18) vanishes for this plane wave, i.e., $\theta = 0$. If it is linearly polarized along the x direction the amplitude of the field is $(0, \mathcal{E}^x, 0, 0)$. The propagation equation (3.20) then simplifies to

$$[\mathcal{E}^x(\epsilon/\dot{\mu})^{1/4}] = 0 \tag{3.27}$$

which implies

$$\mathcal{E}^x \left(\frac{\epsilon}{\mu}\right)^{1/4} = f\left(-ct + \int_{-\infty}^{z} N(z')dz'\right), \tag{3.28}$$

where the function f reflects the time dependence of the source amplitude $\mathcal{E}(t, z)$ at the source, i.e., at $z = -\infty$. For a stable plane wave source, we simply put $f =$ constant.

To compute the energy flux we can use either the spatial part of the general result Eq. (3.22), or because the physical metric is flat and the fluid is at rest, use

the familiar 3-D electric and magnetic fields from Eqs. (3.2) and (3.10)

$$\begin{aligned} \mathbf{E} &= e^{iS/\lambda_0}\mathcal{E}^x\,\hat{\mathbf{i}}, \\ \mathbf{H} &= \sqrt{\epsilon/\mu}\;\hat{\mathbf{k}}\times\mathbf{E}, \end{aligned} \tag{3.29}$$

to evaluate the time averaged Poynting vector directly

$$\begin{aligned} \mathbf{S} &= \frac{c}{8\pi}\Re\{\mathbf{E}\times\mathbf{H}^*\}, \\ &= \frac{c}{8\pi}\Re\{\sqrt{\epsilon/\mu}\}|\mathcal{E}^x|^2 e^{-2S_I/\lambda_0}\hat{\mathbf{k}}. \end{aligned} \tag{3.30}$$

The magnitude of $\mathbf{S}$ can be evaluated using Eq. (3.28) as

$$S(z) = \frac{\cos\beta(z)}{\cos\beta(-\infty)}e^{-2S_I(z)/\lambda_0}S(-\infty), \tag{3.31}$$

where $S(-\infty)$ is the flux at the source and where

$$\cos\beta \equiv \frac{\Re\{\sqrt{\epsilon/\mu}\}}{\sqrt{|\epsilon/\mu|}} = \frac{\Re\{Z\}}{|Z|}. \tag{3.32}$$

The phase β represents the angle by which $\mathbf{H}$ field lags behind the $\mathbf{E}$ field, and $\cos\beta$ is the familiar power factor in the language of circuit analysis. From the imaginary part of the eikonal we can now easily write down the relation between the absorption coefficient α and the classical optical depth τ [61]

$$\tau(z) = 2\frac{\omega}{c}\int_{-\infty}^{z}\kappa(z')dz' = \int_{-\infty}^{z}\alpha(z')dz'. \tag{3.33}$$

3.2.2 Spherical Waves in a Static Spherically Symmetric Spacetime

Because this case is similar to the above, we truncate the discussion and give mainly the results. For an isotropic monochromatic source at rest at the origin of a static spherically symmetric spacetime which is emitting radiation at a steady rate into an optical fluid, which is also at rest, and whose optical properties depend only on the distance from the origin, we have an optical metric of the form

$$d\bar{s}^2 = -\frac{e^{2\Phi(r)}}{N(r)^2}(cdt)^2 + e^{2\Psi(r)}dr^2 + r^2(d\theta^2 + \sin^2\theta d\phi^2), \tag{3.34}$$

and a fluid at rest with respect to the non-rotating Killing flow, i.e., $u^a = e^{-\Phi}\delta^a_0$. For the radial null vectors in Eq. (3.12) we have,

$$\begin{aligned} \bar{k}^a &= N\left(Ne^{-2\Phi}, e^{-\Phi-\Psi}, 0, 0\right), \\ k_a &= (-1, Ne^{-\Phi+\Psi}, 0, 0). \end{aligned} \tag{3.35}$$

The complex eikonal is

$$S = \left[-ct + \int_0^r n(r')e^{-\Phi+\Psi}dr'\right] + i\left[\int_0^r \kappa(r')e^{-\Phi+\Psi}dr'\right]. \tag{3.36}$$

Equations (3.13) and (3.14) simplify to

$$\begin{aligned} e^{-\Phi} &= \lambda\!\!\!^{-}_0\left(\frac{2\pi}{cT}\right), \\ \frac{2\pi}{\lambda} + i\frac{\alpha}{2} &= N\left(\frac{2\pi}{cT}\right), \end{aligned} \tag{3.37}$$

and give an r dependent frequency $\nu \equiv 1/T = c\,e^{-\Phi}/(2\pi\lambda\!\!\!^{-}_0)$, an r dependent wavelength $\lambda = 2\pi\lambda\!\!\!^{-}_0 e^{\Phi}/n(r)$ and an r dependent absorption coefficient $\alpha = 2\kappa(r)e^{-\Phi}/\lambda\!\!\!^{-}_0$. The expansion parameter θ of Eq. (3.18) is

$$\theta = N\frac{e^{-\Phi-\Psi}}{r} = \frac{\dot{r}}{r} = \frac{\dot{\sqrt{A}}}{\sqrt{A}}. \tag{3.38}$$

For a time independent source Eq. (3.20) now gives

$$[r(\epsilon/\dot{\mu})^{1/4}\mathcal{E}] = 0\,, \tag{3.39}$$

where the polarization vector has been written in the form $\mathcal{E}^a = (0, 0, \mathcal{E}/r, 0)$ and points in the $\hat{\mathbf{e}}_\theta$ direction. The flux measured by $u^a = e^{-\Phi}\delta^a_0$ is found from Eq. (3.22) to be

$$\begin{aligned} S(r) &= \frac{c}{8\pi}e^{-2S_I/\lambda\!\!\!^{-}_0}|\mathcal{E}|^2(u^a k_a)^2\Re\{\sqrt{\epsilon/\mu}\}, \\ &= e^{-\tau(r)}\frac{\cos\beta(r)}{\cos\beta(0)}e^{-2\Phi(r)+2\Phi(0)}\frac{\mathcal{L}}{4\pi r^2}, \end{aligned} \tag{3.40}$$

where $\mathcal{L}$ is the total isotropic power radiated by the stationary point source in a narrow frequency range. The optical depth τ changes from Eq. (3.33) to

$$\tau(r) = 2\lambda\!\!\!^{-}_0{}^{-1}\int_0^r \kappa(r')e^{-\Phi+\Psi}dr', \tag{3.41}$$

$$= \int_0^r \alpha(r')e^{\Psi}dr'. \tag{3.42}$$

The spherical result differs from the plane wave result of Eq. (3.31) by a decrease of the flux caused by the wave's expansion ($A^{-1} \propto r^{-2}$) and by a frequency shift in the wave as it moves through the changing gravity field.

3.3 A Real Eikonal

Waves traveling in spacetimes where the imaginary part of the index of refraction is much smaller than the real part must still satisfy the same set of Maxwell's equations (3.3) and (3.9) as before but for them the eikonal S in Eq. (3.2) can be taken as real. The complex index of refraction is caused by a complex permittivity $\epsilon = \epsilon_R + i\epsilon_I$ and/or a complex permeability $\mu = \mu_R + i\mu_I$ whose imaginary parts are much smaller than their real parts. Consequently we write N as

$$N = n + i\kappa = n\left(1 + i\lambda\!\!\!^{-}_0\overline{\kappa} + \mathcal{O}(\lambda\!\!\!^{-}_0{}^2)\right), \tag{3.43}$$

where $n \equiv \sqrt{\epsilon_R \mu_R}$ and the constant parameter $\lambda\!\!\!^{-}_0$ is the same parameter used to keep track of the various orders in the geometrical optics expansion. The absorption coefficient α of Eq. (3.14) is related to $\overline{\kappa}$ by[1] $\alpha = 2\overline{\kappa}\lambda\!\!\!^{-}_0/\lambda$. The optical metric components of Eqs. (3.5) and (1.4) are

$$\bar{g}_{ab} = -\frac{1}{N^2}u_a u_b + g_{\perp\, ab} = \tilde{g}_{ab} - 2\frac{\lambda\!\!\!^{-}_0}{i}\frac{\overline{\kappa}}{n^2}u_a u_b + \mathcal{O}(\lambda\!\!\!^{-}_0{}^2), \tag{3.44}$$

$$\bar{g}^{ab} = -N^2 u^a u^b + g_\perp^{ab} = \tilde{g}^{ab} + 2\frac{\lambda\!\!\!^{-}_0}{i}\overline{\kappa} n^2 u^a u^b + \mathcal{O}(\lambda\!\!\!^{-}_0{}^2), \tag{3.45}$$

where the $\mathcal{O}(\lambda\!\!\!^{-}_0{}^0)$ term of the optical metric, $\tilde{g}_{ab}$, and its inverse, $\tilde{g}^{ab}$, are real

$$\tilde{g}_{ab} = -\frac{1}{n^2}u_a u_b + g_{\perp\, ab}, \tag{3.46}$$

$$\tilde{g}^{ab} = -n^2 u^a u^b + g_\perp^{ab}. \tag{3.47}$$

[1]This comes from Eqs. (3.50), (3.51), (3.53) and the fact that $|\Delta l| = (u_a \bar{k}^a)d\xi = n(u_a k^a)d\xi$.

When the geometrical optics expansion of Eq. (3.2) is inserted into Eqs. (3.3) and (3.9) the $\mathcal{O}(\lambda\!\!\!^{-}{}_0{}^{-1})$ terms result in Eq. (3.10) again, but now with k_a the gradient of the real eikonal S and null with respect to the $\mathcal{O}(\lambda\!\!\!^{-}{}_0{}^{0})$ optical metric $\tilde{g}_{ab}$, i.e.,

$$\tilde{k}^a k_a = 0, \tag{3.48}$$

$$\dot{\tilde{k}}^a = \frac{d\tilde{k}^a}{D\xi} \equiv \tilde{k}^b \tilde{\nabla}_b k^a = 0. \tag{3.49}$$

This gives real geodesics $x^a(\xi)$ with real tangents $dx^a/d\xi = \tilde{k}^a \equiv \tilde{g}^{ab}k_b$, and makes the real metric $\tilde{g}_{ab}$ the important geometric quantity rather than the complex $\bar{g}_{ab}$. The ' ' derivative is now the familiar derivative with respect to an affine parameter ξ along null geodesics. Equations (3.12) are still valid except N is replaced by its real part n and complex $\bar{k}^a$ by the real $\tilde{k}^a$. Equations (3.13) and (3.14) for the frequency and wavelength are replaced by

$$-(S_{,b}u^b) = \lambda\!\!\!^{-}{}_0 \left(\frac{2\pi}{cT}\right), \tag{3.50}$$

and

$$\frac{2\pi}{\lambda} = n\left(\frac{2\pi}{cT}\right). \tag{3.51}$$

The polarization vector $\mathcal{E}_a$ in Eq. (3.10) is now constrained to be orthogonal to $\tilde{k}^a$ and can be, as before, chosen orthogonal to the fluid u_a. The $\mathcal{O}(\lambda\!\!\!^{-}{}_0{}^{1})$ correction terms B_{ab} are still given by Eq. (3.16), the expansion θ in Eq. (3.18) is computed using $\tilde{k}^a$, and the covariant derivatives are all with respect to the real $\tilde{g}_{ab}$ Christoffel connection. The only equation that contains a new term, the extinction term, is

the propagation equation for the amplitude $\tilde{\mathcal{E}}^a$ that replaces Eq. (3.17)[2] ,

$$\dot{\tilde{\mathcal{E}}}^a + \tilde{\mathcal{E}}^a\theta + \tilde{\mathcal{E}}^a\dot{\phi} + \overline{\kappa}n^2(u^b k_b)^2\tilde{\mathcal{E}}^a = \frac{\tilde{k}^a}{2}(\tilde{\nabla}_b\tilde{\mathcal{E}}^b + k_b\tilde{\mathcal{D}}^b + 2\phi_{,b}\tilde{\mathcal{E}}^b). \tag{3.52}$$

The phase ϕ is now computed similarly as for Eq. (3.17) but now using only the $\mathcal{O}({\lambda_0}^0)$ terms of the impedance $2\phi = \log\sqrt{\epsilon_R/\mu_R}$. The integral of Eq. (3.52) which replaces Eq. (3.20) now contains an affine parameter integral

$$\log\left[(\mathcal{E}^*_a\tilde{\mathcal{E}}^a)A\sqrt{\epsilon_R/\mu_R}\right] = -2\int \overline{\kappa}n^2(u^b k_b)^2 d\,\xi\,. \tag{3.53}$$

When the time averaged Poynting vector, Eq. (3.21), is evaluated Eq. (3.22) is replaced by

$$S^a = \frac{c}{8\pi}(\mathcal{E}_a\tilde{\mathcal{E}}^{*a})(S_{,b}u^b)^2\left(\sqrt{\epsilon_R/\mu_R}\right)\left[n\,u^a + \hat{k}^a\right]. \tag{3.54}$$

Comparing Eqs. (3.22) with (3.54) the effects of absorption can easily be seen to have shifted from the eikonal where it belongs if absorption is significant over wavelength scales, to the slowly changing amplitude $\mathcal{E}_a$ where it belongs if extinction is significant only over many wavelengths.

In the next section we give an example of absorption with a real eikonal from observational cosmology. We evaluate luminosity-distance in a FLRW universe when extinction occurs.

3.3.1 Robertson-Walker Spacetime

As an example of weak absorption we apply our complex extension of Gordon's optical theory to a Robertson-Walker universe filled with a time dependent index

[2]See the appendix to this chapter for a detailed derivation of this equation.

of refraction $N(t) = n(t) + i\kappa(t)$ [see Eq. (3.43)] and obtain for the real optical metric, Eq. (3.46),

$$d\tilde{s}^2 = -\frac{(cdt)^2}{n(t)^2} + R^2(t)\left\{\frac{dr^2}{1-kr^2} + r^2(d\theta^2 + \sin^2\theta\, d\phi^2)\right\}. \tag{3.55}$$

The familiar curvature parameter $k = (1, 0, -1)$ distinguishes respectively between spatially closed, flat, and open models. The radial outgoing null geodesics can be solved immediately to give null vectors

$$\tilde{k}^a = R_0\left(\frac{n}{R}, \frac{\sqrt{1-kr^2}}{R^2}, 0, 0\right), \tag{3.56}$$

$$k_a = R_0\left(-\frac{1}{nR}, \frac{1}{\sqrt{1-kr^2}}, 0, 0\right), \tag{3.57}$$

and the related real spherically symmetric eikonal centered at the emission point, $t = t_e$, $r = 0$,

$$S(t, r) = S_R = R_0\left(-\int_{t_e}^{t} \frac{c\, dt'}{n(t')R(t')} + \mathrm{sinn}^{-1}[r]\right), \tag{3.58}$$

where sinn$[r]$ is defined as before. The constant R_0 is the current radius of the universe [from Eq. (3.55)] and has been introduced so that the geometrical optics expansion parameter $\lambda\!\!\!^{-}_0$ corresponds to the rationalized wavelength of the wave when it reaches an observer at t_0, r_0 from an emitting source at $t_e, r = 0$. From Eqs. (3.50) and (3.51) we have the wavelength and frequency redshifts

$$\begin{aligned} 1 + z &\equiv \frac{\lambda_0}{\lambda} = \frac{R_0}{R}, \\ 1 + z_n &\equiv \frac{\nu}{\nu_0} = \frac{n_0}{n}\frac{R_0}{R}, \end{aligned} \tag{3.59}$$

which are thus related by

$$(1 + z_n) = \frac{n_0}{n}(1 + z). \tag{3.60}$$

The conventional RW redshift $(1 + z) \equiv R_0/R$ is valid for both wavelength and frequency when the refracting and absorbing material is absent, i.e., when $N = 1$. We see that even with refraction and absorption the wavelength redshift remains as in RW cosmology. The frequency redshift, however, is affected by the real part of the index of refraction, n, but not by the imaginary part, κ, i.e., not by extinction.

To evaluate the apparent brightness of a source we need to evaluate the magnitude of the spatial part of the Poynting vector, Eq. (3.54), which requires that we know the area A in Eq. (3.53). For a spherical wave emanating from the co-moving origin, $A \propto (rR)^2$, which is confirmed by evaluating the expansion parameter θ using Eq. (3.56). From the transport Eq. (3.53) we have

$$(\mathcal{E}^*_a \tilde{\mathcal{E}}^a)\sqrt{\epsilon_R/\mu_R} \propto \frac{e^{-\tau}}{(Rr)^2}, \tag{3.61}$$

where the optical depth $\tau(t)$ from t to t_0 is

$$\tau(t) = 2c \int_t^{t_0} \frac{\overline{\kappa}(t')}{n(t')} \frac{R_0}{R(t')}\, dt' , \tag{3.62}$$

$$= c \int_t^{t_0} \frac{\alpha(t')}{n(t')}\, dt' . \tag{3.63}$$

When the observer looks back in time, Eq. (3.54) gives the magnitude of the spatial part of flux

$$S(t) \propto \frac{e^{-\tau(t)}}{[n(t)R(t)]^2[r(t)R(t)]^2}. \tag{3.64}$$

The apparent luminosity L in a narrow band is just the value of $S(t)$ at the observer,

$t = t_0$. If the absorption is frequency independent in the observed frequency range, and the constant of proportionality is evaluated at the source at $r(t_e) = 0$ the luminosity becomes

$$L = \frac{\mathcal{L}}{4\pi R_0^2 r_0^2} \frac{e^{-\tau}}{(1+z_n)^2}, \tag{3.65}$$

where $\mathcal{L}$ is the absolute luminosity of an assumed isotropically radiating source in that frequency range. The luminosity distance d_L is easily read from this and differs from RW cosmology, i.e.,

$$d_L = (1+z_n) R_0 r_0 \, e^{\tau/2}, \tag{3.66}$$

however, the apparent size distance remains $d_A = r_0 R_e$. These distances obviously violate the classical reciprocity relation $d_L = (1+z)^2 d_A$ (see [11, 38, 51, 63] and discussion in Sec. 1.3) which is valid for non-refractive non-absorptive optics.

Using the dynamics of the FLRW cosmologies, we find

$$d_L(z_n) = (1+z_n) \frac{c}{H_0} \frac{e^{\tau(z_n)/2}}{\sqrt{|\Omega_k|}} \text{sinn} \sqrt{|\Omega_k|} \int_0^{z(z_n)} \frac{dz'}{n(z')h(z')}, \tag{3.67}$$

where we have used Eq. (3.60) to express distance-redshift as a function of the frequency redshift z_n, and where H_0, $h(z)$ and Ω_k are defined as before. When the optical depth τ is written as a function of the frequency redshift z_n it becomes

$$\tau(z_n) = \frac{c}{H_0} \int_0^{z(z_n)} \frac{\alpha(z')}{(1+z')n(z')h(z')} \, dz'. \tag{3.68}$$

The distance-redshift of Eq. (3.67) can be compared with a similar result but without absorption given in Sec. 2.2 (Ref.[16]). In Sec. 2.4 we have shown that a

cosmological model with a refraction index $n(z) = 1 + p * z^2 + q * z^3$, but with no absorption, can fit the currently available type Ia supernovae data quite well. A source for such refraction remains elusive. For illustrative purposes, we now use the distance-redshift of Eq. (3.67) with a constant absorption coefficient α which does not change with frequency (i.e., is grey) but without refraction to fit this same supernovae data, i.e., we take

$$\Omega_\Lambda = 0,\ n(z) = 1,\ \alpha(z) = \text{const.} \tag{3.69}$$

The Hubble constant we use is $H_0 = 65\,\text{km} \cdot \text{s}^{-1} \cdot \text{Mpc}^{-1}$. Since we are concerned with the matter dominated era, we exclude radiation ($\Omega_r = 0$). The function $h(z)$ in Eqs. (3.67) and (3.68) simplifies to

$$h(z) = (1 + z)\sqrt{1 + \Omega_m z}, \tag{3.70}$$

and our model has just two parameters (Ω_m, α). We compare the distance modulus versus redshift, $\mu(z)$, of the concordance model ($\Omega_\Lambda = 0.7$, $\Omega_m = 0.3$) with five $\Omega_\Lambda = 0$ extinction models (three open, one flat and one closed). The result is shown in Fig. 3.1, where the distance-modulus μ is compared to the same set of supernova data as used in Chapter 2. In Fig. 3.1, the solid green curve represents the flat concordance model dominated by dark energy. The dotted red curve models an open universe with baryonic only matter, $\Omega_\Lambda = 0$, $\Omega_\text{m} = 0.05$, $n = 1$ and $\alpha(z) = 6{\times}10^{-5}\text{Mpc}^{-1}$. The short dashed red curve is an open model containing only dark matter, $\Omega_\Lambda = 0$, $\Omega_\text{m} = 0.3$, $n = 1$ and $\alpha(z) = 1.2 \times 10^{-4}\,\text{Mpc}^{-1}$. The solid black curve is our least χ^2 model (see Fig. 3.2) with $\Omega_\Lambda = 0$, $\Omega_\text{m} = 0.73$,

$\alpha(z) = 2.2 \times 10^{-4}\,\mathrm{Mpc}^{-1}$. The longer dashed green curve represents a flat universe dominated solely by matter, with $\Omega_\Lambda = 0$, $\Omega_\mathrm{m} = 1.0$, $\alpha(z) = 2.6 \times 10^{-4}\,\mathrm{Mpc}^{-1}$. The longest dashed blue curve is a closed model, where $\Omega_\Lambda = 0$, $\Omega_\mathrm{m} = 1.3$, $\alpha = 3.2 \times 10^{-4}\,\mathrm{Mpc}^{-1}$. The black dashed curve is the now disfavored matter dominated $\Omega_\Lambda = 0$, $\Omega_\mathrm{m} = 0.3$ model (without extinction). In the inset we show $\Delta\mu$ versus z (relative to the disfavored matter dominated case) for each model. To produce roughly the same amount of change in the distance-modulus a larger absorption coefficient α is needed for a larger Ω_m (α is positively correlated to Ω_m). As the reader can easily see in Fig. 3.1 the effects of a suitable value of the simplest absorption coefficient $\alpha(z) = \text{const}$ can simulate the accelerating effects of a cosmological constant.

In Fig. 3.2, we show the confidence contours for our model parameters, α versus Ω_m. The best fitting parameters are $\Omega_m = 0.73, \alpha = 2.2 \times 10^{-4}\mathrm{Mpc}^{-1}$, with $\chi^2_\mathrm{min} = 1.04$ (per degree of freedom). The innermost contour encloses the 68.3% confidence region, and the next one encloses the 95.4% confidence region, the outermost one encloses the 99.73% confidence region. For each fixed Ω_m selected in Fig. 3.1, α is the value that gives the least χ^2.

If we extract a density factor ρ from the absorption coefficient, i.e., $\sigma \equiv \alpha/\rho$ we obtain an opacity in e.g., $\mathrm{cm}^2 \cdot \mathrm{g}^{-1}$. The density ρ with units of $\mathrm{g} \cdot \mathrm{cm}^{-3}$ is the density of the relevant species causing the absorption. A competitive absorption model should properly account for both the cosmic expansion and the physical/chemical evolution of the inter-galactic medium [81]. Here we are content with an order of magnitude estimate noting that an opacity $\sigma = 10^5\,\mathrm{cm}^2 \cdot \mathrm{g}^{-1}$ as proposed for the carbon needle model in [1], requires a density ρ the order of $10^{-33}\,\mathrm{g} \cdot \mathrm{cm}^{-3}$ to produce the absorption needed for the above fitting. This density is only a factor of $\sim 10^{-4}$ of the current critical mass density $\rho_c \approx 8 \times 10^{-30}\mathrm{g} \cdot \mathrm{cm}^{-3}$. For fine-tuned

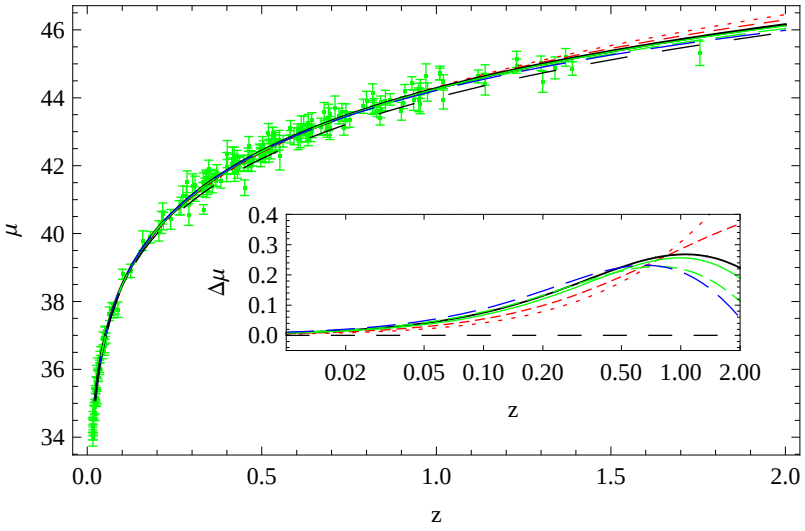

Figure 3.1: Distance modulus μ versus redshift z. The two red and one solid black curves are open models, the two green curves are flat models, and the blue curve is a closed model. (looking downward at redshift $z = 1.5$) Dotted red curve: $\Omega_\Lambda = 0$, $\Omega_\mathrm{m} = 0.05$, $\alpha(z) = 6 \times 10^{-5}\ \mathrm{Mpc}^{-1}$. Short dashed red curve : $\Omega_\Lambda = 0$, $\Omega_\mathrm{m} = 0.3$, $\alpha(z) = 1.2 \times 10^{-4}\ \mathrm{Mpc}^{-1}$. Solid black curve (our best fit): $\Omega_\Lambda = 0$, $\Omega_\mathrm{m} = 0.73$, $\alpha(z) = 2.2 \times 10^{-4}\ \mathrm{Mpc}^{-1}$. Solid green curve (concordance model): $\Omega_\Lambda = 0.7$, $\Omega_\mathrm{m} = 0.3$, $\alpha = 0$. Longer dashed green curve: $\Omega_\Lambda = 0$, $\Omega_\mathrm{m} = 1.0$, $\alpha(z) = 2.6 \times 10^{-4}\ \mathrm{Mpc}^{-1}$. Longest dashed blue curve: $\Omega_\mathrm{m} = 1.3$, $\alpha(z) = 3.2 \times 10^{-4}\ \mathrm{Mpc}^{-1}$. Black dashed curve: $\Omega_\Lambda = 0$, $\Omega_\mathrm{m} = 0.3$, $\alpha = 0$. Inset: $\Delta\mu$ versus z curve for each model, the fiducial model (black dashed curve): $\Omega_\Lambda = 0$, $\Omega_\mathrm{m} = 0.3$, $\alpha = 0$.

dust absorption models, see e.g., [1, 2, 12, 40, 74].

3.4 Discussion

In this chapter we have demonstrated how the 4-D optical metric of Gordon [see Eq. (3.5)] can be extended and used even in cases where absorption is present. We looked at both 'strong' and 'weak' absorption, the distinction being whether absorption is significant on wavelength scales or only over a multitude of wavelengths. The two cases are distinguished respectively by complex and real eikonals. For the

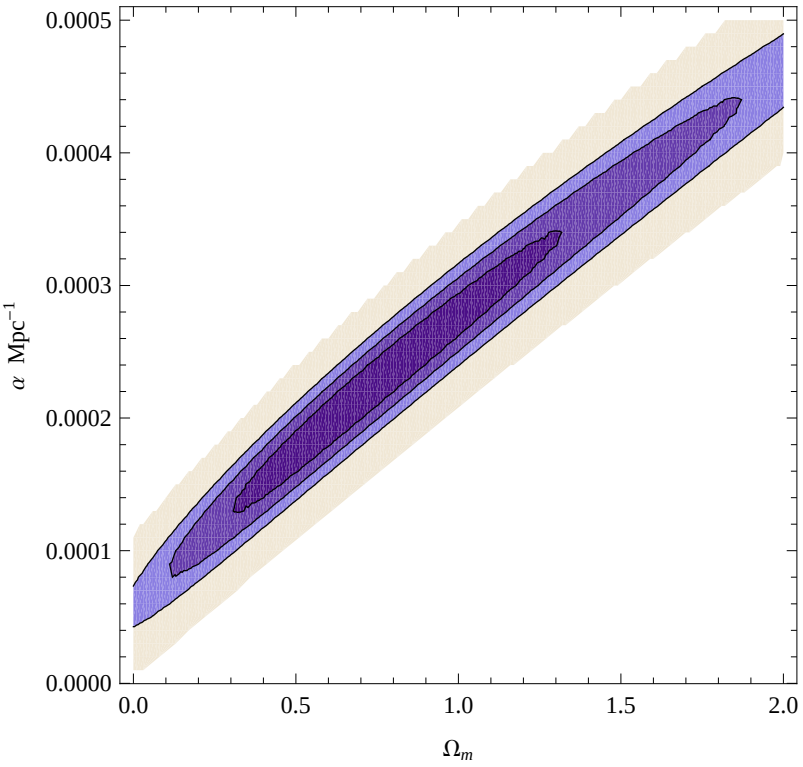

Figure 3.2: α versus $\Omega_{\rm m}$. The best fitting parameters are $\Omega_{\rm m} = 0.73, \alpha = 2.2 \times 10^{-4}{\rm Mpc}^{-1}$, with $\chi^2_{\rm min} = 1.04$ (per degree of freedom). The innermost contour encloses the 68.3% confident region, the next one encloses the 95.4% confidence region, and the outermost one encloses the 99.73% confidence region.

complex eikonal case the optical metric must remain complex (see Sec. 3.2), however, for the weak absorption case the real part of the optical metric (essentially the same as Gordon's original proposal) remains as the significant geometrical structure (see Sec. 3.3). The two cases differ on how absorption appears in the geometrical optics field. In the 'strong' absorption case the imaginary part of the eikonal reduces the wave's intensity [see Eq. (3.22)] but in the 'weak' case the amplitude's reduction [see Eq. (3.53)] is responsible for the intensity decrease.

A geometrical optics wave is like a single frequency wave even though the wave's frequency changes from spacetime point to spacetime point. To superimpose multiple frequencies is straightforward, however, to superimpose optical metrics, real or complex, makes no sense. Consequently a useful single optical metric only exists when the optical properties are insensitive to the superimposed frequencies. Such frequency independence approximations are often designated as 'grey' in astrophysical applications.

The two examples we gave in Sec. 3.2 can be used to study the impact of refraction and/or absorption on light propagation in stellar atmospheres. The classical radiation transport equation (see e.g. [32, 56]) is derived assuming that light follows null geodesics in curved spacetimes. With the presence of light refraction, both the direction and speed of light change. This would require the radiative transfer equation to be written using the optical metric instead of the physical metric. The optical metric might also be of some use in hydrodynamical simulations of stellar interiors. For an example, the slowing down of light will reduce the efficiency of energy transport outward via the radiation field. Our first example (flat spacetime) can be used to study the 1-D case; a comparison of results of a numerically solved radiation transport equation with/without a refraction in-

dex $n(z)$ would be interesting. Similarly, our second example (curved spherically symmetrical spacetime) can be used to model the atmospheres of neutron stars. Further non-spherically symmetric examples could be useful in radiation transport calculations in accretion disks of black holes.

Our last example, the real eikonal case, allowed us to give luminosity distance redshift for observations in standard cosmologies where both refraction and absorption were present. As an example of the usefulness of this theory we went on to fit the gold sample of type Ia supernovae to a Hubble curve corrected for grey extinction. In Sec. 3.3 we showed that it is possible to explain the current supernova observations via a simple absorption model instead of requiring the existence of dark energy. Our best fit was an open $\Omega_m = 0.73$ model with constant absorption $\alpha = 2.2 \times 10^{-4}\text{Mpc}^{-1}$, see Fig. 3.2 for confidence contours. More realistic z dependent models for α are in order.

3.5 Appendix

In this appendix, we give the detailed derivation of the GO approximation for the real eikonal case discussed in Sec. 3.3.

We write the electric field/magnetic induction bivector as

$$F_{ab}^{\lambda\!\!\!^{-}_0} = \Re\left\{ e^{\frac{i}{\lambda\!\!\!^{-}_0}(S_R + \frac{\lambda\!\!\!^{-}_0}{i} S_I)} \left(A_{ab} + \frac{\lambda\!\!\!^{-}_0}{i} B_{ab} + O(\lambda\!\!\!^{-2}_0) \right) \right\}. \tag{3.71}$$

Note that by writing the complex eikonal $S(x^a)$ as $S = S_R + (\lambda\!\!\!^{-}_0/i)S_I$ we have explicitly assumed the smallness of the imaginary part of $S(x^a)$ compared with the

real part S_R. We define $k_a \equiv \partial_a S$. Note that[3]

$$\bar{\nabla}_b(e^{2\phi}\bar{F}^{ab}) = 0 \tag{3.72}$$

is equivalent to

$$\tilde{\nabla}_b(e^{2\phi}\bar{F}^{ab}) = 0 \tag{3.73}$$

for our approximation using

$$\nabla_c A^{bc} = \frac{1}{\sqrt{-g}}(\sqrt{-g}A^{bc})_{,c}. \tag{3.74}$$

Inserting Eq. (3.71) into the modified Maxwell equations we obtain for oder $\lambda\!\!\!^{-}_0{}^{-1}$

$$\begin{aligned} A_{[ab}k_{c]} &= 0, \\ \tilde{A}^{ab}k_b &= 0, \end{aligned} \tag{3.75}$$

and for order $\lambda\!\!\!^{-}{}^0$

$$\begin{aligned} \partial_{[a}A_{bc]} + S_{I,[a}A_{bc]} + k_{[a}B_{bc]} &= 0, \\ \tilde{\nabla}_b\tilde{A}^{ab} + \tilde{A}^{ab}(2\phi_{,b} + S_{I,b}) + \tilde{B}^{ab}k_b + (2\bar{\kappa}n^2)2k_b u^{[b}g^{a]c}A_{cd}u^d &= 0, \end{aligned} \tag{3.76}$$

where when deriving the second of the equations above we have made use of

$$\bar{A}^{ab} = \tilde{A}^{ab} + \frac{\lambda\!\!\!^{-}_0}{i}(2\bar{\kappa}n^2)2u^{[b}g^{a]c}A_{cd}u^d. \tag{3.77}$$

[3]In this appendix barred quantities are with respect to the complex optical metric $\bar{g}_{ab}$ [Eq. (3.44)], and tilde quantities are with respect to Gordon's original (real) optical metric $\tilde{g}_{ab}$ [Eq. (3.46)].

By arguments similar to those in Sec. 1.2, we found

$$\begin{aligned} A_{ab} &= -2k_{[a}\mathcal{E}_{b]}, \\ B_{ab} &= 2\mathcal{E}_{[a,b]} + 2\mathcal{E}_{[a}S_{I,b]} - 2k_{[a}D_{b]}, \end{aligned} \tag{3.78}$$

where $\mathcal{E}_a\tilde{k}^a = 0$. We furthermore constrain $\mathcal{E}_a$ to be orthogonal to u^a via a gauge choice. Inserting the above expressions into the second of Eqs. (3.76) we obtain the propagation equation of $\tilde{\mathcal{E}}^a$

$$\dot{\tilde{\mathcal{E}}}^a + \tilde{\mathcal{E}}^a[\theta + \dot{\phi} + \dot{S}_I + \overline{\kappa}n^2(u^b k_b)^2] = \frac{\tilde{k}^a}{2}(\tilde{\nabla}_b\tilde{\mathcal{E}}^b + S_{I,b}\tilde{\mathcal{E}}^b + k_b\tilde{\mathcal{D}}^b + 2\phi_{,b}\tilde{\mathcal{E}}^b). \tag{3.79}$$

Redefining $\mathcal{E}^a$, i.e., $\mathcal{E}^a \to \mathcal{E}^a e^{S_I}$, and $\mathcal{D}^a \to \mathcal{D}^a e^{S_I}$, we finally obtain

$$\dot{\tilde{\mathcal{E}}}^a + \tilde{\mathcal{E}}^a[\theta + \dot{\phi} + \overline{\kappa}n^2(u^b k_b)^2] = \frac{\tilde{k}^a}{2}(\tilde{\nabla}_b\tilde{\mathcal{E}}^b + k_b\tilde{\mathcal{D}}^b + 2\phi_{,b}\tilde{\mathcal{E}}^b). \tag{3.80}$$

Chapter 4

An Optical Metric that Includes Absorption

In this chapter [18] we show that it is possible to equate the intensity reduction of a light wave caused by weak absorption with a geometrical reduction in intensity caused by a "transverse" conformal transformation of the spacetime metric in which the wave travels. We are consequently able to modify Gordon's optical metric to situations in which the electromagnetic properties of the optical material filling the spacetime include both refraction and absorption. Unlike refraction alone however, including absorption requires a modification of the optical metric that depends on the eikonal of the wave itself. We derive the distance-redshift relation from the modified optical metric for Friedman-Lemaître-Robertson-Walker spacetimes whose cosmic fluid has associated refraction and absorption coefficients. We then fit the current supernovae data and provide an alternate explanation (other than dark energy) of the apparent acceleration of the universe expansion.

4.1 Introduction

In Chapter 3 we modified Gordon's theory and showed that Gordon's optical metric could be generalized to include absorption by allowing the metric to become complex. We defined a complex refraction index $N = n + i\kappa$, and distinguished two different cases, i.e., strong and week absorption. In the case of strong absorption the real and imaginary parts of the index of refraction are of the same order ($\kappa \sim n$), the eikonal $S(x^a)$ has an imaginary part, and the optical metric is complex. In the weak absorption case ($k \ll n$), the eikonal $S(x^a)$ can be taken as real, and the real part of the optical metric (Gordon's original metric) remains as the significant geometrical structure. In this chapter we show that for weak absorption another generalization of Gordon's metric exists that can account for absorption as well as refraction. The generalization amounts to a transverse conformal transformation (see Sec. 4.2) of Gordon's original optical metric. This new optical metric remains real but does include absorption. Including absorption via a transverse conformal transformation requires an optical metric that depends on the eikonal of the wave itself.

In the next section we define transverse conformal transformations. In Sec. 4.3 we consider the geometrical optics approximation and relate wave properties in the two spacetimes, the physical and optical. In Sec. 4.4 we compare the effects of the transverse conformal transformation with absorption and relate the conformal factor σ to optical depth τ. In Sec. 4.5 we construct the optical metric that accounts for absorption in Robertson-Walker spacetimes. In Sec. 4.6 we include refraction by generalizing Gordon's metric [41] to including absorption. In Sec. 4.7 we derive the refraction/absorption corrected distance-redshift relation from the generalized

Gordon's optical metric in RW spacetimes. In Sec. 4.8 we fit the current supernovae data with the Hubble curve of a cosmological model in which the cosmic fluid has both an associated refraction index n and a constant opacity parameter α, and provide an alternate interpretation of the apparent acceleration of the cosmic expansion. In Sec. 4.9 we summarize our results.

4.2 The "Transverse" Conformal Transformation

A conformal transformation [33] is defined as a rescaling of the metric and is usually written in a form similar to

$$\hat{g}_{ab} = e^{2\sigma} g_{ab}, \tag{4.1}$$

where $\sigma(x^a)$ is an arbitrary scalar function defined on the spacetime manifold. The vacuum Maxwell equations

$$\begin{aligned} F_{[ab,c]} &= 0, \\ \nabla_b F^{ab} &= 0, \end{aligned} \tag{4.2}$$

are formally invariant under a conformal transformation[1], i.e.,

$$\begin{aligned} \hat{F}_{[ab,c]} &= 0, \\ \hat{\nabla}_b \hat{F}^{ab} &= 0, \end{aligned} \tag{4.3}$$

provided that the covariant electromagnetic field tensor F_{ab} transforms as

$$\hat{F}_{ab} = F_{ab}, \tag{4.4}$$

[1]Refer to the proof in Sec. 1.1.

and hence the contravariant field transforms as

$$\hat{F}^{ab} = e^{-4\sigma} F^{ab}. \tag{4.5}$$

The above is a purely mathematical observation and simply says that if you have a solution to Maxwell's vacuum equations in one spacetime then you have a related solution to Maxwell's vacuum equations in any conformally related spacetime. Nothing is being said by this about the existence of any new physically relevant field. One can and does make good use of such transformations to compactify spacetimes and to analyze fields at "∞", see e.g., [64]. However, by modifying these conformal transformations to be "transverse" [see Eq. (4.10) and (4.11)] we are able to construct new and useful solutions to Maxwell's equations.

Because the two metrics are defined on the same differentiable manifold we can make unique correspondences between events, world lines, and various fields in these two spacetimes. We call the original metric and manifold physical spacetime and the manifold with the conformally transformed metric the conformal spacetime. For example a normalized fluid 4-velocity, $\hat{u}^a(x)$, defined in the conformal spacetime would be related to the corresponding physical fluid 4-velocity by $\hat{u}^a(x) = e^{-\sigma} u^a(x)$. If we compare observed properties of radiation fields that are related as in Eqs. (4.4) and (4.5) and as seen in these two spacetimes by corresponding observers, we find that energy fluxes are diminished by a factor of $e^{-4\sigma}$. This net effect can be looked at as the result of the area of the radiation's wave front changing by a factor $e^{2\sigma}$, and the energies and rates each changing by a factor $e^{-\sigma}$. We will make use of this intensity reduction to account for absorption in physical spacetime. However, because a pure conformal transformation has the undesirable

property of altering a wave's frequency and wavelength it must be appropriately modified to represent absorption, which does not.

We assume that our physical spacetime is filled with two vector fields. The first is the normalized velocity field u^a ($u^a u_a = -1$) of a fluid whose optical properties we know and the second is a null field k^a ($k^a k_a = 0$) corresponding to the eikonal of a given electromagnetic wave (see Sec. 4.3 for details of the geometrical optics approximation). These two fields define a 2-dimensional timelike subspace at each point of the manifold. We are hence able to decompose the tangent space at each point of the 4-dimensional spacetime manifold into two orthogonal 2-dimensional subspaces, one timelike $g_{\parallel ab}$ and spanned by the pair (u^a, k^a)[2] and the other spacelike $g_{\perp ab}$. The full metric can be decomposed in terms of these two orthogonal pieces as

$$g_{ab} = g_{\parallel ab} + g_{\perp ab}. \tag{4.6}$$

We can give a simple expression for $g_{\parallel ab}$ by defining a second null vector m^a lying in the two dimensional timelike subspace spanned by u^a and k^a as

$$m^a \equiv \frac{k^a}{2(u \cdot k)^2} + \frac{u^a}{(u \cdot k)}, \tag{4.7}$$

from which it follows that

$$m^a m_a = 0,\ m^a u_a = -\frac{1}{2(u \cdot k)},\ m^a k_a = 1. \tag{4.8}$$

[2]See the discussion of the projection tensor P_{ab} in Sec. 1.5.2.

The metrics on the orthogonal 2-dimensional surfaces can be written as

$$\begin{aligned} g_{\parallel ab} &= 2m_{(a}k_{b)}, \\ g_{\perp ab} &= g_{ab} - 2m_{(a}k_{b)}. \end{aligned} \tag{4.9}$$

We conformally transform the 2-dimensional spacelike subspace only and arrive at the desired optical metric

$$\begin{aligned} \tilde{g}_{ab} &\equiv g_{\parallel ab} + e^{2\sigma} g_{\perp ab} \\ &= e^{2\sigma} g_{ab} + (1 - e^{2\sigma})\, 2m_{(a}k_{b)}, \end{aligned} \tag{4.10}$$

with inverse

$$\begin{aligned} \tilde{g}^{ab} &\equiv g_{\parallel}^{ab} + e^{-2\sigma} g_{\perp}^{ab} \\ &= e^{-2\sigma} g^{ab} + (1 - e^{-2\sigma}) 2m^{(a}k^{b)}. \end{aligned} \tag{4.11}$$

By straightforward tensor algebra we find that[3]

$$\det \tilde{g} = e^{4\sigma} \det g. \tag{4.13}$$

We would have obtained $\det \hat{g} = e^{8\sigma} \det g$ were we conformally transforming the entire metric g_{ab} as in Eq. (4.1). We call these transformations transverse conformal because they scale directions transverse to a wave's propagation direction k^a as

[3] *Proof.* First show that

$$\tilde{g}_{ab} = e^{2\sigma} g_{ac} [\delta^c{}_e + (e^{-2\sigma} - 1) m^c k_e][\delta^e{}_b + (e^{-2\sigma} - 1) k^e m_b] \tag{4.12}$$

using $m^a k_a = 1$, and $k^a k_a = 0$. Then use identity $\det(\delta^a{}_b + A^a B_b) = 1 + A^a B_a$.

seen by an observer u^a moving with the optical fluid. We find that the vacuum Maxwell equations (4.2) remain invariant in form under the transverse conformal transformation of Eq. (4.10), i.e.,

$$\begin{aligned} \tilde{F}_{[ab,c]} &= 0, \\ \tilde{\nabla}_b \tilde{F}^{ab} &= 0, \end{aligned} \tag{4.14}$$

provided that the covariant electromagnetic field tensor F_{ab} transforms as

$$\tilde{F}_{ab} = F_{ab}, \tag{4.15}$$

and that the contravariant field tensor $\tilde{F}^{ab}$ defined by

$$\tilde{F}^{ab} \equiv \tilde{g}^{ac}\tilde{g}^{bd}\tilde{F}_{cd} \tag{4.16}$$

is constrained to satisfy

$$\tilde{F}^{ab} = e^{-2\sigma}F^{ab}. \tag{4.17}$$

This constraint requires that two of the following three terms, i.e., F_0^{ab} and F_2^{ab}, originating from Eq. (4.16) vanish:

$$\tilde{F}^{ab} = F_0^{ab} + e^{-2\sigma}F_1^{ab} + e^{-4\sigma}F_2^{ab}, \tag{4.18}$$

where

$$\begin{aligned} F_0^{ab} &\equiv 2m^{[a}k^{b]}\left(F_{cd}k^c m^d\right), \\ F_1^{ab} &\equiv -2k^{[a}F^{b]}{}_c m^c - 2m^{[a}F^{b]}{}_c k^c - 2F_0^{ab}, \end{aligned}$$

$$F_2^{ab} \equiv F^{ab} - F_0^{ab} - F_1^{ab}. \tag{4.19}$$

Consequently F_{ab} must satisfy

$$F_{cd}k^c m^d = 0, \tag{4.20}$$

and

$$F^{ab} = -2k^{[a}F^{b]}{}_c m^c - 2m^{[a}F^{b]}{}_c k^c. \tag{4.21}$$

As we will see in the next section [see Eq. (4.33)] a radiation field whose eikonal generates the null field k^a satisfies these constraints. For a familiar example, choose the physical metric to be Minkowskian, i.e.,

$$ds^2 = -c^2dt^2 + dr^2 + r^2(d\theta^2 + \sin^2\theta\, d\phi^2), \tag{4.22}$$

with a stationary optical fluid $u^a = (1/c, 0, 0, 0)$, and radial null geodesics $k^a = k\,(1/c, 1, 0, 0)$. From Eq. (4.7) we find

$$m^a = \frac{1}{2k}\left(-\frac{1}{c}, 1, 0, 0\right). \tag{4.23}$$

Equations (4.20) and (4.21) then give

$$F_{01} = -F_{10} = 0,\ F_{23} = -F_{32} = 0, \tag{4.24}$$

i.e., F^{ab} is a transverse field, hence motivating the designation of Eq. (4.10) as a "transverse" conformal transformation. Equations (4.20) and (4.21) simply express the transversality condition for an arbitrary wave. In the following section we

review the geometrical optics approximation and relate electromagnetic quantities in the physical and optical spacetimes.

4.3 Geometrical Optics Approximation

As before we write the covariant field tensor as

$$F_{ab} = \Re\left\{e^{iS/\lambda\!\!\!^{-}_0}\left(A_{ab} + \frac{\lambda\!\!\!^{-}_0}{i}B_{ab} + O(\lambda\!\!\!^{-}_0{}^2)\right)\right\}. \tag{4.25}$$

The A_{ab} term represents the geometrical optics approximation and the B_{ab} term is its first order correction. Defining the unitless (also metric independent) wave vector $k_a = \partial_a S$ and inserting Eq. (4.25) into the vacuum Maxwell equations we obtain to order $\lambda\!\!\!^{-}_0{}^{-1}$

$$\begin{aligned} A_{[ab}k_{c]} &= 0, \\ A^{ab}k_b &= 0, \end{aligned} \tag{4.26}$$

and to order $\lambda\!\!\!^{-}_0{}^{0}$

$$\begin{aligned} \partial_{[a}A_{bc]} + k_{[a}B_{bc]} &= 0, \\ \nabla_b A^{ab} + B^{ab}k_b &= 0. \end{aligned} \tag{4.27}$$

Equations (4.26) tell us that $k^a \equiv g^{ab}k_b$ is tangent to null geodesics of g_{ab}, i.e.,

$$\begin{aligned} k^a k_a &= 0, \\ k^b\nabla_b k^a &= 0, \end{aligned} \tag{4.28}$$

and that A_{ab} is of the form:

$$A_{ab} = -2k_{[a}\mathcal{E}_{b]}, \tag{4.29}$$

where $\mathcal{E}_a$ is spacelike and constrained by $\mathcal{E}_a k^a = 0$ with the remaining gauge freedom (to order $\lambda\!\!\!^{-}_0{}^0$) $\mathcal{E}_a \to \mathcal{E}_a + f(x)k_a$. Since $k^a m_a = 1$, we can use this freedom to choose $\mathcal{E}_a$ such that $\mathcal{E}_a m^a = 0$ or equivalently $\mathcal{E}_a u^a = 0$. For this choice, $\mathcal{E}^a$ is (up to a factor ω^{-1}) the amplitude of the electric field seen by observers at rest with respect to the fluid u^a. It is the geometrical optics approximation, i.e., Eq. (4.29) that makes the Maxwell field of Eq. (4.25) satisfy the needed transverse constraints of Eqs. (4.20) and (4.21) and hence allows us to introduce the transverse conformal transformation of Eq. (4.10). Before doing so we first finish the geometrical optics approximation for F^{ab} in the physical spacetime.

Equation (4.27) tells us that the order $\lambda\!\!\!^{-}_0{}^1$ correction to geometrical optics is of the form

$$B_{ab} = 2(\mathcal{E}_{[a,b]} - k_{[a}\mathcal{D}_{b]}), \tag{4.30}$$

with a remaining gauge freedom, to $O(\lambda\!\!\!^{-}_0{}^1)$, $\mathcal{D}_a \to \mathcal{D}_a + g(x)k_a$ and also gives the propagation equation for $\mathcal{E}^a$

$$\dot{\mathcal{E}}^a + \theta\mathcal{E}^a = \frac{k^a}{2}(\nabla_b\mathcal{E}^b + k_b\mathcal{D}^b), \tag{4.31}$$

where '$\cdot$' is the affine parameter rate of change along the null ray, $\dot{\mathcal{E}}^a \equiv k^b\nabla_b\mathcal{E}^a$, and θ is the expansion rate of the null congruence, $\theta \equiv \nabla_a k^a/2$. By splitting $\mathcal{E}^a = \mathcal{E}e^a$ into a scalar amplitude $\mathcal{E}$ and a unit polarization vector $e^a e^*_a = 1$, the

transport equation for the amplitude $\mathcal{E}$ becomes

$$\dot{\mathcal{E}} + \mathcal{E}\theta = 0. \tag{4.32}$$

The geometrical optics approximation, i.e., the $O(\lambda_0{}^0)$ term in Eq. (4.25), hence simplifies to

$$F^{ab} = -2\mathcal{E}\,\Re\{e^{iS/\lambda_0} k^{[a} e^{b]}\}. \tag{4.33}$$

As we have indicated above, because both the physical metric g_{ab} and optical metric $\tilde{g}_{ab}$ of Eq. (4.10) are defined on the same manifold we can compare properties of a common field such as F_{ab} in both spacetimes. For the above geometrical optics field all covariant quantities such as $\tilde{F}_{ab}, \tilde{k}_a, \tilde{m}_a$, and $\tilde{\mathcal{E}}_a$ in the optical spacetime are exactly the same as F_{ab}, k_a, m_a, and $\mathcal{E}_a$ in the physical spacetime. All contravariant components that lie in the k-m plane are also unchanged, i.e., $\tilde{k}^a = k^a, \tilde{m}^a = m^a$, and $\tilde{u}^a = u^a$. Consequently, quantities such as affine parameters, frequencies and wavelengths are the same in both spacetimes. However, transverse contravariant components, i.e., components in the orthogonal 2-dimensional spacelike surface are scaled by the conformal factor $e^{-2\sigma}$, e.g., $\tilde{\mathcal{E}}^a = e^{-2\sigma}\mathcal{E}^a$. This changes the magnitude to $\tilde{\mathcal{E}} = e^{-\sigma}\mathcal{E}$ with a new unit polarization vector $\tilde{e}^a = e^{-\sigma}e^a$ and the expansion parameter θ of Eq. (4.32) to $\tilde{\theta} = \theta + \dot{\sigma}$.

The time averaged 4-flux seen by an observer moving with the optical fluid is in general

$$S^a \equiv \frac{c}{8\pi}\Re\left\{H^{*ac}F_{cb} - \frac{1}{4}\delta^a_b H^{*dc}F_{cd}\right\}u^b. \tag{4.34}$$

In the physical and optical spaces (in vacuum) they are related by

$$\tilde{S}^a = e^{-2\sigma} S^a = -e^{-2\sigma} \frac{c}{8\pi} (u^b k_b) \mathcal{E}\mathcal{E}^* k^a, \tag{4.35}$$

and from the 3-D Poynting vector $S^a_\perp \equiv (g^{ab} + u^a u^b) S_b$ we find magnitudes related by

$$\tilde{S}_\perp = e^{-2\sigma} S_\perp = e^{-2\sigma} \frac{c}{8\pi} \mathcal{E}\mathcal{E}^* (u^b k_b)^2. \tag{4.36}$$

This result says that the intensity of a monochromatic wave can be reduced by a factor $e^{-2\sigma}$ at any point in spacetime by a transverse conformal transformation without altering the wave's frequency or wavelength. In the next section we equate this reduction of energy flux with absorption. In Sec. 4.6 when we combine absorption with refraction we reverse the process and assume that physical spacetime possesses the absorbing material and the transverse conformal transformation to the optical spacetime removes it.

4.4 A Transverse Conformal Transformation Versus Absorption

The attenuation coefficient κ_ν ($\mathrm{cm}^2 \cdot \mathrm{g}^{-1}$) is defined by looking at the amount of energy absorbed, dE_ν, in time dt by a pencil beam of radiation as it passes through a small slab of material of density ρ ($\mathrm{g} \cdot \mathrm{cm}^{-3}$), cross-section dA and length dl (see e.g. [61]),

$$dE_\nu = (\rho \kappa_\nu) I_\nu d\Omega d\nu dt dA dl. \tag{4.37}$$

All quantities are defined in the local rest (co-moving) frame of the optical fluid u^a. The specific intensity I_ν ($\times d\Omega d\nu$) measures the wave's intensity directed into solid angle $d\Omega$ and within the frequency range ν to $\nu + d\nu$. In the absence of emission the specific intensity $I_\nu(\tau)$, after traveling an optical depth $\tau \equiv \int \rho\kappa_\nu dl$ along a "characteristic" direction, differs from the value $I_\nu(0)$ it would have without absorption by

$$I_\nu(\tau) = I_\nu(0)e^{-\tau}. \tag{4.38}$$

Evaluating τ can be complicated because the frequency in the integrand is continually Doppler shifted due to the non-static nature of the optical fluid and/or the curvature of spacetime. The specific flux S_ν at any point is the first moment of specific intensity I_ν, i.e.,

$$S_\nu = 2\pi \int_{-1}^{1} \mu I_\nu d\mu. \tag{4.39}$$

For any I_ν that has a delta function dependence on direction, e.g., a geometrical optics wave, the corresponding value of the flux $S_\nu(\tau)$ seen by the observer in the presence of absorption is similarly related to the non-absorption value, i.e.,

$$S_\nu(\tau) = S_\nu(0)e^{-\tau}. \tag{4.40}$$

Comparing Eqs. (4.36) and (4.40) we find that a conformal factor σ reduces the flux by the exact same amount as absorption if

$$\sigma = \frac{1}{2}\tau. \tag{4.41}$$

If this conformal factor is to be unique, then either a single frequency is present at any spacetime point or the attenuation is "grey", i.e., the opacity $\alpha \equiv \rho\kappa_\nu$

is frequency independent. Even if there is only a single frequency present the frequency dependence in the absorption makes the calculation complicated. We must follow the frequency of each wave, starting from the source, as it is red/blue shifted and selectively absorbed while moving through the optical medium. In general a different conformal factor would exist for each source frequency. However, for the "grey" case the $\sigma(x^a)$ is unique. For a geometrical optics wave emanating from the world line of a point source, $\sigma(x^\mu)$ is defined on forward light cones (surfaces on which the eikonel S remains constant), i.e.,

$$\sigma(x^a) = \frac{1}{2}\int_{x_s^a}^{x^a} \rho(x'^b)\kappa_\nu(x'^b)dl. \tag{4.42}$$

The integration is performed along the null geodesic connecting the emitting event x_s^a and the spacetime point x^a. The density, attenuation coefficient, and spatial length element, respectively ρ, κ_ν, and dl, are measured in a sequence of local inertial frames ($u^a \propto \delta_0^a$) which are at rest with respect to the material along the null geodesic. We caution the reader that $\sigma(x^a)$ might not be globally defined, or even uniquely defined. The integral above is only defined for x^a which lies on forward light cones of the source. If the light source is turned on/off at some time (star birth/death) σ will only be defined on part of the spacetime manifold. However, its value can be taken as zero on the remainder. Furthermore, we might have multiple null geodesics connecting the emitting event S and receiving event O. For an example, when an Einstein ring occurs in a gravitational lensing configuration we have, in principle, an infinite number of null geodesics connecting S and O. These rays might pass through regions with different ρ's and κ_ν's and therefore give us different σ's. Rather than limiting the domain over which the conformal

transformation is defined to keep it single valued, we can extend the manifold to multiple layers and make the conformal factor unique on each layer. This is in direct analogy with Riemann's extension of the domain of a multi-valued complex function on R^2 to a Riemann surface on which its value is unique. This extended domain could be truly convoluted as for example in an inhomogeneous cosmology where strong lensing is prevalent.

The simplest example to illustrate a transverse conformal transformation is a plane electromagnetic wave traveling in Minkowski spacetime filled with stratified weakly absorbing gas. We suppose a monochromatic light source is lying infinitely far away ($z = -\infty$) and is producing a plane wave propagating in the $+z$ direction. The needed properties of a stratified gas filling the spacetime are summarized by the density $\rho(z)$ and attenuation coefficient $\kappa_\nu(z)$. The physical metric is

$$ds^2 = -c^2dt^2 + dx^2 + dy^2 + dz^2, \tag{4.43}$$

and the vector fields k^a and m^a in Eq. (4.7) are trivially ($u^a = \delta^a_t/c$)

$$\begin{aligned} k^a &= k\left(\frac{1}{c}, 0, 0, 1\right), \\ m^a &= \frac{1}{2k}\left(-\frac{1}{c}, 0, 0, 1\right). \end{aligned} \tag{4.44}$$

Equation (4.10) then gives

$$d\tilde{s}^2 = -c^2dt^2 + e^{2\sigma(z)}(dx^2 + dy^2) + dz^2, \tag{4.45}$$

where the conformal factor is related to the integral of the opacity by

$$\sigma(z) = \frac{1}{2}\int_{-\infty}^{z} \alpha(z')dz'. \tag{4.46}$$

We can now give a geometrical interpretation of Eq. (4.36). Because the rays in Eq. (4.44) are all running parallel to the z-axis the cross-sectional area of any bundle of rays is expanded by a factor $e^{2\sigma(z)}$ for the conformally transformed spacetime, Eq. (4.45), relative to initial the physical spacetime, Eq. (4.43). From the definition of flux, we can conclude that it will be reduced by the reciprocal factor $e^{-2\sigma}$. The reason the conformal factor was not applied to the whole 4-D metric now becomes clear: a $e^{2\sigma}$ factor in front of the entire physical metric would produce an undesirable time dilation factor e^{σ} as well as a frequency shift factor $e^{-\sigma}$. These two combined would have contributed another factor of $e^{-2\sigma}$ to the wave's flux in the conformal spacetime. We can also look at the electric field $\mathbf{E}$ and the magnetic field $\mathbf{H}$ in both spacetimes and see that in the conformal spacetime they are each diminished by a factor $e^{-\sigma}$. Consequently the flux, $\mathbf{E} \times \mathbf{H}$, is reduced by $e^{-2\sigma}$. (This reduction in amplitude/intensity matches that of weak absorption given in [17] but, not unexpectedly, differs from that of strong absorption, i.e., Eqs. (28)-(30) of [17]).

4.5 Absorption in Robertson-Walker Spacetimes

The interesting example for cosmology is absorption by the Intergalactic Medium (IGM) which is modeled as absorption by the cosmological fluid in Robertson-Walker spactimes. The familiar RW metric can be written in co-moving coordinates

$(u^a = \delta^a_t/c)$ as

$$ds^2 = -c^2\,dt^2 + R^2(t)\left\{\frac{dr^2}{1-kr^2} + r^2(d\theta^2 + \sin^2\theta\,d\phi^2)\right\}, \tag{4.47}$$

where $k = 1, 0, -1$ for a closed, flat or open universe, respectively. The eikonal of Eq. (4.33) for a point source located at $r = 0$ (see [17]) is

$$S(t,r) = R_0\left(-\int_{t_e}^{t}\frac{c\,dt'}{R(t')} + \mathrm{sinn}^{-1}[r]\right), \tag{4.48}$$

where R_0 is radius of the universe at the observation time t_0. The corresponding radial null geodesics are

$$k^a = R_0\left(\frac{1}{c\,R(t)}, \frac{\sqrt{1-kr^2}}{R^2(t)}, 0, 0\right), \tag{4.49}$$

for which Eq. (4.7) gives

$$m^a = \frac{R(t)}{2R_0}\left(-\frac{1}{c}, \frac{\sqrt{1-kr^2}}{R(t)}, 0, 0\right), \tag{4.50}$$

and from which it follows that

$$2m_{(a}k_{b)} = \mathrm{diag}\left[-c^2, \frac{R^2(t)}{1-kr^2}, 0, 0\right]. \tag{4.51}$$

Equation (4.10) then gives the optical metric

$$d\tilde{s}^2 = -c^2\,dt^2 + R^2(t)\left\{\frac{dr^2}{1-kr^2} + e^{2\sigma}r^2(d\theta^2 + \sin^2\theta\,d\phi^2)\right\}. \tag{4.52}$$

An observer at (r,t) will see the source redshifted an amount z as a function of

co-moving radius r and observing instant t, which can be obtained by integrating Eq. (4.49). If the dynamics of the RW spacetime is determined by general relativity, and the gravity source is a mixture of non-interacting perfect fluids, the redshift can be found by inverting

$$r(t,z) = \mathrm{sinn}\left[\frac{c}{R(t)H(t)}\int_0^z \frac{dz'}{h(z')}\right], \tag{4.53}$$

where $h(z)$ was defined in Eq. (1.96).

For spatially homogeneous and nondispersive (grey) absorption the differential optical depth $d\tau$ is related to the opacity α by

$$\begin{aligned} d\tau =& -\alpha(cdt) \\ =& \ \alpha\frac{c}{H}\frac{1}{(1+z)}\frac{dz}{h(z)}, \end{aligned} \tag{4.54}$$

and the total optical depth $\tau(r,t)$ of a source at $(0, t_e(r,t))$ seen by an observer at (r,t) is the integral

$$\tau(z) = \frac{c}{H(t)}\int_0^z \frac{\alpha(z')}{(1+z')h(z')}dz'. \tag{4.55}$$

The conformal factor σ of Eq. (4.52) is therefore one-half this value.

The presence of absorption changes the distance modulus-redshift relation $\mu(z)$, e.g., the magnitudes of supernovae are corrected for absorption by the IGM before drawing a Hubble diagram. From the definition of distance modulus

$$\mu \equiv 5\log\frac{d_L}{1\mathrm{Mpc}} + 25, \tag{4.56}$$

and luminosity distance d_L in terms of flux S

$$d_L = \left(\frac{L}{4\pi S}\right)^{1/2}, \tag{4.57}$$

we immediately obtain via Eq. (4.40) the absorption-corrected luminosity distance

$$\tilde{d}_L = e^{\tau/2} d_L, \tag{4.58}$$

and the corrected distance modulus $\tilde{\mu}$

$$\tilde{\mu} = \mu + \frac{5}{2\ln 10}\tau. \tag{4.59}$$

This is the normal interpretation of the increase in luminosity distance caused by light absorption. If we use the optical metric to compute luminosity distance (see e.g. [35]) we find that compared with the physical metric the cross-sectional area of the ray bundle is expanded by a factor $e^{2\sigma}$ which reduces the received flux by a factor of $e^{-2\sigma}$, i.e., from Eq. (4.52)

$$\tilde{d}_L = e^{\sigma(r_o,t_o)}(1+z)R_0 r = e^{\sigma} d_L. \tag{4.60}$$

We see that by identifying σ with $\tau/2$ we have the same luminosity distance in the optical spacetime with no absorption as in the physical spacetime with absorption.

4.6 Incorporating Both Refraction and Absorption into the Optical Metric

Up to now, we have been considering only absorption, however, we know that besides having its flux reduced, a light wave's path and speed can be altered (refracted) due to the presence of a polarizable material. Recall that Gordon modified Einstein's physical spacetime metric to include the effects of a nondispersive refractive material on Maxwell's theory. His theory accounts for any polarizable material whose constitutive properties are summarized by two scalar functions, a permittivity $\epsilon(x^a)$ and a permeability $\mu(x^a)$. His optical metric $\bar{g}_{ab}$ [41] is defined on the same differentiable manifold as Einstein's spacetime metric g_{ab} and is related to it by

$$\bar{g}_{ab} = g_{ab} + \left(1 - \frac{1}{n^2}\right) u_a u_b, \quad \bar{g}^{ab} = g^{ab} + \left(1 - n^2\right) u^a u^b, \tag{4.61}$$

where $n(x^a) = \sqrt{\epsilon\mu}$ is the refractive index and u^a is the 4-velocity of the optical fluid, normalized using the physical spacetime metric g_{ab}. Even though we can incorporate absorption of only geometrical optics waves into Gordon's metric, his index of refraction theory applies to all Maxwell fields, see [17] for some related examples. The modified Maxwell equations are

$$\begin{aligned} \bar{F}_{[ab,c]} &= 0, \\ \bar{\nabla}_b \left(\sqrt{\epsilon/\mu}\, \bar{F}^{ab}\right) &= 0, \end{aligned} \tag{4.62}$$

and the fields in optical and physical spacetimes are connected by

$$H^{ab} = \frac{1}{\mu}\bar{F}^{ab},$$
$$F_{ab} = \bar{F}_{ab}. \tag{4.63}$$

We now generalize Gordon's optical metric to include effects of an additional isotropic and frequency independent (grey) attenuation coefficient κ_ν on a radiation field described by the geometrical optics approximation. To obtain this result we simply apply a transverse conformal transformation of Eq. (4.10) to Gordon's metric Eq. (4.61). The geometrical optics theory in Gordon's optical spacetime is almost identical to the geometrical optics theory of the physical spacetime given in Sec. 4.3 (see Sec. III of [17]), e.g., the contravariant components of the Maxwell field are correctly given by Eq. (4.33)

$$\bar{F}^{ab} = -2\mathcal{E}\,\Re\{e^{iS/\lambda_0}\bar{k}^{[a}\bar{e}^{b]}\}. \tag{4.64}$$

Here

$$\bar{k}^a = \bar{g}^{ab}\partial_b S, \tag{4.65}$$

is tangent to null geodesics of the optical metric, and tangent to the corresponding timelike "slower than light" curves of the physical metric, $\bar{e}^b$ is the unit (in the optical metric) polarization vector, and S is the eikonal function. The significantly different equation is the transport equation for the amplitude of the wave given by Eq. (4.32), which becomes

$$\dot{\mathcal{E}} + \theta\mathcal{E} + \dot{\phi}\mathcal{E} = 0, \tag{4.66}$$

(see Eq. (18) of [17]). The presence of the additional term $\phi \equiv (1/4)\ln(\epsilon/\mu)$ is due to the afore mentioned modification of Maxwell's equations [see Eq. (4.62)] in Gordon's optical spacetime.

From Eqs. (4.10) and (4.11) the new optical metric becomes

$$\tilde{g}_{ab} = e^{2\sigma}\bar{g}_{ab} + (1 - e^{2\sigma})2\bar{m}_{(a}\bar{k}_{b)}, \quad \tilde{g}^{ab} = e^{-2\sigma}\bar{g}^{ab} + (1 - e^{-2\sigma})2\bar{m}^{(a}\bar{k}^{b)}. \quad (4.67)$$

where $\bar{m}^a$ from Eq. (4.7) is a null vector field in Gordon's optical spacetime defined by

$$\bar{m}^a = \frac{\bar{k}^a}{2(\bar{u}_b\bar{k}^b)^2} + \frac{\bar{u}^a}{(\bar{u}_b\bar{k}^b)}, \quad (4.68)$$

and $\bar{u}^a$ the fluid's 4-velocity normalized using Gordon's optical metric

$$\bar{u}^a = nu^a, \;\; \bar{u}_a = \frac{1}{n}u_a. \quad (4.69)$$

The reader should observe that the transverse conformal transformation does not alter the orthogonality of the two 2-D subspaces nor does it alter the metric structure of the timelike 2-D space spanned by $\bar{u}^a$ and $\bar{k}^a$. Rewriting the new optical metric Eq. (4.67) in terms of the physical metric g_{ab} and physical observer u_a we have

$$\tilde{g}_{ab} = e^{2\sigma}g_{ab} + e^{2\sigma}\left(1 - \frac{1}{n^2}\right)u_a u_b + \frac{1 - e^{2\sigma}}{n^2(u\cdot k)^2}\left[k_a k_b + 2(u\cdot k)k_{(a}u_{b)}\right], \quad (4.70)$$

with inverse

$$\tilde{g}^{ab} = e^{-2\sigma}g^{ab} + (1 - n^2)e^{-2\sigma}u^a u^b + \frac{1 - e^{-2\sigma}}{n^2(u\cdot k)^2}[\tilde{k}^a\tilde{k}^b + 2n^2(u\cdot k)u^{(a}\tilde{k}^{b)}], \quad (4.71)$$

where

$$\tilde{k}^a \equiv \tilde{g}^{ab} S_{,b} = \bar{g}^{ab} S_{,b} = g^{ab} S_{,b} + (1 - n^2) u^a (u^b S_{,b}), \tag{4.72}$$

and determinant

$$\det \tilde{g} = \frac{e^{4\sigma}}{n^2} \det g. \tag{4.73}$$

The new Maxwell field

$$\begin{aligned} \tilde{F}^{ab} &= \mu e^{-2\sigma} H^{ab}, \\ \tilde{F}_{ab} &= F_{ab}, \end{aligned} \tag{4.74}$$

satisfies the same equations as $\bar{F}^{ab}$, i.e., Eq. (4.62), but $\tilde{g}_{ab}$ has the advantage of incorporating both refraction and absorption. We now have a correspondence of geometrical optics waves in two spacetimes, the physical and the optical. In the physical spacetime the wave travels at a reduced speed c/n with an intensity that is reduced by absorption as in Eq. (4.38) whereas in the optical spacetime the wave travels at speed c with no extinction.

4.7 The Optical Metric in FLRW Cosmology with Both Refraction and Absorption

The formalism developed above appears complicated when applied to an arbitrary spacetime, however, for specific cases the formalism is more transparent. For example we reconsider RW spacetime, but this time with both refraction n and absorption κ associated with the cosmic fluid. The result is elegantly simple. The

optical metric for the RW metric [17] is

$$d\bar{s}^2 = -\frac{c^2}{n^2}dt^2 + R^2(t)\left\{\frac{dr^2}{1-kr^2} + r^2(d\theta^2 + \sin^2\theta\, d\phi^2)\right\}. \tag{4.75}$$

For spherical waves the radial null geodesics are

$$\bar{k}^a = R_0\left(\frac{n}{c\,R}, \frac{\sqrt{1-kr^2}}{R^2}, 0, 0\right), \tag{4.76}$$

and from Eq. (4.68) we find

$$\bar{m}^a = \frac{R}{2R_0}\left(-\frac{n}{c}, \frac{\sqrt{1-kr^2}}{R}, 0, 0\right). \tag{4.77}$$

Immediately we find

$$2\bar{m}_{(a}\bar{k}_{b)} = \text{diag}\,\left(-\frac{c^2}{n^2}, \frac{R^2}{1-kr^2}, 0, 0\right), \tag{4.78}$$

which gives us

$$d\tilde{s}^2 = -\frac{c^2}{n^2}dt^2 + R^2(t)\left\{\frac{dr^2}{1-kr^2} + e^{2\sigma}r^2(d\theta^2 + \sin^2\theta\, d\phi^2)\right\}. \tag{4.79}$$

With dynamics supplied by the FLRW solutions the scalar function σ in the above equation is

$$\begin{aligned}\sigma(r,t) &\equiv \frac{1}{2}\int_{t_e}^{t}\alpha\,\frac{c\,dt'}{n} \\ &= \frac{1}{2}\frac{c}{H(t)}\int_0^{z(z_n)}\frac{\alpha(z')}{n(z')(1+z')h(z')}dz'.\end{aligned} \tag{4.80}$$

Note the difference between wavelength redshift z and frequency redshift z_n (see Sec. 2.2 and [17]):

$$1+z=\frac{R_0}{R(t_e)},\ 1+z_n=\frac{n(t_o)}{n(t_e)}\frac{R_0}{R(t_e)}. \tag{4.81}$$

We have discussed the impact of light refraction on the distance-redshift relation in [17]. Now incorporating absorption we find from Eq. (4.79) that the angular diameter distance $\tilde{d}_A$ in $\tilde{g}_{ab}$ is

$$\tilde{d}_A=R(t_e)e^{\sigma(0,t_e)}r=R(t_e)r=\bar{d}_A, \tag{4.82}$$

($\sigma(0,t_e)$ vanishes because of the zero optical depth from the source event to itself) where

$$\bar{d}_A(z_n)=\frac{1}{[1+z(z_n)]}\frac{c}{H_0}\frac{1}{\sqrt{|\Omega_k|}}\mathrm{sinn}\left[\sqrt{|\Omega_k|}\int_0^{z(z_n)}\frac{dz}{n(z)h(z)}\right]. \tag{4.83}$$

Finally the luminosity distance $\tilde{d}_L$ is (see [35, 17])

$$\tilde{d}_L=(1+z_n)(1+z)e^{\sigma}d_A=e^{\sigma}\bar{d}_L. \tag{4.84}$$

We thus obtained the same luminosity-redshift relation we obtained in [17] for the real eikonal case (refer to Eq. (66) of [17]) by changing the geometry rather than absorbing some of the wave's intensity. Just as in [17], Eq. (4.84) differs from the standard reciprocity relation $d_L(z)=(1+z)^2d_A(z)$ in two aspects: first, the existence of refraction causes photon orbits to deviate from null geodesics in the physical spacetime, this giving the $1+z_n$ factor instead of $1+z$; second, light absorption (expressed by the conformal factor σ) violates the photon number con-

servation law which is required to obtain the reciprocity relation. For an interesting discussion about using cosmic distance-duality as a probe of acceleration/exotic physics, see [8].

4.8 An Application: FLRW Spacetime with Both Refraction and Absorption

In Chapter 2 and 3 (see [16, 17]) we have interpreted the observed apparent increase in the universe's expansion rate as caused by light refraction and absorption respectively, instead of by a cosmological constant Λ. In Chapter 2 [16] we used a two parameter pure refraction model, i.e., $n(z) = 1 + pz^2 + qz^3$, without absorption to fit the supernovae gold sample [43]. In Chapter 3 [17] we fit the sample with a pure absorption model, i.e., we took $n = 1$, and the opacity $\alpha(z) \equiv \rho(z)\kappa(z) = \text{const}$. In this section, we fit the same data set with a CDM model containing both refraction and absorption. We use simple expressions $n(z) = 1 + pz^2$ and $\alpha(z) = \text{const}$ that depend on only two parameters. Since we are concerned with the matter dominated era, we have excluded radiation ($\Omega_r = 0$) and since we are trying to only emulate acceleration we take $\Lambda = 0$. We choose the current Hubble constant to be $H_0 = 65\,\text{km/s/Mpc}$ and fit our two parameter $(\alpha,\ p)$ model for different choices of Ω_m. The scaled Hubble function $h(z)$ in this case simplifies to

$$h(z) = (1+z)\sqrt{1+\Omega_\text{m} z}. \tag{4.85}$$

The refraction and absorption corrected distance-redshift relation is now written as

$$\tilde{d}_L(z_n) = (1+z_n)\frac{c}{H_0}\frac{e^{\sigma(z_n)}}{\sqrt{|\Omega_k|}}\mathrm{sinn}\sqrt{|\Omega_k|}\int_0^{z(z_n)}\frac{dz'}{n(z')h(z')}, \tag{4.86}$$

where

$$\sigma(z_n) = \frac{\alpha}{2}\frac{c}{H_0}\int_0^{z(z_n)}\frac{dz'}{(1+z')n(z')h(z')}, \tag{4.87}$$

and

$$1+z_n = \frac{1+z}{1+pz^2}. \tag{4.88}$$

Our results are shown in Figures 4.1 and 4.2. In Fig. 4.1, we show the $\Delta\mu(z)$ curves for different model parameters. Here $\Delta\mu(z) \equiv \mu(z) - \mu_F(z)$, where $\mu_F(z)$ is the distance modulus of the fiducial, matter only, model (horizontal black dashed curve in Fig. 4.1), i.e., $\Omega_\Lambda = 0, \Omega_\mathrm{m} = 0.3, \alpha = 0, p = 0$. In each of the four frames the green curve is the concordance model, $\Omega_\Lambda = 0.7, \Omega_\mathrm{m} = 0.3, \alpha = 0, p = 0$. In the upper left panel we show a few absorption models with no refraction index ($\Omega_\mathrm{m} < 1$ for all curves in this panel). The dotted red curve has: $\Omega_\Lambda = 0, \Omega_\mathrm{m} = 0.05, \alpha = 0.7 \times 10^{-4}\mathrm{Mpc}^{-1}, n = 1$. The short-dashed red curve has: $\Omega_\Lambda = 0, \Omega_\mathrm{m} = 0.3, \alpha = 1.3 \times 10^{-4}\mathrm{Mpc}^{-1}, n = 1$. The solid black curve has: $\Omega_\Lambda = 0, \Omega_\mathrm{m} = 0.73, \alpha = 2.2 \times 10^{-4}\mathrm{Mpc}^{-1}, n = 1$. In the upper right panel the models are flat. The blue curve has: $\Omega_\Lambda = 0, \Omega_\mathrm{m} = 1.0, \alpha = 2.5 \times 10^{-4}\mathrm{Mpc}^{-1}, p = 0$. The red curve has: $\Omega_\Lambda = 0, \Omega_\mathrm{m} = 1.0, \alpha = 2.5 \times 10^{-4}\mathrm{Mpc}^{-1}, p = 0.024$. In the bottom left panel the blue curve has: $\Omega_\Lambda = 0, \Omega_\mathrm{m} = 1.5, \alpha = 3.3 \times 10^{-4}\mathrm{Mpc}^{-1}, p = 0$. The red curve has: $\Omega_\Lambda = 0, \Omega_\mathrm{m} = 1.5, \alpha = 3.3 \times 10^{-4}\mathrm{Mpc}^{-1}, p = 0.042$. In the bottom right panel the blue curve has: $\Omega_\Lambda = 0, \Omega_\mathrm{m} = 2.0, \alpha = 4.1 \times 10^{-4}\mathrm{Mpc}^{-1}, p = 0$. The red curve has: $\Omega_\Lambda = 0, \Omega_\mathrm{m} = 2.0, \alpha = 4.1 \times 10^{-4}\mathrm{Mpc}^{-1}$, and $p = 0.049$.

In Fig. 4.2 we show the confidence contours (68.3%, 95.4%, and 99.73%) of our two parameter (α, p) model with different choices of $\Omega_{\rm m}$. We show 6 different cases with $\Omega_{\rm m} = 0.05$ (baryonic matter only), $\Omega_{\rm m} = 0.3$ (dark matter only), $\Omega_{\rm m} = 0.73$ (our least χ^2 pure absorption model, see [17]), $\Omega_{\rm m} = 1.0$ (flat universe), $\Omega_{\rm m} = 1.5$ and 2.0 (closed universe model). We restrict the parameter p to be nonnegative to keep the light speed $v = c/n$ less than c. For the first three cases, i.e., $\Omega_{\rm m} = 0.05, 0.3$ and 0.73, the best fits occurs for $p = 0$, which suggests that introducing additional refraction parameters would not significantly improve the fitting when absorption is present. However, as $\Omega_{\rm m}$ increases, nonvanishing p values give better fits. For $\Omega_{\rm m} = 1.0$, the best fitting parameters ($\chi^2 = 1.04$) are $\alpha = 2.5 \times 10^{-4}{\rm Mpc}^{-1}, p = 0.024$. For $\Omega_{\rm m} = 1.5$, the best fitting ($\chi^2 = 1.05$) parameters are $\alpha = 3.3 \times 10^{-4}{\rm Mpc}^{-1}, p = 0.042$. For $\Omega_{\rm m} = 2.0$, the best fitting ($\chi^2 = 1.06$) parameters are $\alpha = 4.1 \times 10^{-4}{\rm Mpc}^{-1}, p = 0.049$. This can also be seen from Fig. 4.1: In the upper right and two bottom frames, the blue and red curves have the same absorption coefficient α, the difference is that the red curve has p nonzero whereas the blue curve has $p = 0$. The inclusion of p for these large $\Omega_{\rm m}$ cases improves the fitting.

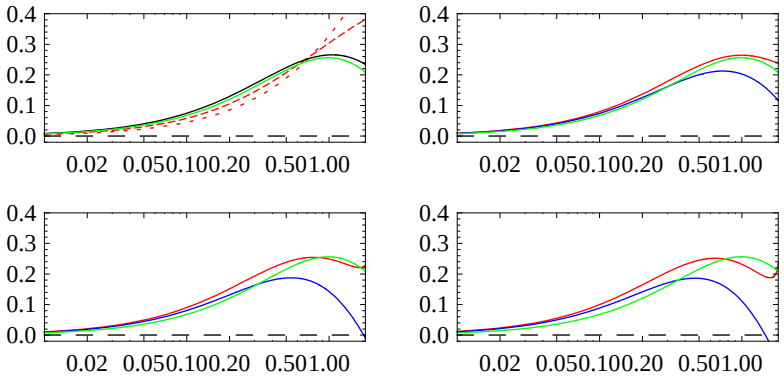

Figure 4.1: $\Delta\mu$ versus z. In each of the four frames the fiducial model (horizontal black dashed) is the now disfavored dark matter only model, i.e., $\Omega_\Lambda = 0, \Omega_{\rm m} = 0.3, \alpha = 0, p = 0$, and the green curve is the concordance model, $\Omega_\Lambda = 0.7, \Omega_{\rm m} = 0.3, \alpha = 0, p = 0$. Upper left panel: pure absorption models with no refraction. Dotted red curve, $\Omega_\Lambda = 0, \Omega_{\rm m} = 0.05, \alpha = 0.7 \times 10^{-4}{\rm Mpc}^{-1}, n = 1$. Short-dashed red curve, $\Omega_\Lambda = 0, \Omega_{\rm m} = 0.3, \alpha = 1.3 \times 10^{-4}{\rm Mpc}^{-1}, n = 1$. Solid black curve: $\Omega_\Lambda = 0, \Omega_{\rm m} = 0.73, \alpha = 2.2 \times 10^{-4}{\rm Mpc}^{-1}, n = 1$. Upper right panel: blue curve, $\Omega_\Lambda = 0, \Omega_{\rm m} = 1.0, \alpha = 2.5 \times 10^{-4}{\rm Mpc}^{-1}, p = 0$. Red curve, $\Omega_\Lambda = 0, \Omega_{\rm m} = 1.0, \alpha = 2.5 \times 10^{-4}{\rm Mpc}^{-1}, p = 0.024$. Bottom left panel: blue curve, $\Omega_\Lambda = 0, \Omega_{\rm m} = 1.5, \alpha = 3.3 \times 10^{-4}{\rm Mpc}^{-1}, p = 0$. Red curve, $\Omega_\Lambda = 0, \Omega_{\rm m} = 1.0, \alpha = 3.3 \times 10^{-4}{\rm Mpc}^{-1}, p = 0.042$. Bottom right panel: blue curve, $\Omega_\Lambda = 0, \Omega_{\rm m} = 2.0, \alpha = 4.1 \times 10^{-4}{\rm Mpc}^{-1}, p = 0$. Red curve, $\Omega_\Lambda = 0$, $\Omega_{\rm m} = 2.0$, $\alpha = 4.1 \times 10^{-4}{\rm Mpc}^{-1}$, $p = 0.049$.

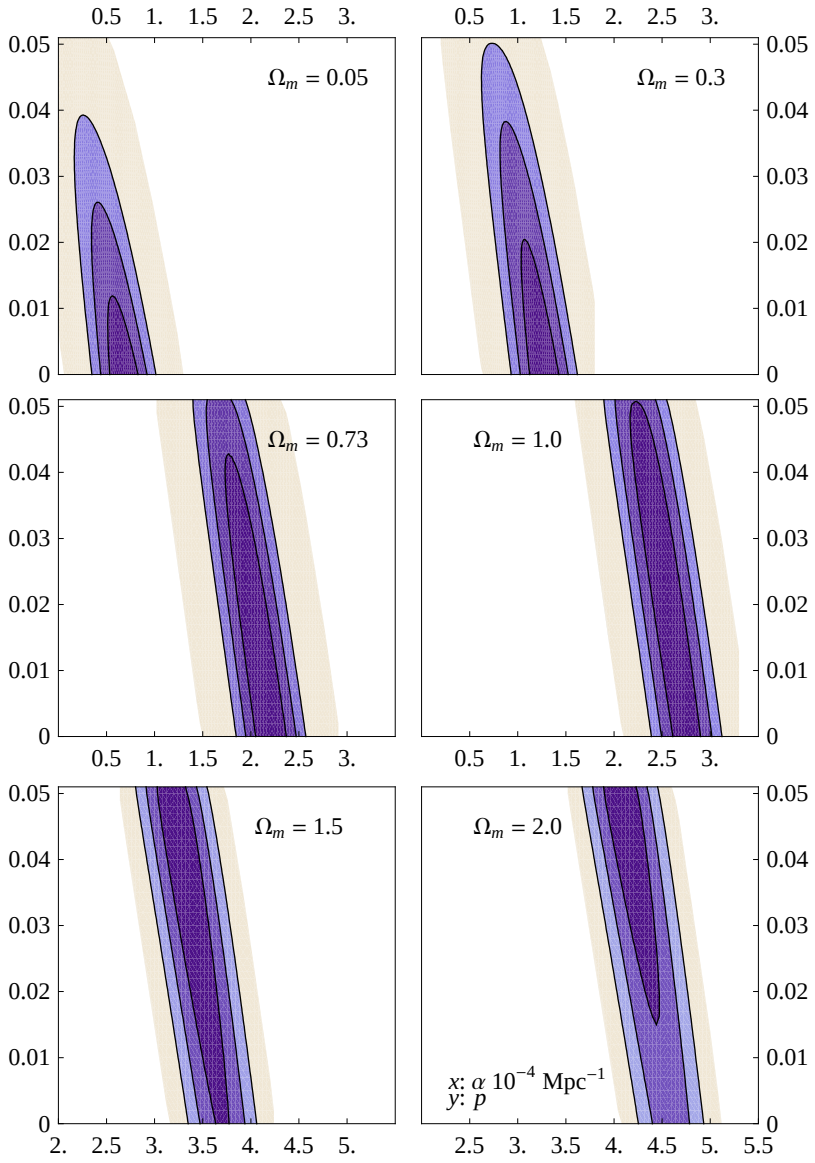

Figure 4.2: Confidence contours (68.3%, 95.4%, and 99.73%) for each fixed $\Omega_{\rm m}$ model. The x coordinate is absorption coefficient α in unit of $10^{-4}{\rm Mpc}^{-1}$, and the y-axis is refraction index parameter p ($n = 1+pz^2$). Top left panel, $\Omega_{\rm m} = 0.05$, with least chi-square (per degree of freedom) $\chi^2 = 1.09$, the best fitting parameters are $\alpha = 0.7 \times 10^{-4}{\rm Mpc}^{-1}$, $p = 0$. Top right panel, $\Omega_{\rm m} = 0.3$, least $\chi^2 = 1.05$, the best fitting parameters are $\alpha = 1.3 \times 10^{-4}{\rm Mpc}^{-1}$, $p = 0$. Middle left panel, $\Omega_{\rm m} = 0.73$, least $\chi^2 = 1.035$, the best fitting parameters are $\alpha = 2.2 \times 10^{-4}{\rm Mpc}^{-1}$, $p = 0$. Middle right panel, $\Omega_{\rm m} = 1.0$, least $\chi^2 = 1.042$, at $\alpha = 2.5 \times 10^{-4}{\rm Mpc}^{-1}$, $p = 0.024$. Bottom left, $\Omega_{\rm m} = 1.5$, least $\chi^2 = 1.05$, the best fitting parameters are $\alpha = 3.3 \times 10^{-4}{\rm Mpc}^{-1}$, $p = 0.042$. Bottom right, $\Omega_{\rm m} = 2.0$, least $\chi^2 = 1.06$, the best fitting parameters are $\alpha = 4.1 \times 10^{-4}{\rm Mpc}^{-1}$, $p = 0.049$.

4.9 Discussion

In this chapter, we introduced the concept of a "transverse" conformal transformation, which allowed us to equate the intensity reduction of light caused by absorption with a geometrical reduction caused by the expansion of the cross-sectional area of the ray bundle without changing other desirable properties of geometrical waves, such as frequency and wavelength. This application of conformal transformations is new. We use it to generalize Gordon's optical metric to include light absorption via such a conformal transformation. This generalization is fundamentally different from chapter 3 in which we included light absorption by making Gordon's metric complex. In the complex metric formalism, we distinguished two different cases: strong and weak absorption. The strong case is where a non-negligible amount of absorption occurs on a wavelength scale and the weak case is where absorption is significant only over multitudes of wavelengths. In the strong case the eikonal remains complex but in the weak case it can be taken as real. In this paper we were able to replace the effects of weak absorption by a special conformal transformation. The disadvantage of this formalism is that the optical metric depends on the eikonal of the wave itself whereas in [17] it did not. We used this new optical metric to derived the absorption and refraction corrected distance-redshift relation for RW spacetimes and obtained exactly the same expression as in [17] for weak absorption. In [16] we fit supernovae Hubble data with a pure refraction model, and in [17] we fit it with a pure absorption model. In this chapter, we fit the data with a cosmological model possessing both refraction and absorption. We have shown that a single parameter polynomial for the refraction index, i.e., $n(z) = 1 + pz^2$, together with a constant opacity parameter α fits the

data well. More realistic z dependent models for α and n are appropriate.

The Supernova data is currently considered to be the most compelling evidence for the existence of dark energy because of the apparent acceleration observed in the expansion of the universe (see e.g. [70, 65]). Competing interpretations have been proposed, e.g., evolutionary effects [29, 23], local Hubble bubbles [24, 96], absorption [75], modified gravity [37, 52, 10] and others such as slowly changing fundamental constants [3, 7]. There are at least four different sources of opacity: the Milky Way, the hosting galaxy, intervening galaxies, and the IGM that should be taken into account. The Galactic absorption has been studied extensively [81, 59] and early constraints on properties of IGM were often obtained assuming the applicability of Galactic dust properties (see e.g. [95]). The luminosity of high redshift supernovae have been corrected for host galaxy absorption using the Galactic reddening law, see e.g. [65, 68, 69, 70]. We have to be careful when applying Galactic dust properties to the IGM, since the composition, size, shape, and alignment of intergalactic dust could be significantly different than that of Milky Way dust. Aguirre [1, 2] introduced a carbon needle model and showed that dust grains of larger size ($\geq 1\,\mu m$), which should be preferentially ejected by star burst galaxies, would have relatively higher opacities (e.g. $\kappa \sim 10^5\,\mathrm{cm}^2\,g^{-1}$) and much greyer absorption curves, and therefore might escape the reddening censorship based on Galactic reddening law. Evidence against this model appeared in [26, 49, 86]. Goobar et al. [40] introduced a replenishing dust model in which the dilution caused by cosmic expansion is continually replenished ($\rho = \rho_0(1+z)^3$ for $z < 0.5$, $\rho = \rho_0$ for $z \geq 0.5$). This dust model is indistinguishable from Ω_Λ and cannot be ruled out by Supernovae data alone (see table 5 of [72]). Bassett et al. [8] claimed to rule out the replenishing model at more than 4σ by con-

sidering violations of distance duality (reciprocity relation). Östman & Mörtsell [62] further constrained the magnitude of grey dust absorption from Quasar colors and spectra and claimed that for a wide range of intergalactic dust models, extinction larger than 0.2 mag is ruled out (see also [46, 25]). A new grey dust model is proposed in [74]. More complicated and fine tuned dust models will keep emerging in the future until dark matter/energy has been identified, if in fact it exists. In this application we ignored effects of inhomogeneities including the possibility of having a multi-valued conformal factor. We assumed that none of the SN Ia used were strongly lensed. Since the flat concordance model is supported by other observations, e.g., the angular position of the first acoustic peak as measured by WMAP (Wilkinson Microwave Anisotropy Probe) team [84, 85], and baryonic acoustic oscillations (BAO) detected in galaxy surveys [34, 88, 89], an absorption and/or refraction theory cannot be on firm ground unless it is consistent with these additional observations. We leave these and other applications to future efforts.

Conclusions

In this dissertation we reviewed Gordon's optical metric theory and generalized it to include light absorption in two different ways: first, by defining a complex refraction index $N(x^a)$ and allowing Gordon's metric to become complex, and second, by applying a "transverse" conformal transformation to Gordon's original metric. The first case was applicable to both strong and weak absorptions, whereas the latter case works only for weak absorption.

We applied our theory to cosmology and provided an alternate explanation of the apparent acceleration of the universe's expansion by fitting the current supernovae data to three simple models: a model with only refraction ($n(z) = 1 + pz^2 + qz^3$), a model with pure absorption ($n = 1$, and $\alpha = \text{const}$), and a model with both refraction and absorption ($n = 1 + pz^2$ and $\alpha = \text{const}$). We also tried to explain the flatness of universe as implied by the WMAP data via our refraction corrected angular-diameter distance redshift relation in Chapter 2. One important cosmological subject we did not tackle was baryonic acoustic oscillations; this we leave to future work.

In Sec. 2.3 we have shown that up to 1^{st} order approximation, the inhomogeneity of a flat ($k = 0$) FLRW universe can be identified with an equivalent effective refraction index and therefore incorporated in our optical metric theory. To extend

the formalism in [76] to the non-flat case, in particular, to the open universe case ($k < 0$), and to estimate the magnitude of the perturbations needed to fit the cosmological data is an interesting problem to work on.

In Sec. 1.5 we introduced the concept of optical scalars and their transport equations. Assuming that the background spacetime is filled with dielectric material, i.e., with a real/complex refraction index, how would the transport equations of optical scalars be impacted? This also is an interesting problem to work on.

Throughout this dissertation, one important assumption we have made about the dielectric property of the materials filling the spacetime is its nondispersiveness, i.e., its greyness. Can we generalize Gordon's formalism to more realistic cases where the permittivity ϵ and permeability μ, or the refraction index n actually depend on frequency? This would give us an optical metric defined on the phase space of photons (the tangent bundle of the spacetime manifold). Can we build up the formalism using a more advanced theory in differential geometry, such as a Finsler geometry or a complex manifold [19, 20]?

Bibliography

[1] A. N. Aguirre, Astrophys. J. 512, L19 (1999).

[2] A. N. Aguirre, Astrophys. J. 525, 583 (1999).

[3] A. Albrecht & J. Magueijo, Phys. Rev. D 59, 043516 (1999).

[4] H. Alnes, M. Amarzguioui, and O. Gron, Phys. Rev. D 73, 083519 (2006).

[5] H. Alnes & M. Amarzguioui, Phys. Rev. D 74, 103520 (2006).

[6] P. Astier et al. Astron. Astrophys. 447, 31 (2006).

[7] J. D. Barrow, Phys. Rev. D 59, 043515 (1999).

[8] B. A. Bassett, S. Liberati, C. Molina-Paris, and M. Visser, Phys. Rev. D 62, 103518 (2000).

[9] B. A. Bassett & M. Kunz, Phys. Rev. D 69, 101305(R) (2004).

[10] E. Bertschinger & P. Zukin, Phys. Rev. D 78, 024015 (2008).

[11] B. Bertotti, Proc. R. Soc. A. 294, 195 (1966).

[12] S. Bianchi & A. Ferrara, Mon. Not. R. Astron. Soc. 358, 379 (2005).

[13] N. Brouzakis, B. Tetradis, and E. Tzavara, arXiv:astro-ph/0703586v2.

[14] C. Boehm & R. Schaeffer, Astron. Astrophys. 438, 419 (2005).

[15] M. P. Carmo, *Riemannian Geometry* (Birkhäuser, Boston, 1992).

[16] B. Chen & R. Kantowski, Phys. Rev. D 78, 044040 (2008).

[17] B. Chen & R. Kantowski, Phys. Rev. D 79, 104007 (2009).

[18] B. Chen & R. Kantowski, arXiv:0907.5042v1, Phys. Rev. D (to be published).

[19] S. S. Chern, W. H. Chen & K. S. Lam, *Lectures on Differential Geometry* (World Scientific, Singapore, 1999).

[20] S. S. Chern, *Complex Manifolds without Potential Theory* (Springer-Verlag, New York, 2008).

[21] C. H. Chuang, J. A. Gu, and W. Y. P. Hwang, arXiv:astro-ph/0512651.

[22] D. J. H. Chung & A. E. Romano, Phys. Rev. D 74, 103507 (2006).

[23] F. Combes, New Astron. Rev. 48, 583 (2004).

[24] A. Conley et al., Astrophys. J. 664, L13 (2007).

[25] P. S. Corasaniti, Mon. Not. R. Astron. Soc. 372, 191 (2006).

[26] R. A. C. Croft, R. Davé, L. Hernquist and N. Katz, Astrophys. J. 534, L123 (2000).

[27] S. Davidson, S. Hannestad, and G. Raffelt, JHEP 0005, 3 (2000).

[28] T. M. Davis et al. arXiv:astro-ph/0701510.

[29] P. S. Drell, T. J. Loredo, and I. Wasserman, Astrophys. J. 530, 593 (2000).

[30] J. Ehlers, in *Perspectives in Geometry and Relativity*, edited by B. Hoffmann (Indiana Univ., Indiana, 1966), p. 127.

[31] J. Ehlers, Z. Naturforsch. 22 a, 1328 (1967).

[32] J. Ehlers, in *General Relativity and Cosmology*, edited by R. K. Sachs (Academic, London, 1971), p. 1.

[33] L. P. Eisenhart, *Riemannian Geometry* (Princeton Univ., Princeton, 1926).

[34] D. J. Eisenstein et al. Astrophys. J. 633, 560 (2005).

[35] G. F. R. Ellis, in *General Relativity and Cosmology*, edited by R. K. Sachs (Academic, New York, 1971), p 104.

[36] G. F. R. Ellis, Gen. Relativ. Gravit. 39, 511 (2007).

[37] M. Ishak, A. Upadhye & D. N. Spergel, Phys. Rev. D 74, 043513 (2006).

[38] I. M. H. Etherington, Philos. Mag. 15, 761 (1933).

[39] S. Gardner & D. C. Latimer, arXiv:hep-ph/0904.1612v2.

[40] A. Goobar, L. Bergström, and E. Mörtsell, Astron. Astrophys. 384, 1 (2002).

[41] W. Gordon, Ann. Phys. (Leipzig) 72, 421 (1923).

[42] J. B. Hartle, *Gravity An Introduction to Einstein's General Relativity* (Addison Wesley, San Francisco, 2003).

[43] http://braeburn.pha.jhu.edu/∼ariess/R06/.

[44] K. Ichikawa, M. Kawasaki, T. Sekiguchi, and T. Takahashi, arXiv:astro-ph/0605481v2.

[45] K. Ichikawa & T. Takahashi, arXiv:astro-ph/0612739v2.

[46] A. K. Inoue & H. Kamaya, Mon. Not. R. Astron. Soc. 350, 729 (2004).

[47] R. Kantowski, Astrophys. J. 155, 89 (1969).

[48] R. Kantowski, Astrophys. J. 507, 483 (1998).

[49] R. Knop et al. Astrophys. J. 598, 102 (2003).

[50] E. W. Kolb, S. Matarrese, and A. Riotto, New J. Phys. 8, 322 (2006).

[51] J. Kristian & R. K. Sachs, Astrophys. J. 143, 379 (1966).

[52] M. Kunz & D. Sapone, Phys. Rev. Lett 98, 121301 (2007).

[53] L. D. Landau, E. M. Lifshitz, and L.P. Pitaevskii, *Electrodynamics of Continuous Media* (Butterworth-Heinenann, Oxford, 2002).

[54] E. M. Lifshitz, J. Phys. (Moscow) 10, 116 (1946).

[55] E. M. Lifshitz and I. M. Khalatnikov, Adv. Phys. 12, 185 (1963).

[56] R. W. Lindquist, Ann. Phys. 37, 487 (1966).

[57] V. Marra, E. W. Kolb, S. Matarrese, and A. Riotto, Phys. Rev. D 76, 123004 (2007).

[58] V. Marra, E. W. Kolb, and S. Matarrese, arXiv:0710.5505M.

[59] J. S. Mathis, Ann. Rev. Astron. Astrophys. 28, 37 (1990).

[60] T. Mattsson, arXiv:astro-ph/0711.42264.

[61] D. Mihalas, *Stellar Atmospheres* (W. H. Freeman and Company, San Francisco, 1970).

[62] L. Östman & E. Mörtsell, J. Cosmol. Astropart. Phys. 2, 005 (2005).

[63] R. Penrose, in *Perspectives in Geometry and Relativity*, edited by B. Hoffmann (Indiana Univ., Indiana, 1966), p. 259.

[64] R. Penrose, *An Analysis of the Structure of Space-Time, Adams Prize Essay* (Princeton Univ., Princeton, 1967).

[65] Perlmutter et al. Astrophys. J. 517, 565 (1999).

[66] A. Raychadhuri, Phys. Rev. 98, 1123 (1955).

[67] A. Raychadhuri, Z. Astrophys. 43, 161 (1957).

[68] A. G. Riess, W. H. Press, and R. P. Kirshner, Astrophys. J. 473, 88 (1996).

[69] A. G. Riess, W. H. Press, and R. P. Kirshner, Astrophys. J. 473, 588 (1996).

[70] A. G. Riess et al., Astron. J. 116, 1009 (1998).

[71] A. G. Riess et al., Astrophys. J. 607, 665 (2004).

[72] A. G. Riess et al., Astrophys. J. 659, 98 (2007).

[73] A. E. Romano, Phys. Rev. D 75, 043509 (2007).

[74] A. R. Robaina & J. Cepa, Astron. Astrophys. 464, 465 (2007).

[75] M. Rowan-Robinson, Mon. Not. R. Astron. Soc. 332, 352 (2002).

[76] R. K. Sachs, Proc. R. Soc. A 264, 309 (1961).

[77] R. K. Sachs & A. M. Wolfe, Astrophys. J. 147, 73 (1967).

[78] R. K. Sachs & H. Wu, *General Relativity for Mathematicians* (Springer-Verlag, New York, 1977).

[79] S. Sarkar, arXiv:astro-ph/0710.5307.

[80] P. Schneider, J. Ehlers, and E. E. Falco, *Gravitational Lenses* (Springer-Verlag, Berlin, 1992).

[81] L. Spitzer, *Physical Processes in the Interstellar Medium* (John Wiley & Sons, Inc., New York, 1978).

[82] J. Simon, L. Verde, and R. Jimenez, Phys. Rev. D 71, 123001 (2005).

[83] K. Sigurdson, M. Doran, A. Kurylov, R. R. Caldwell, and M. Kamionkowski, Phys. Rev. D 70, 083501 (2004).

[84] D. N. Spergel et al. Astrophys. J. Suppl. Ser. 148, 175 (2003).

[85] D. N. Spergel et al. Astrophys. J. Suppl. Ser. 170, 377 (2007).

[86] M. Sullivan et al. Mon. Not. R. Astron. Soc. 340, 1057 (2003).

[87] M. Taoso, G. Bertone, and A. Masiero, arXiv:astro-ph/0711.4996v2.

[88] M. Tegmark et al. Phys. Rev. D 69, 103501 (2004).

[89] M. Tegmark et al. Astrophys. J. 606, 702 (2004).

[90] R. A. Vanderveld, E. E. Flanagan, and I. Wasserman, Phys. Rev. D 74, 023506 (2006).

[91] W. M. Wood-Vasey et al. arXiv:astro-ph/0701041.

[92] Y. Wang, Astrophys. J 536, 531 (2000).

[93] Y. Wang & P. Mukherjee, Astrophys. J. 606, 654 (2004).

[94] Y. Wang & M. Tegmark, Phys. Rev. D 71, 103513 (2005).

[95] E. L. Wright, Astrophys. J. 250, 1 (1981).

[96] I. Zehavi et al., Astrophys. J. 503, 483 (1998).

[97] Y. B. Zeldovich & I. D. Novikov, *The Structure and Evolution of the Universe* (Univ. of Chicago, Chicago, 1983), Vol. 2, Chap. 12.